The Thesis Committee for Clarke Austin Clayton
Certifies that this is the approved version of the following thesis:

Linking Gulf of Mexico Margin Submarine Canyons to Regional Tectonics and Interaction of Paleogene Lower Wilcox High Frequency Sequences with the Yoakum Canyon

APPROVED BY
SUPERVISING COMMITTEE:

Supervisor:

Ronald J. Steel

Co-Supervisor:

Cornel Olariu

William Fisher

Linking Gulf of Mexico Margin Submarine Canyons to Regional Tectonics and Interaction of Paleogene Lower Wilcox High Frequency Sequences with the Yoakum Canyon

by

Clarke Austin Clayton, BS

Thesis

Presented to the Faculty of the Graduate School of

The University of Texas at Austin

in Partial Fulfillment

of the Requirements

for the Degree of

Master of Science in Geological Sciences

The University of Texas at Austin

May 2017

Dedication

I would like to dedicate this work to Allyson, my parents, and my sister.

Acknowledgements

I would like to sincerely thank Dr. Cornel Olariu for his countless hours helping me develop ideas for this project. Without his help, guidance, and friendship this project would not have been possible. I also would like to express my sincere thanks to Dr. Ronald Steel for his help with completing this project and his insight throughout my undergraduate and graduate studies. I would also like to thank Dr. William Fisher for his great insight and deep knowledge on submarine canyons, which this project is based around.

Thank you to Statoil for giving support to this project. The funding provided for this project and the previous Wilcox Project helped build the database that made this possible. David Conwell allowed for this project to start smoothly with his previous project focusing on the Upper Wilcox.

Thank you to my friends from the Jackson School of Geosciences. The Dynamic Stratigraphy Group provided great support and insight on how to further improve my project throughout the process. I would also like to thank John Bucholz, Takonporn Kunpitaktakun, Rattanaporn Fong-Ngern, and Yang Peng for their support and friendship during my time working on this project.

A great group of assistants, Ryan Herring, Ryan Kraft, Moonsoo Shin, and Jae Jun Lee, provided countless hours of digitizing well logs, creating the backbone of this project. Thank you very much for your help.

Finally, I would like to thank Allyson and my family for providing me with support and inspiration during my time pursing this project.

Abstract

Linking Gulf of Mexico Margin Submarine Canyons to Regional Tectonics and Interaction of Paleogene Lower Wilcox High Frequency Sequences with the Yoakum Canyon

Clarke Austin Clayton, MS Geo. Sci.

The University of Texas at Austin, 2017

Supervisor: Ronald J. Steel

Co-Supervisor: Cornel Olariu

In northern Gulf of Mexico, a clustering in a 100-150 km wide area of six Late Cretaceous-Paleogene age incisions up to 1000 m deep and 100 km long suggests a structural, rather than eustatic, control. The incisions counterintuitively align with the basinward trend of the San Marcos Uplift instead of forming in front of large sediment fairways (rivers) that formed depocenters of the Rio Grande and Houston embayments. The Sabine Arch and LaSalle Arch also uplift regions around the Gulf of Mexico Basin, which align with large slope incisions that indicate a possible main control of tectonism on canyon formation. This study proposes three new possible mechanisms, shelf edge bulge model, low uplift rate model (LUR), and high uplift rate model (HUR), for canyons formation in addition to the two 'conventional' models of cutting during lowstand (Posamentier et al., 1991) and cutting during transgression (Galloway, 1991)

In addition to the tectonic control of canyon formation, canyon evolution can be longer lived than previously described for some of the Wilcox Group large-scale incisions. By mapping 12 high frequency regressive-transgressive sequences within the Lower Wilcox in the San Marcos Arch region: (1) Sand thickening patterns towards the Yoakum Canyon margin (2) Mis-match of log signature correlation across the Yoakum Canyon (indicating the canyon acted as a "sediment barrier" in the study region) suggest that canyon was active for a longer period than previously described. With the Yoakum Canyon being active during Lower Wilcox time, the canyon(s) evolution would be in the scale of 4 to 5 million years rather than 1 million to 100,000 years. Over this time scale, the deep-water sediment was delivered into the submarine canyon(s) when lateral switching of the shelf-delta depocenters reached close to the head of the canyon during delta transits across the inner to outer shelf. The relationship of Wilcox Group incisions with tectonics and long-lived evolution of canyons provides insight into the large volume of clastic sediment and possible new mechanisms for sediment delivery to the deep water Gulf of Mexico.

Table of Contents

List of Figures xi

Chapter 1 Introduction 1

Chapter 2 Linking Cretaceous and Paleogene Gulf of Mexico Large Scale Canyon Incisions to Tectonics 3

Introduction 3,h3 style 2

Large Scale Incisions of the Gulf of Mexico 3,h3 style 6

Uplifted Areas (Arches) Around the Gulf of Mexico 12

Discussion 14

Location of Canyons, Arches and Sediment Fairways 14

Arche Uplifts as a Mechanism for Canyon Formation 15

Conclusions 16

Chapter 3: Interaction of Paleogene Lower Wilcox High Frequency Sequences with the Yoakum Canyon 22

Introduction 22

Background/Geologic Setting 28

Wilcox 28

Submarine Canyons 34

Methods and Dataset 39

Dataset 39

Mapping 44

Cross Sections 45

Results 48

Regional Cross Sections 48

Lower Wilcox Sequence Maps 49

Sequence 1 49

Sequence 2 52

Sequence 3 54

Sequence 4 58

Sequence 5 62
Sequence 6 64
Sequence 7 66
Sequence 8 70
Sequence 9 74
Sequence 10 76
Sequence 11 78
Sequence 12 80
Discussion 82
Implications for the Evolution of the Yoakum Canyon 86
Comparison to the Mississippi Canyon 88
Relationship with the Deepwater 90
Conclusions 93
Chapter 4: Thesis Findings and Future Work 94
Future Proposed Research 95
Bibliography 97
Vita 101

List of Figures

Figure 1: Regional overview of the Gulf of Mexico highlighting location of paleocanyons, regional tectonic features, shelf edge margins, and Wilcox Group Embayments (modified from Fisher and McGowen, 1967; Hutchinson, 1984; Laubach and Jackson, 1990; Lawless and Hart, 1990; Galloway, 2008).....5

Figure 2: San Marcos Arch region submarine paleocanyons: A) Cretaceous Trinity Canyon (Culotta et al., 1992) B) Halletsville Complex/Smothers Channel (Devine and Wheeler, 1989) C) Lavaca Canyon (Galloway et al., 1991) D) Yoakum Canyon (Dingus and Galloway, 1990) E) Upper Wilcox “Cornish” Canyons (Cornish, 2013). Numbers provided describe the length and width of each submarine canyon. Dashed lines denote location of previous underlying canyon.....7

Figure 3: Chart depicting timing of the San Marcos Arch region with an emphasis on canyon formation timing. (1) The stratigraphic column is for the specific formations present in the San Marcos Arch region and approximate thicknesses of each formation are displayed next to the column. (2) San Marcos Arch movement column depicts periods of “Emergence” (when the San Marcos Arch was actively uplifting), and “Submergence” (when the San March Arch was not tectonically active). (3) Eustatic sea level curve is provided by Haq et al., (1988). (4) Third-order clastic wedges for the Wilcox Group in the San Marcos Arch region as interpreted by Crabaugh and Elsik, (2000). 8

Figure 4: Block Diagrams depicting proposed mechanisms of tectonic uplift associated with submarine canyon formation.. 20
Figure 5: Link between San Marcos Arch region submarine canyons and the basin floor fans (modified from Zarra, 2007; McDonnell et al., 2008). 23
Figure 6: San Marcos Arch region and cluster of Cretaceous and Paleogene submarine canyons.....25
Figure 7: Seismic cross section of the Yoakum Canyon with the previous interpretation of a single cut and fill phase for the canyon evolution (Dingus and Galloway, 1990; HGS Bulletin 2006). No scale or orientation was provided by the HGS Bulletin (2006), but the canyon is likely on the scale of 10 to 15 km wide in this section and the orientation is likely along depositional strike.. 26
Figure 8: Seismic cross section of the Yoakum Canyon with the previous interpretation of a single cut and fill phase for the canyon evolution (Dingus and Galloway, 1990; HGS Bulletin 2006) and a new interpretation of multiple cut and fill events that we would like to argue in this study. No scale or orientation was provided by the HGS Bulletin (2006), but the canyon is likely on the scale of 10 to 15 km wide in this section and the orientation is likely along depositional strike 27
Figure 9: Compilations of different stratigraphic columns and associated clastic wedges for the study area (modified from Crabaugh and Elsik, 2000).. 29
Figure 10: Lower Wilcox Deltas A, B, and C across the Houston embayment for the Rockdale Delta System with the location of the Yoakum Canyon (modified from Fisher and McGowen [1967]). 30

Figure 11: Depositional Environments of the Lower Wilcox in the Houston Embayment and relationship with the Yoakum Canyon (modified from Fisher and McGowen [1967]). 32
Figure 12: Location of Wilcox Group paleocanyons (Hutchinson, 1984).. 35
Figure 13: Schematic figures showing mechanisms for canyon cutting. A) Sea level lowing and fluvial incision during lowstand (Vail, 1987; Cornish, 2013). B and Stage 1 through 4) overloading of shelf edge initiating failure and transgressive headward erosion of the canyon within the shelf (Dingus and Galloway, 1990; Galloway et al., 1991).. 38
Figure 14: Study Region and location of cross sections and type log. 40
Figure 15: Type log defining sequences, flooding surfaces, regressive surfaces, and Bebout (1987) defined Wilcox surfaces. 43
Figure 16: Regional cross section A-A' dissecting the proximal portion of the Yoakum Canyon. 46
Figure 17: Regional cross section B-B' dissecting the basinward portion of the Yoakum Canyon.. 47
Figure 18: Isopach maps for the total sequence, regressive phase, and transgressive phase for Sequence 1. Isopach maps included are gross thickness, net sand thickness, and net to gross ratio. White arrows indicate location of trends for the sequence.....51
Figure 19: Isopach maps for the total sequence, regressive phase, and transgressive phase for Sequence 2. Isopach maps included are gross thickness, net sand thickness, and net to gross ratio. White arrows indicate location of trends for the sequence.....53

Figure 20: Isopach maps for the total sequence, regressive phase, and transgressive phase for Sequence 3. Isopach maps included are gross thickness, net sand thickness, and net to gross ratio. White arrows indicate location of trends for the sequence.....55
Figure 21: Cross-section C-C' depicting sand thickening trend towards the Halletsville Complex.. 57
Figure 22: Isopach maps for the total sequence, regressive phase, and transgressive phase for Sequence 4. Isopach maps included are gross thickness, net sand thickness, and net to gross ratio. White arrows indicate location of trends for the sequence.....59
Figure 23: Cross-section D-D' depicting sand thickening trend towards the Lavaca Canyon. 61
Figure 24: Isopach maps for the total sequence, regressive phase, and transgressive phase for Sequence 5. Isopach maps included are gross thickness, net sand thickness, and net to gross ratio. White arrows indicate location of trends for the sequence.....63
Figure 25: Net sand thickness maps for Sequences 4-6 illustrating the progradation of the system across the shelf. Shorelines (interpreted based on the break between sandy and muddy lithology) represented for Sequences 4 and 5. Sequence 6 shoreline estimated to be basinward of the study area ..64
Figure 26: Isopach maps for the total sequence, regressive phase, and transgressive phase for Sequence 6. Isopach maps included are gross thickness, net sand thickness, and net to gross ratio. White arrows indicate location of trends for the sequence.....65

Figure 27: Isopach maps for the total sequence, regressive phase, and transgressive phase for Sequence 7. Isopach maps included are gross thickness, net sand thickness, and net to gross ratio. White arrows indicate location of trends for the sequence.....67

Figure 28: Cross-section E-E' illustrating the sand thickening trend of sequence 7 towards the Yoakum Canyon margin. 69

Figure 29: Isopach maps for the total sequence, regressive phase, and transgressive phase for Sequence 8. Isopach maps included are gross thickness, net sand thickness, and net to gross ratio. White arrows indicate location of trends for the sequence.....71

Figure 30: Cross-section H-H' illustrating matching log patterns across the Yoakum Canyon. 73

Figure 31: Isopach maps for the total sequence, regressive phase, and transgressive phase for Sequence 9. Isopach maps included are gross thickness, net sand thickness, and net to gross ratio. White arrows indicate location of trends for the sequence.....75

Figure 32: Isopach maps for the total sequence, regressive phase, and transgressive phase for Sequence 10. Isopach maps included are gross thickness, net sand thickness, and net to gross ratio. White arrows indicate location of trends for the sequence.....77

Figure 33: Isopach maps for the total sequence, regressive phase, and transgressive phase for Sequence 11. Isopach maps included are gross thickness, net sand thickness, and net to gross ratio. White arrows indicate location of trends for the sequence.....79

Figure 34: Isopach maps for the total sequence, regressive phase, and transgressive phase for Sequence 12. Isopach maps included are gross thickness, net sand thickness, and net to gross ratio. White arrows indicate location of trends for the sequence.....81

Figure 35: Evolution of the Lower Wilcox sequence depocenters based on trends depicted in isopach maps of each sequence and log patterns. Morphology and location of depocenters interpreted from isopach maps for the regressive phase of each sequence. 84

Figure 36: Location of different Delta systems of the Mississippi Delta Complex illustrating that the Mississippi Canyon did not capture shelfal sediments during the last lowstand (Suter and Beryhill, 1985) 89

Figure 37: Paleogeographic map of Wilcox 2 showing the basin floor fan downdip of the Yoakum Canyon (Zarra, 2007).....92

Chapter 1: Introduction

Economically, the Paleocene-Eocene Wilcox Group has been a highly sought after resource play that has included extensive reserves of fresh water, lignite, natural gas, and oil (Hargis 1962, Fisher and McGowen, 1967; Zarra, 2007). The first Wilcox wells were drilled in the late 1920's and more wells have now been drilled in northeast Mexico, Texas, Louisiana, Mississippi and Alabama both on shore as well as offshore into deep water (Zarra, 2007). By the 1990's a total of 30 billion cubic feet of natural gas has been discovered within the Wilcox Group out of a total of approximately 30 trillion cubic feet believed to be in the entire Gulf of Mexico for the Wilcox Group (Nehring Database, 1997; Zarra, 2007). These reserves were limited to the 'shelfal' Wilcox Group deposits below southern Texas and mainly contain gas. The Wilcox Group, within this shelf segment, is primarily characterized by fluvial, deltaic, and shallow-marine environments (Fisher and McGowen, 1967). In 2001, a deep-water Wilcox well, Baha #2, successfully discovered a thick (4,500 ft/ 1500 m) Wilcox Group turbidite trend (Zarra, 2007). Following this discovery, the deep-water Wilcox Group has been a highly sought after reservoir in deepwater GOM exploration. Due to the discovery of deep-water reservoirs, the link between these deposits and the shelf became a renewed topic of interest especially within a sediment source-to-sink framework that is lately of significant interest for scaling of depositional environments (Somme et al., 20009) and basin evolution.

The Wilcox Group shelf system contains multiple submarine canyons at different locations and active at different geologic times (Hoyt, 1959; Chuber, 1979; Dingus and

Galloway, 1991; Galloway, 2008). These canyons are the key features within ancient source-to-sink sediment dispersal system, are shelf dissecting (for tens of kilometers), connect with paleo-shorelines and provide one of the main conduits for sediment bypass of the slope. Many of the canyons seems to cluster in a specific area on the shelf. The goal of this study is (1) to provide an insight into location of canyon clusters, suggest possible mechanisms for canyon formation, and (2) to provide a detailed evolution for the largest Wilcox Group canyon (Yoakum Canyon) in the San Marcos Arch region.

Chapter 2: Linking Cretaceous and Paleogene Gulf of Mexico Large Scale Canyon Incisions to Tectonics

INTRODUCTION:

In the Late Cretaceous to Paleogene Gulf of Mexico Basin, large incisions were commonly recognized since the earliest stratigraphic studies (Hoyt, 1959). Submarine canyon formation is conventionally attributed to initiation during eustatic sea level falls (Mitchum, 1985; Vail, 1987). The lowstand incisions enlarge during subsequent transgressions resulting from an interplay of sediment supply, subsidence rate, and eustatic sea level change (Galloway, 1989) Using previous maps and publications, this study shows that large-scale incisions have a strong correlation with areas of tectonic uplift (arches) that have a long axis orientation perpendicular to the basin margin. The focus of this study is on four recurrent episodes of submarine canyon formation occurring within the Wilcox Group in the "Yoakum" area (Figure 1) directly overlying the extended axis of the San Marcos Arch, west of the "Houston Embayment" which was actively uplifting during the Paleogene. The Paleogene or earlier subduction of the Pacific Plate caused stress and may possibly have created the uplifted (arches) areas (Laubach and Jackson, 1990) that in turn fostered canyon formation. The correlation between the onshore uplift and offshore canyons occurs at multiple locations along the Gulf of Mexico margin during the Late Cretaceous to Paleogene suggesting that shelf "arching" may have been a more common mechanism for canyon formation than thought. While a tectonic control mechanism for

canyons was alluded to by (Galloway, 2008) a formation mechanism was not proposed. The tectonic control mechanism for canyon formation would have a significant implication for GOM basin margin architecture and deepwater sediment delivery because (1) it would have encouraged significant shelf incision even during greenhouse times (low amplitudes of isostatic sea levels) and (2) it would have caused potential capture of highstand shoreline sediments and transfer of these to deepwater areas.

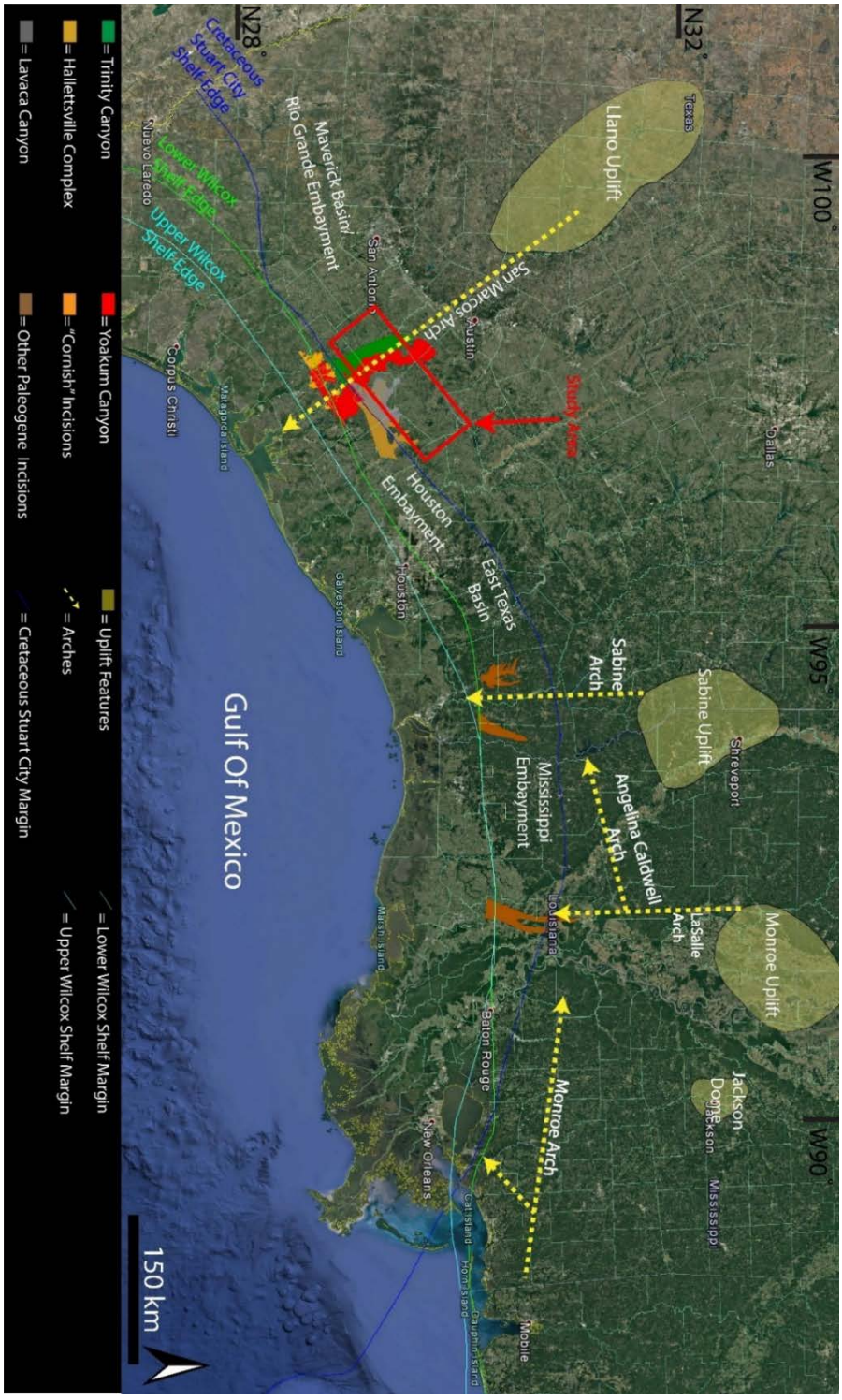

Figure 1: Regional overview of the Gulf of Mexico highlighting location of paleocanyons, regional tectonic features, shelf edge margins, and Wilcox Group

Embayments (modified from Fisher and McGowen, 1967; Hutchinson, 1984; Laubach and Jackson, 1990; Lawless and Hart, 1990; Galloway, 2008).

LARGE SCALE INCISIONS OF THE GULF OF MEXICO:

The Late Cretaceous to Paleogene margin of the Gulf of Mexico has multiple large incisions clustered in specific areas (Figures 2, 3). The Trinity (Culotta et al. 1992), Yoakum (Dingus and Galloway, 1990), Lavaca (Chuber, 1979), Hallettsville Complex (Chuber, 1979), and "Cornish" (Cornish, 2013) canyons are all located within close proximity, covering DeWitt, Lavaca, and Colorado counties (Figures 1, 2). The canyons relate with each other because of overlap in localized areas (Figure 2), but are of different ages (Figure 3). The age distribution ranges from Late Cretaceous (Cenomanian) (oldest) to Early Eocene (Ypresian) youngest: Trinity Canyon, Hallettsville complex, Lavaca Canyon, Yoakum Canyon, and "Cornish" incisions (Figures 2, 3).

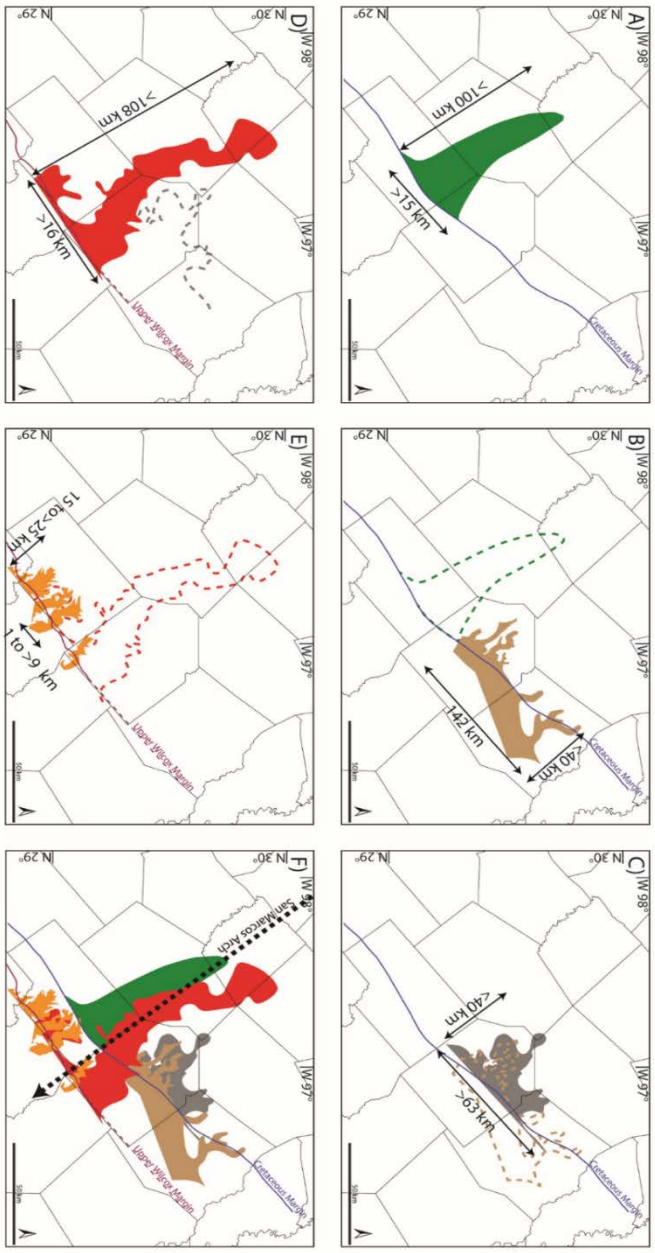

Figure 2: San Marcos Arch region submarine paleocanyons: A) Cretaceous Trinity Canyon (Culotta et al., 1992) B) Halletsville Complex/Smothers Channel (Devine and Wheeler, 1989) C) Lavaca Canyon (Galloway et al., 1991) D) Yoakum Canyon (Dingus and Galloway, 1990) E) Upper Wilcox "Cornish" Canyons (Cornish, 2013). Numbers provided describe the length and width of each submarine canyon. Dashed lines denote location of previous underlying canyon.

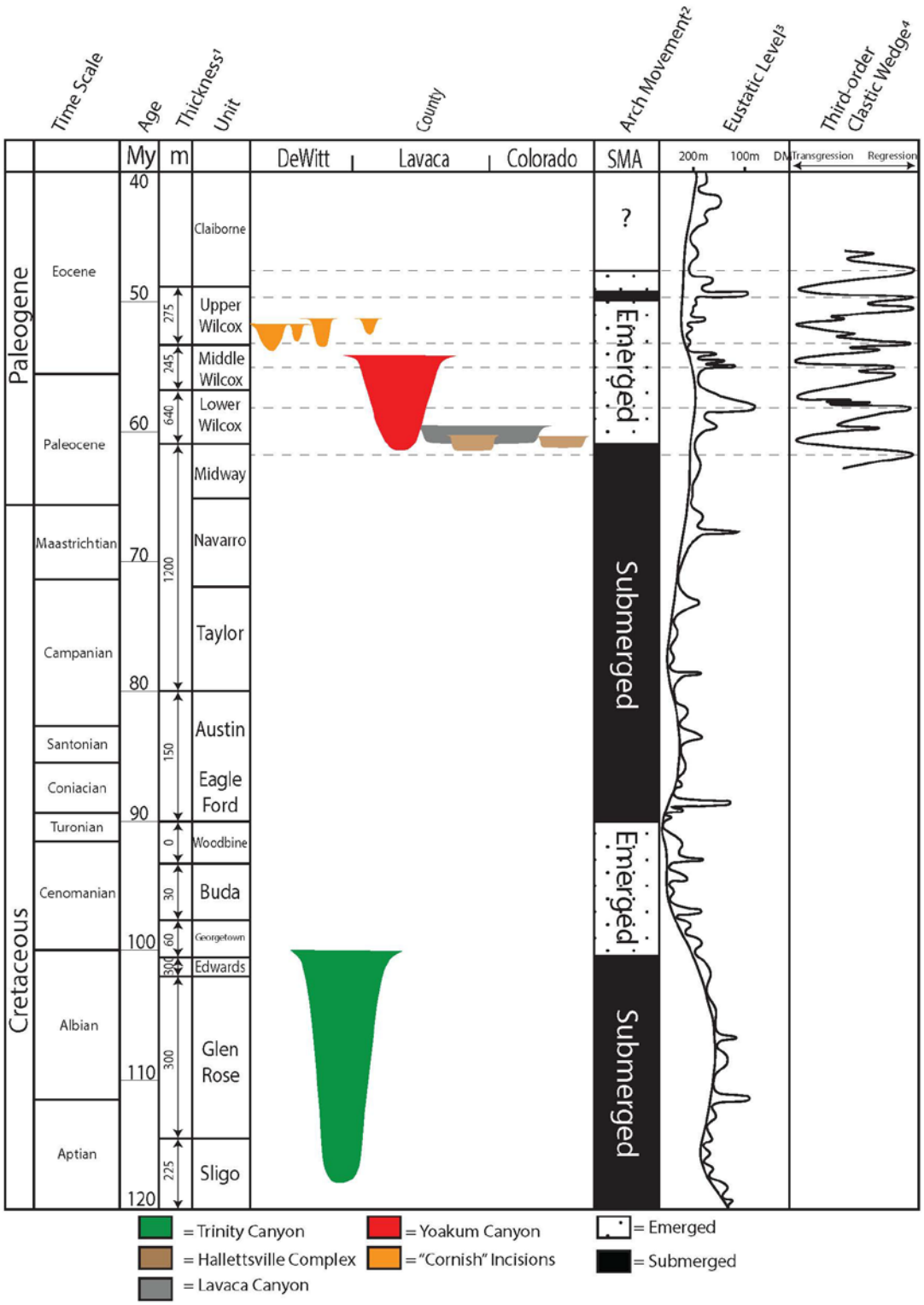

Figure 3: Chart depicting timing of the San Marcos Arch region with an emphasis on canyon formation timing. (1) The stratigraphic column is for the specific

formations present in the San Marcos Arch region and approximate thicknesses of each formation are displayed next to the column. (2) San Marcos Arch movement column depicts periods of "Emergence" (when the San Marcos Arch was actively uplifting), and "Submergence" (when the San March Arch was not tectonically active). (3) Eustatic sea level curve is provided by Haq et al., (1988). (4) Third-order clastic wedges for the Wilcox Group in the San Marcos Arch region as interpreted by Crabaugh and Elsik, (2000).

The Trinity Canyon (Culotta et al., 1992) is the oldest canyon that cut into the carbonate deposits of the Glen Rose and Sligo formations (Figure 3). The regional strike-oriented seismic survey indicates the dimensions of this canyon could be 2 km deep, 15 km wide, and was inferred to be greater than 100 km long (Figure 2) (Culotta et al. 1992). The 2-D seismic correlations suggest that the canyon cuts through the outer shelf and shelf edge of the Cretaceous Trinity Group's upper Sligo shelf and that it was filled with the deposits of Edwards unit. The Trinity canyon is not extensively studied and further insight is needed to understand timing and processes of the canyon excavation and filling.

The Smothers "channel" is the oldest incision (Devine and Wheeler, 1989) into the Paleocene (Selandian) siliciclastic deposits. This channel incision is relatively small compared to the other incisions with a depth of about 400 ft (122 m), a sinuous channel length of 3 miles or (4.8 km), and a width larger than 2 miles (3.2 km) (Chuber, 1979; Devine and Wheeler, 1989). The Smothers Channel is part of a broader complex of outer shelf incisions, the Hallettsville complex. The width of this complex is large, over 140 km (Figure 2). The morphology of the complex is characterized by slumping and scalloping similar to the younger Lavaca Canyon (Galloway et al., 1991). Devine and Wheeler (1989) suggested that the Smothers Channel and Hallettsville complex eroded during a sea level

lowering. The channel cut through the Kubena Sand of the Lower Wilcox into the Midway Shale and extended with associated growth faulting past the underlying Cretaceous margin (Devine and Wheeler, 1989). The channel and the complex subsequently filled during progradation of the next deltaic unit (referred to as Delta A by Fisher and McGowen [1967], Devine and Wheeler [1989]). The channel fill is predominantly marine shales with more sandstones and conglomerates near the proximal end.

The progradation of Lower Wilcox Delta A (Fisher and McGowan, 1967) led to sediment loading on the shelf margin and subsequent slope failure, initiating the incision of the Lavaca Canyon (Hoyt, 1959; Devine and Wheeler, 1989; Galloway et al., 1991). Canyon head slumping widened the incised area and formed a broad-scalloped canyon morphology (Figure 2). Where the canyon opens to the lower slope, the canyon depth is nearly 4,000 ft (>1300m) (Galloway and McGilvery, 1995). The central region of the canyon has a length to width ratio of 0.8 (i.e., wider than longer) and the floor of the canyon is largely flat with steep margin walls (Galloway et al., 1991). The Lavaca Canyon fill is dominantly mudstone, similar to the other Paleogene Gulf of Mexico incisions. The Lavaca Canyon fill, however, does contain deep-water sandstone deposits (turbidite beds and deformed beds up to meters thick) in cores from Howell Allen #2 well (Galloway and McGilvery 1995). The lower portion of the canyon fill consists of onlapped mudstone and bidirectional offlapping sandstone mounds on the basal canyon surface (Galloway et al., 1991).

The most prominent canyon in the region is the Yoakum Canyon, which dissects the shelf over a length of more than 67 mi (108 km), has a width larger than 10 mi (16 km)

and is more than 3500 ft (1067 m) deep (Figure 2) (Dingus and Galloway, 1990). The geometry of the Yoakum Canyon is elongate unlike the broader morphologies of the Hallettsville Complex, Lavaca Canyon, and younger "Cornish" incisions. Dingus and Galloway (1990) proposed that the canyon excavation was initiated due to regression of the upper Middle Wilcox shelf deposits atop lower Middle Wilcox shelf margin mudstones, that together loaded the shelf edge resulting in slump failure. Headward erosion extended the canyon landward during subsequent transgression. Finally, the canyon completed its infilling by Upper Wilcox hemiplegic and prodelta muds. The canyon fill, interpreted from well logs, is predominantly mudstone with some sandstone lenses, similar to the fills of the Lavaca, Smothers, and "Cornish" canyons. There are no cores available from the Yoakum Canyon fill, but well logs suggest that also the facies here are likely dominated by mudstone and similar to the turbidite and deformed facies found in the Howell Allen #2 core in the Lavaca Canyon.

Finally, the youngest incisions in this region are within the Upper Wilcox (Cornish, 2011). Four separate, large Upper Wilcox shelf-edge incisions of two different ages have been mapped. The Meyersville and Anna Barre incisions are slightly older than the Jennie Bell and Hope incisions. The depths of these incisions range from 425 to 1150 feet (140 to 350 m), widths range from 0.5 to 5.8 miles (0.7 to 9 km), and lengths range from 9.1 to 15 miles (14 to 25 km). The Hope, Jennie Bell, and Anna Barre incisions were made by simple streams with a single trunk system and short tributaries while the Meyersville incision is more complex with two major trunk streams and numerous tributaries (Cornish, 2011). The location and thickness suggests large shelf-edge erosion during two rapid sea level falls of

over 400 feet (130 m) in drawdown after which the incisions fill with mud (Cornish, 2011) as have been suggested in other Wilcox canyons.

While the interpretations of canyon evolution (age of incision) differ between the systems, it is significant to note that the incisions all occur in the same region extending throughout a period of about 50 My (Figures 2 and 3). Each incision fill is predominantly mudstone (hundreds of meters thick) but also contain discontinuous meters, tens of meters' thick sandstone bodies. The incisions are large, ranging from 130 to 1300 m in depth, a few km to 100 km in width and lengths from a few km to over 110 within the shelf. While eustatic sea level fluctuations would seem like the easiest and most common mechanism to invoke for starting the incisions, it cannot be the sole cause for the formation of the large incisions. Headward erosion and slumping during rising relative sea level and transgression has also been suggested as an important mechanism. Another factor, tectonics (as will be argued in the next section) may have controlled the formation and location of these features.

UPLIFTED AREAS (ARCHES) AROUND THE GULF OF MEXICO:

Areas of prominent regional uplift (arches) formed along the Gulf of Mexico margin during the Late Cretaceous and early Tertiary (Figure 1). The San Marcos Arch and the Sabine Arch have been most studied. The San Marcos Arch extends from the Llano Uplift plunging to the southeast while the Sabine Arch extends from exposed basement of the Sabine uplift plunging towards the south to southeast basinward to the Gulf of Mexico

(Figure 1). Between the two arches are major, long-lived sediment depocenters, the Houston Embayment and East Texas Basin (Figure 1).

The San Marcos Arch's anticline is the most prominent with an axial trace in excess of 400 km (Laubach and Jackson, 1990). This arch has about 1.5 km of structural relief separating the Lower Cretaceous units on the crest of the arch compared to the same units in the Rio Grande Embayment depocenter to the west. The Sabine arch has multiple anticlines with smaller dimensions than the San Marcos arch. The Sabine arch anticlines have different plunge angles due to flexure and salt structures, but the 80 km long main axis of the uplift is towards the south-southeast (Laubach and Jackson, 1990). The structural relief between the Sabine arch and the adjacent depocenters is approximately 1.3 km.

First movement of the arches occured in the Late Cretaceous and continued into the early Tertiary (Figure 3) (Laubach and Jackson, 1990). A structural high forming at both the Sabine Arch and San Marcos Arch that disrupted the large stratigraphic trends during the late Cretaceous denotes the initial movement. The early Cretaceous deposits near and atop the San Marcos arch were largely uniform in thickness with trends indicating no structural high between the Houston Embayment and Maverick Basin/Rio Grande Embayment. During the late Cretaceous the Upper Eagle Ford Group preferentially deposited (and thickened) away from the arch axis into the Maverick Basin/Rio Grande Embayment to the west and Houston Embayment to the east (Hentz and Ruppel, 2010). The Turonian-Coniacian Upper Eagle Ford shale thinned from the Maverick Basin/Rio Grande Embayment towards the San Marcos Arch suggesting a topographic high during

this period. Another pulse of uplift has been inferred during the early Tertiary (Figure 3) based on the tectonic movements and stratigraphic trends (Murray, 1961; Laubach and Jackson, 1990). Timing of other uplift structures, such as the LaSalle Arch, around the Gulf of Mexico (Figure 1) are less certain but also have been linked with large scale tectonics and thought to initiate around late Cretaceous (Lawless and Hart, 1990).

DISCUSSION:

Location of Canyons, Arches and Sediment Fairways

The large incisions along the Gulf of Mexico during the late Cretaceous and Paleogene form in distinct clusters that align with landward uplifted regions. For the Yoakum area, the prominent regional San Marcos Arch uplift runs along the axis of the six distinct time periods of canyon excavation showing a preferential recurrent region for erosion (Figures 1 and 2). The time of significant erosion correlates with San Marcos arch uplifting during the Late Cretaceous and again during the Early Paleogene (Laubach and Jackson, 1990).

One of the most used mechanisms for canyon formation is fall and lowstand of eustatic sea level, when the shoreline was at or below the shelf edge and the river cut a shelf valley. The shelf valley would have extended incision across the shelf edge and the upper slope (Vail, 1987; Mitchum, 1985). One of the problems with such a model (lowstand-river incision) is that the incisions in the Yoakum area occur not within but between large depocenters, the Rio Grande Embayment and Houston embayments, where there was primary delivery of sediments along the main fluvial fairways during Paleogene

(Figure 1) (Fisher and McGowen, 1969). The Wilcox deltaic systems deposited in these two main fairways have no mapped large incision at the shelf edge but rather large deposition rates that triggered the formation of growth faults (Fisher and McGowen, 1967; Winker and Edwards, 1983; Olariu and Ambrose, 2016). Thus, it is significant and somehow counterintuitive, that canyons were excavated basinward from the structurally high locations associated with the uplifts, while there are no canyons in the structurally low area of the Rio Grande Embayment, Houston Embayment or East Texas Basin. Another problem with the eustatic mechanism of canyon generation is that the amplitude of eustatic fall and rise of sea level during late Cretaceous through lower Eocene was neither large nor frequent because this was a greenhouse period with generally relatively high sea levels.

Arch Uplifts as a Mechanism for Canyon Formation

While the link between tectonic uplift and shelf-edge incision during the late Cretaceous and Paleogene seems obvious, the mechanism for such incisions have not been described and are debatable. We propose three different possible mechanisms (Figure 4) for shelf edge incision with a tectonic influence. i) The low uplift rate model (LUR) proposes that fluvial erosion triggered by relative sea-level fall from localized tectonic uplift (Figure 4C). The tectonic uplift must be slow and a preexisting river will cut through the uplift (similar to the Colorado River cutting the Grand Canyon into Colorado Plateau, McKee and McKee, 1972) to readjust the stream gradient increase on the outer shelf (Zaitlin et al., 1994). The river eventually will erode the shelf and the shelf-edge will be incised. As a result, the river will form large canyon conduits and connect to the deep water

similar to the modern Zaire Canyon (Babonneau et al., 2002) ii) The shelf edge bulge model (Figure 4A) proposes that the outer shelf to shelf-edge gradient increases slowly from tectonic uplift creating upper slope instability. The instability leads to subaqueous slumping and incision of the shelf-edge. Continuous landward uplift supports subaqueous canyon headward erosion into the shelf edge. The incision will fill, subsequently, by progradational shoreline/ delta units as proposed by Galloway et al. (1991). iii) The high uplift rate (HUR) model (Figure 4B) bulges the paleo-shoreline creating a headland with a relatively narrow shelf along the uplifted region. This bulging of the shoreline directs longshore currents basinward to the shelf margin triggering dense sediment-laden shelf-water cascading over the shelf-edge. The cascading of dense water can be erosive for an extensive period, during lowstand and highstands, creating deep incisions (Covault et al., 2007; Palanques et al., 2006; Puig et al, 2014). A modern analog where shelf dense water (with dissolved salts) cut a canyon is to the eastern end of the Pyrenees Mts. where the regional structural trend ends into the Mediterranean basin. During the summer season, salty and dense water from the Gulf of Lions (think Houston Embayment, Fig. 1) cascades over the shelf edge eroding the largest Canyon in the area (Palanques et al. 2006). A modern example where longhore current diverted by a headland/ island) feed deep-water basin margin was described from southeast Australia (Boyd et al., 2008).

The formation of the Paleogene incisions has been described by different theories that have been useful to understand many basin margins and canyons. a) Isolation of the Gulf of Mexico leading to a large scale evaporitic drawdown and subsequent refilling of the Gulf of Mexico (Rosenfeld and Pindell, 2003; Cossey et al., 2016). This is still

controversial for Gulf of Mexico but widely accepted as a mechanism in the Mediterranean Basin (Ryan and Cita,, 1978; Riding et al., 1998). b) Shelf edge failure and headward erosion initially forming gullies (Pratson and Coakley, 1996). This failure is enhanced during transgression where a canyon is excavated through the shelf and subsequent progradation fills the incisions (Galloway et al., 1991). c) Fluvial incision during lowstand and subsequent filling of the incision during highstand (Cornish, 2013). These theories each uniquely postulate GOM Paleogene incision for occurrence but ignore the important fact that these incision occur in clustered regions. Here we propose that tectonic uplift emergence that strongly correlates with each cluster of Paleogene incision along the ancient Gulf of Mexico (Figure 1) is the main controlling factor. Thus, the Pacific Plate subduction, which increased plate stresses to build foreland basin uplifts (Laubach and Jackson, 1990), to form large folds (arches) plunging toward GOM that triggered shelf edge incision (canyon formation) eventually transporting large sand volumes (Figure 3) to basin floor fans in the Gulf of Mexico (Zarra et al., 2005).

The proposed model for canyon formation is supported by multiple canyon clusterings in proximity of structural highs around GOM, not only in the Yoakum area. The Sabine Arch has the same emergence history as the San Marcos Arch, and aligns with other large offshore Paleogene Wilcox incisions. Although less studied, two prominent canyons lie along the axis and flank of Sabine arch (Figure 1), the Tyler Hardin (Hutchinson, 1984) and Bleakwood (Galloway et al., 1991). While these incisions are less studied, they have similar dimensions and fills (mudstone) as the Yoakum area Paleogene incisions.

While the location and timing correlation between the submarine canyon network of the Wilcox Group are strong for both the San Marcos and Sabine Arches, it would be inadequate to ignore the numerous other incisions of the Wilcox Group. These incisions, while less extensively studied, also seem to have a correlation with tectonically active areas (Figure 1). Northeast of the Sabine Arch, the St. Landry (McCulloh, 1986), and Mississippi Embayment Axis (Watkins, 2014) canyons overly the LaSalle Arch (Figure 1). The LaSalle Arch is also associated with the Sabine and San Marcos Arch and its emergence time frame is similar to these arches (Lawless and Hart, 1990). The Chicontepec Canyon (Busch and Govela 1978) overlies a structurally complex region of faulting associated with the Sierra Madre Oriental with Tamaulipas Arch (Salvador, 1991, Pindell et al., 2006). The canyon overlies a heavily faulted area, but also an uplifted feature is directly underlying the canyon as seen by seismic data published by Cossey et al., (2016).

CONCLUSIONS:

Paleo-incisions along the Gulf of Mexico during the late Cretaceous and Paleogene are common and tend to form in clusters. They are significant in having lengths ranging from 10 miles to over 65 miles within the shelf and depths ranging from 400 feet (120 m) to over 4,000 feet (1200 m). These incisions are described as valleys, channels, and canyons, but due to their significant size, association with the shelf-edge and dominant muddy fills, we argue that they can all be considered submarine canyons.

It is striking that multiple uplift-canyon system clusters along the Gulf of Mexico margin correlate spatially extremely well. Close examination of Yoakum-San Marcos

Arch system indicates that tectonic uplift “pulses” in regional arches of the foreland basin, triggered by Pacific plate subduction under North American, influenced the location of canyons along the Gulf of Mexico Margin. Despite not being fully tested, we propose three mechanisms (Figure 4) for the formation of canyons with a tectonic influence. i) The low uplift rate (LUR) model proposes fluvial erosion triggered by relative sea-level fall from localized tectonic uplift. The tectonic uplift must be slow and a preexisting river will cut through the uplift to readjust the stream gradient increase. Eventually the shelf will erode and the shelf edge will incise. ii) The shelf edge bulge model proposes that the outer shelf to shelf-edge gradient increases slowly from tectonic uplift creating sediment instability. The instability leads to slumping and incision of the shelf-edge and upper slope. Continuous landward uplift supports subaqueous canyon headward erosion into the shelf edge. iii) The high uplift rate (HUR) model bulges the paleo-shoreline creating a headland with a relatively narrow shelf along the uplifted region. This bulging of the shoreline directs longshore currents basinward to the shelf margin triggering dense sediment-laden shelf-water cascading over the shelf-edge incising it.

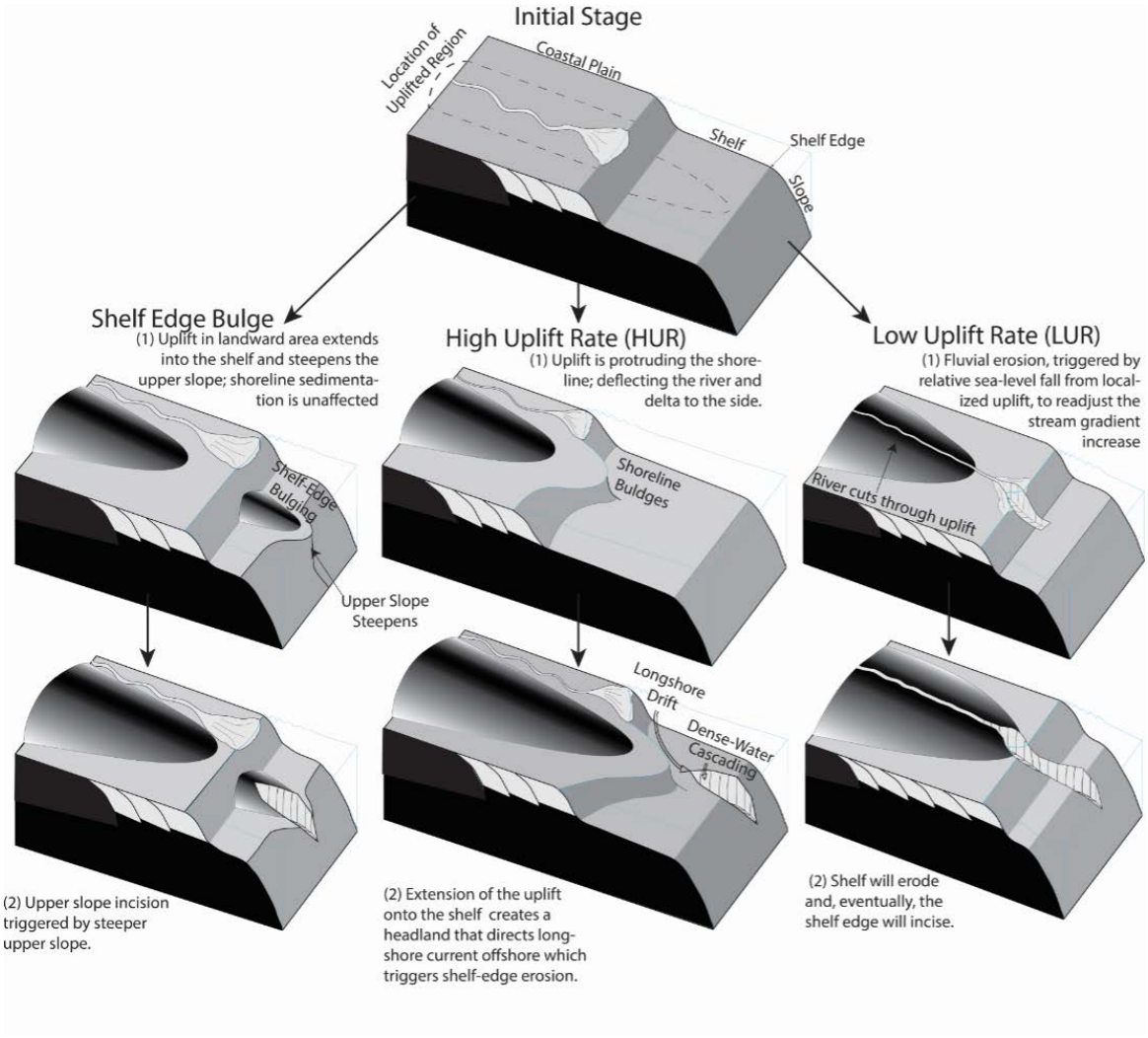

Figure 4: Block Diagrams depicting proposed mechanisms of tectonic uplift associated with submarine canyon formation.

Further work is necessary to confirm the formation mechanism that links canyon clustering and tectonic uplift. Mapping the delta depocenters and analyzing their interaction with the coeval canyon margins can bring additional information related to test any of the proposed mechanisms. Additionally, modeling and comparing the rates of uplift

with the canyons morphology, dimensions, timing can confirm the interaction between tectonics and incisions.

Chapter 3: Interaction of Paleogene Lower Wilcox High Frequency Sequences with the Yoakum Canyon

INTRODUCTION

Significant volumes of Wilcox aged sand bypassed the basin margin slope and deposited in the basin floor during the Paleogene (Zarra, 2007; McDonnel et al., 2008; Conwell, 2015; Figure 5). One of the main mechanisms that contributes sand deposition to the deepwater is shelf-dissecting canyons (Nardin et al., 1979). The Wilcox Group contains multiple large-scale incisions (up to 1000 m deep and 100 km long) which dissect the shelf (Chuber, 1982; McCoulough, 1986; Hutchinson 1987; Dingus and Galloway, 1990; Galloway et al., 1991). These incisions occur in clusters throughout the Gulf of Mexico margin, at times re-incising the same location (Figure 1). The canyon clustering, as described in Chapter 1, can be attributed, at a My or longer time scale, to a tectonic control linked to the subduction of the Pacific Plate increasing plate stresses resulting in foreland basin basement to form broad folds (arches). However, at shorter time scale (few 100 Ky) as shown by the high-frequency regressive-transgressive sequences in the Wilcox succession, the mechanism for shelf building and canyon infilling is most likely an interplay between the long-term tectonic deformation, the short-term sea level changes and sediment supply and proximity to sediment fairways. The evolution of each canyon is still debatable.

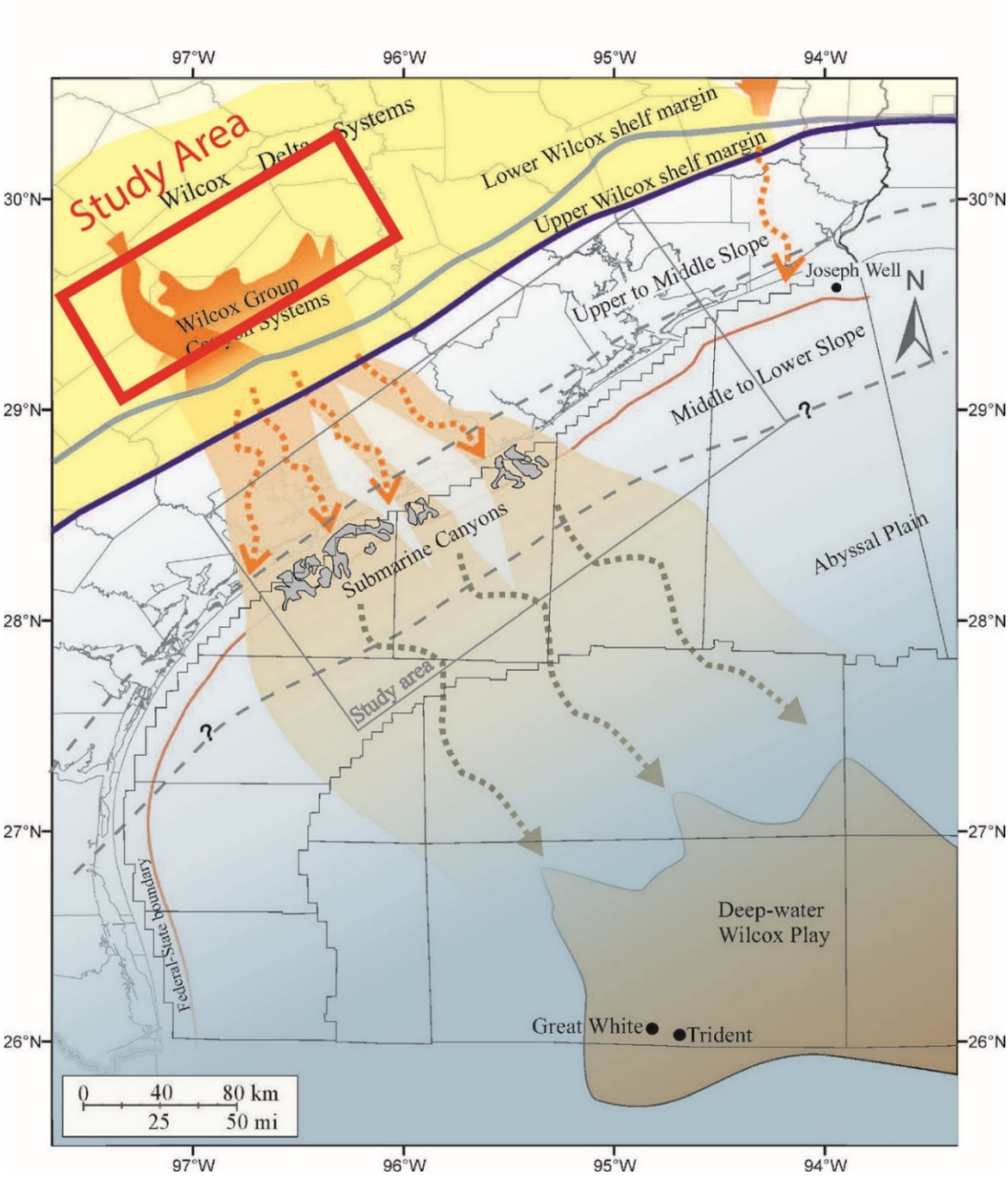

Figure 5: Link between San Marcos Arch region submarine canyons and the basin floor fans (modified from Zarra, 2007; McDonnell et al., 2008).

The study area for this project is southeast of Austin, Texas covering the area of Lavaca, DeWitt, Gonzales, Fayette, Austin, and Washington counties. Within the study area, the uplift of the San Marcos Arch impacted the stratigraphy and multiple Wilcox Group submarine canyons (Figure 6). The largest shelf-dissecting canyon in the study area is the Yoakum Canyon (Hoyt 1959, Chuber, 1982; Dingus and Galloway, 1990). Multiple mechanisms have been attributed to the formation of this canyon, but all mechanisms involve a relatively short (100Ky) lifespan for the canyon that represents one sea-level cycle (Hoyt, 1959; Dingus and Galloway, 1990). The elongate canyon morphology (100 km), over 1000 m deep incision within the shelf, and multiple erosive surfaces observed in a seismic strike oriented cross-section (Figure 7 and 8), suggest that Yoakum Canyon could have a more complex history than what has been previously described. The current literature model describes Yoakum Canyon as initiated during a 3rd order low sea level stand, retrogressively eroded during transgression and filled during the following highstand (Dingus and Galloway, 1990), i.e., during a time period of 1.5 My to 100Ky. The objectives of this study are to define higher frequency (4th order) sequences within the Lower Wilcox and to determine if higher frequency sequences within the Lower Wilcox have a relation (were coeval) with the Yoakum Canyon. The hypothesis to be tested is that Yoakum Canyon was initiated during the Lower Wilcox and that its development can be recognized by mapping the depositional character (isocores maps, sand thickness maps, log pattern variability) of the sequences adjacent to Yoakum Canyon.

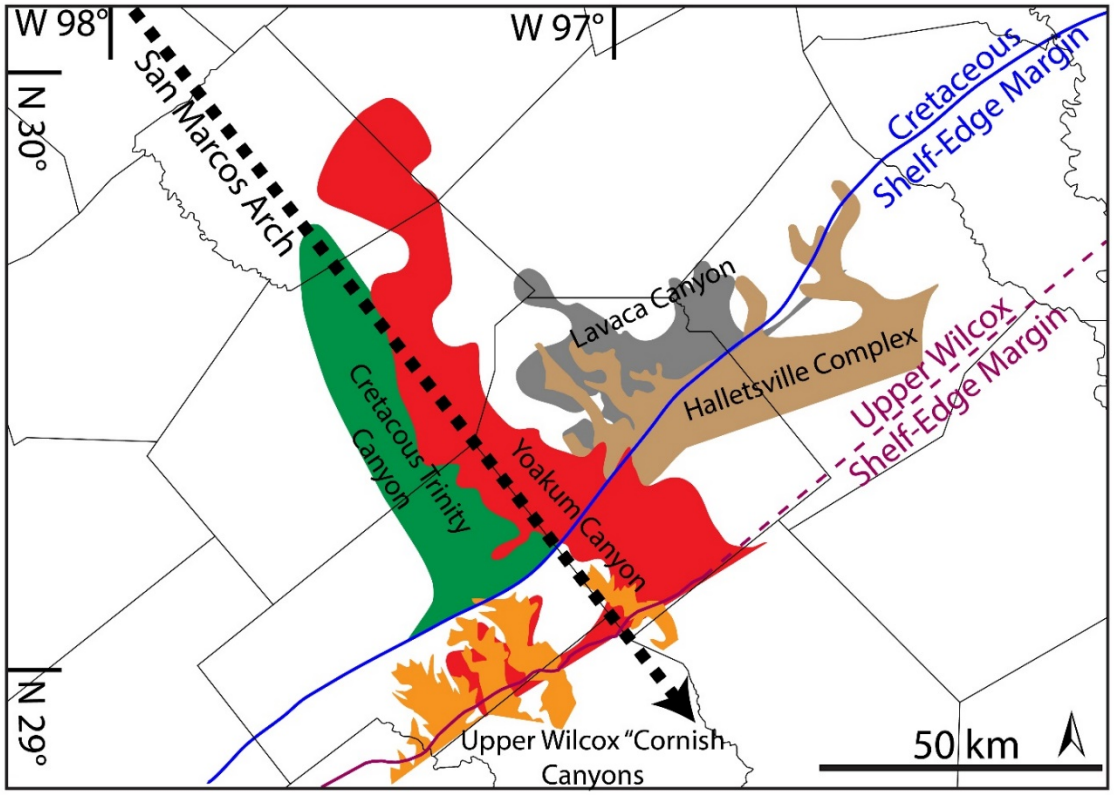

Figure 6: San Marcos Arch region and cluster of Cretaceous and Paleogene submarine canyons.

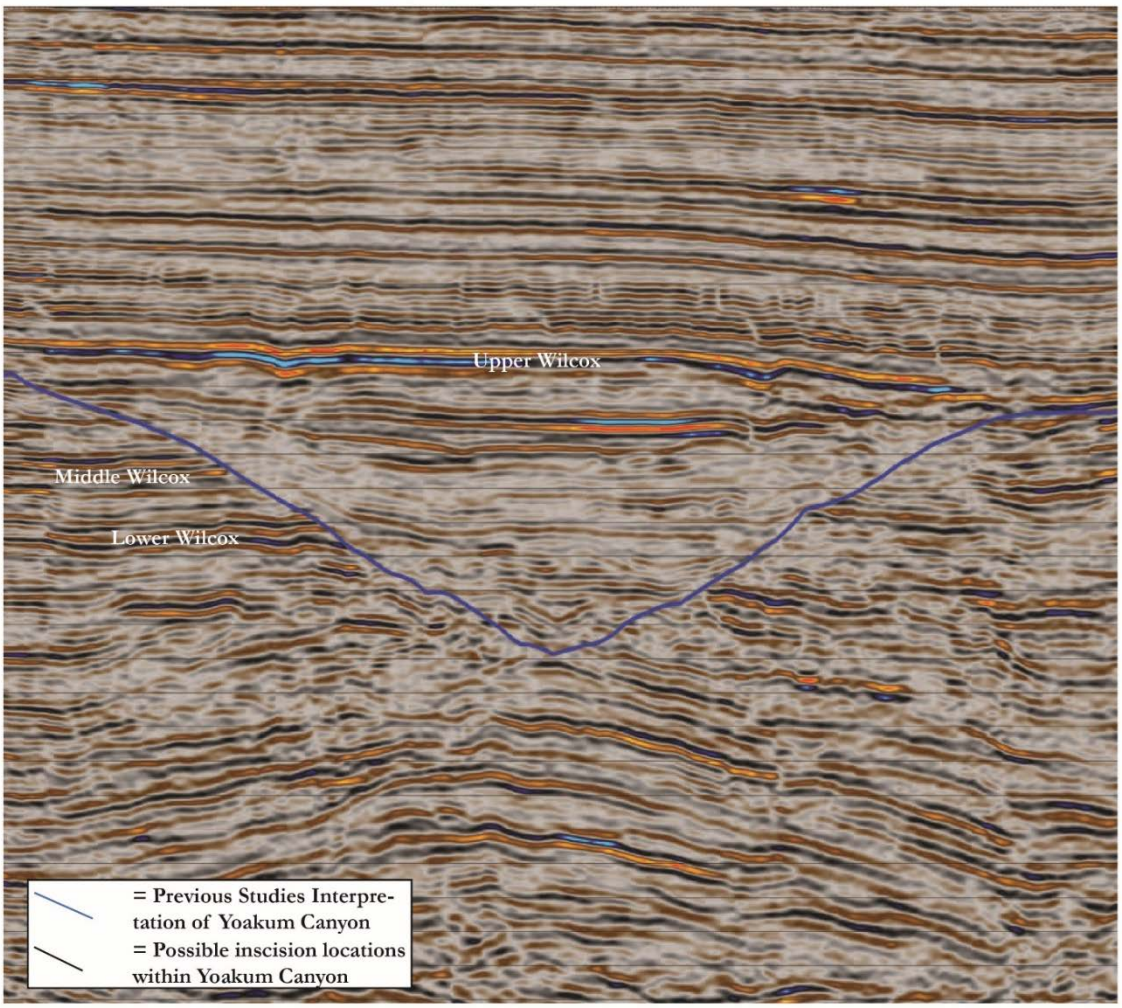

Figure 7: Seismic cross section of the Yoakum Canyon with the previous interpretation of a single cut and fill phase for the canyon evolution (Dingus and Galloway, 1990; Britt, 2006). No scale or orientation was provided by the HGS Bulletin (2006), but the canyon is likely on the scale of 10 to 15 km wide in this section and the orientation is likely along depositional strike.

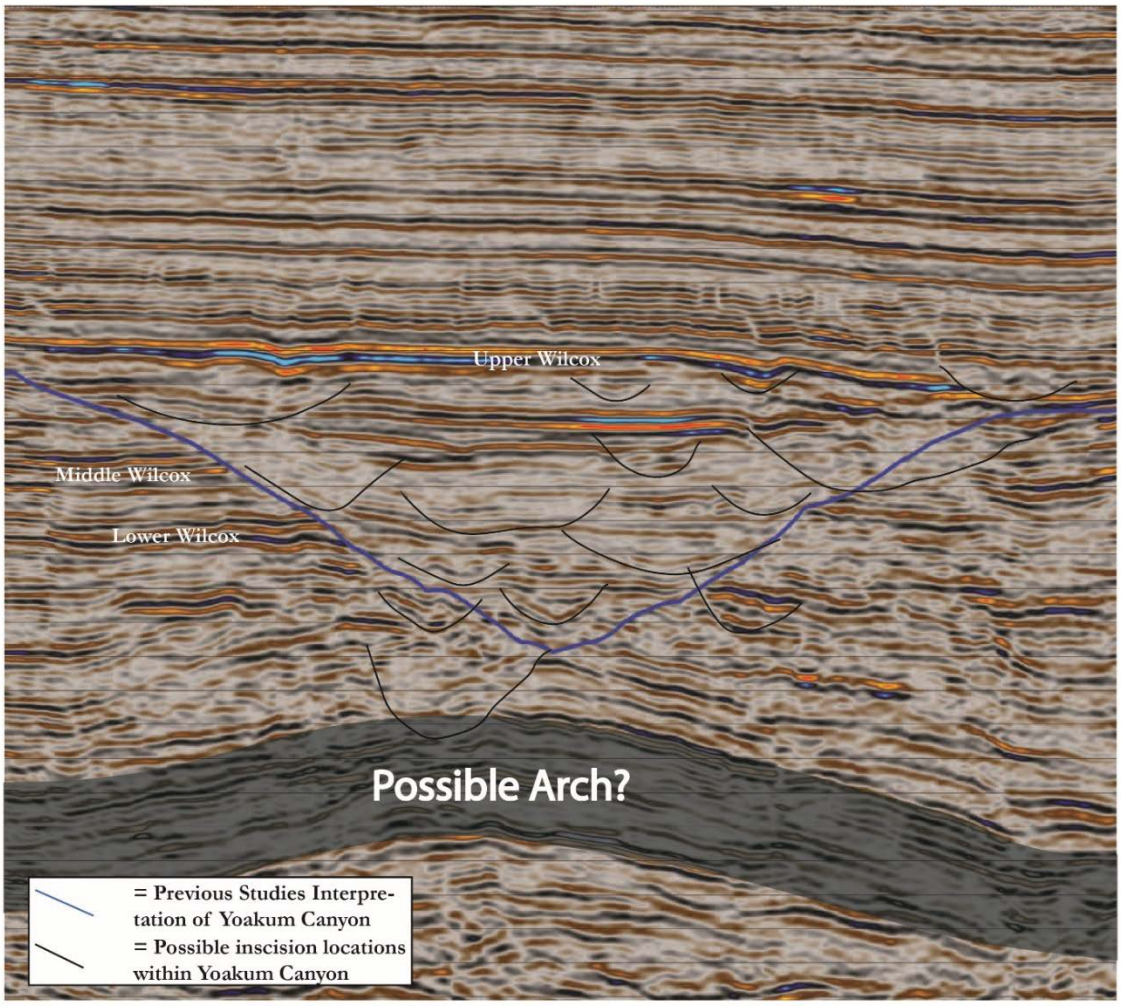

Figure 8: Seismic cross section of the Yoakum Canyon with the previous interpretation of a single cut and fill phase for the canyon evolution (Dingus and Galloway, 1990; Britt, 2006) and a new interpretation of multiple cut and fill events that we would like to argue in this study. No scale or orientation was provided by the HGS Bulletin (2006), but the canyon is likely on the scale of 10 to 15 km wide in this section and the orientation is likely along depositional strike.

BACKGROUND/GEOLOGIC SETTING

Wilcox:

The Wilcox Group records the first major Cenozoic influx of clastic sediments into the northwestern portion of the Gulf of Mexico (Fisher and McGowen 1967; Xue and Galloway 1995; Crabaugh and Elsik 2000). Clastic deposition dominated the Gulf of Mexico margin since Paleogene to present from northern Mexico to southeastern Louisiana (Fisher and McGowen 1967). Underlying the Wilcox Group is the early Paleocene Midway shale which consists primarily of hundreds of meters of marine mudstones (Galloway et al., 2000). The Wilcox Group consists of three to four major third-order clastic wedges ranging from late Paleocene to early Eocene, spanning over 11 million years (Crabaugh and Elsik 2000; Galloway et al., 2011; Galloway, 1989) (Figure 9). The clastic supply was sourced from the eastern flank of the Laramide Orogeny in the Central and Southern Rocky Mountains down to the Sierra Madre Oriental in northern Mexico (Winker and Edwards 1983; Galloway 2005, Mackey et al., 2012). The northern Gulf of Mexico had three main depocenters during Wilcox time, Mississippi, Houston, and Rio Grande embayments (Fisher and McGowen 1967, Galloway 1989; Figure 10). This study focuses on the western part of the Houston Embayment depocenter and its relationship with Yoakum Canyon.

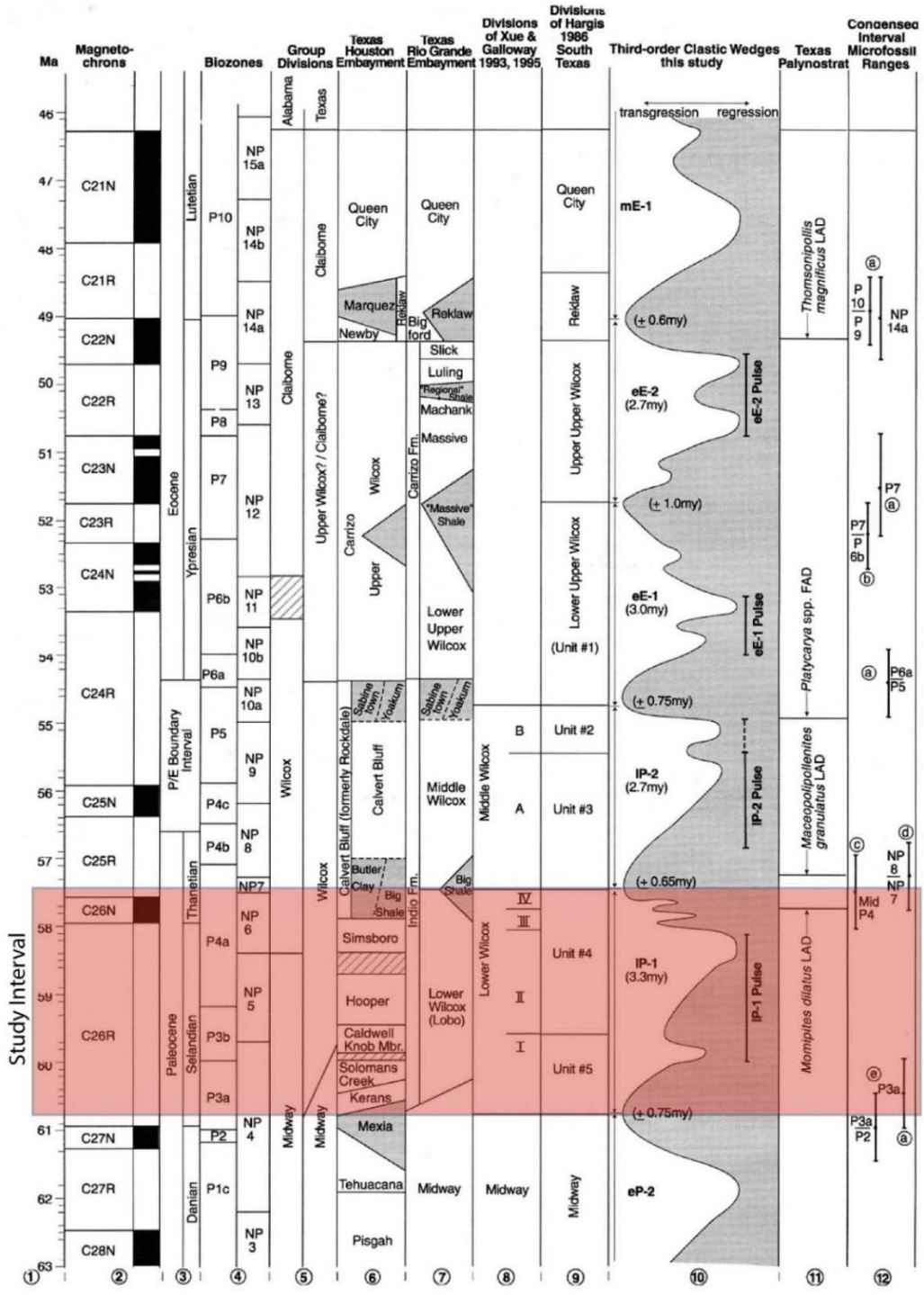

Figure 9: Compilations of different stratigraphic columns and associated clastic wedges for the study area (modified from Crabaugh and Elsik, 2000).

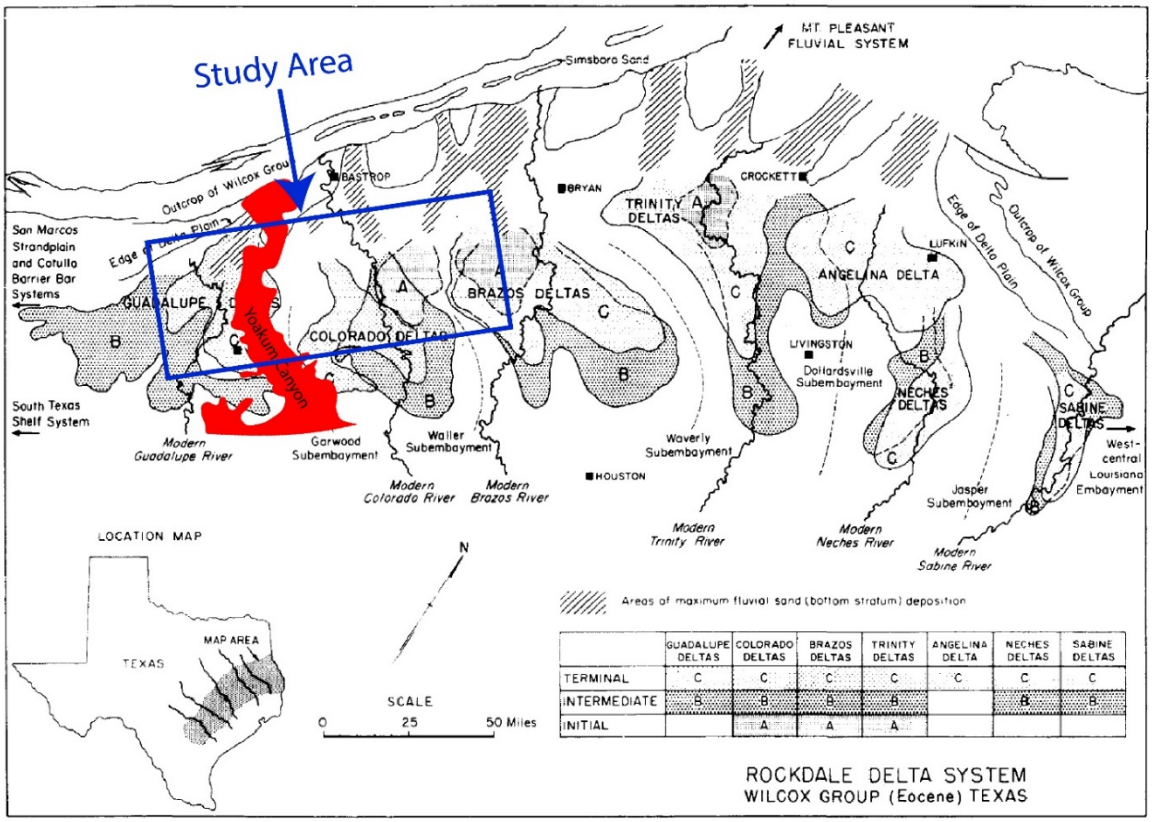

Figure 10: Lower Wilcox Deltas A, B, and C across the Houston embayment for the Rockdale Delta System with the location of the Yoakum Canyon (modified from Fisher and McGowen [1967]).

The early Paleocene Midway shale transgressed over terrestrial muds that prograded over the Cretaceous carbonate platform (Xue and Galloway 1995). Following the deposition of the Midway shale, the Wilcox Group clastic input began with the Lower Wilcox that had an overall regressive character. Galloway (1989) defined three third-order genetic sequences from oldest to youngest: Lower, Middle, and Upper Wilcox. Previously, Fisher and McGowen (1967) described three large delta systems, A, B, and C, within the Lower and Middle Wilcox. The large delta depocenters correspond to the Rockdale Delta

system in the Houston Embayment (Fisher and McGowen 1967). The Rockdale Delta system is one of the seven constituents of Fisher and McGowen's (1967) distinct depositional systems of the Lower Wilcox (Figure 11). The other six systems are the Penleton bay lagoon system, Mt. Pleasant fluvial system, San Marcos strand-plain-bay, Cotulla barrier-bar, Indio lagoon system, and South Texas shelf systems. During the formation of the Rockdale Delta system, seven different deltas (sediment depocenters) fed the region (Fisher and McGowen 1967). From north to south the Fisher and McGowen (1967) defined them as Sabine, Neches, Angelina, Trinity, Brazos, Colorado, and Guadalupe deltas (Figure 10). The thickest deltas occurred to the south with thickness reaching upwards of 1500 meters.

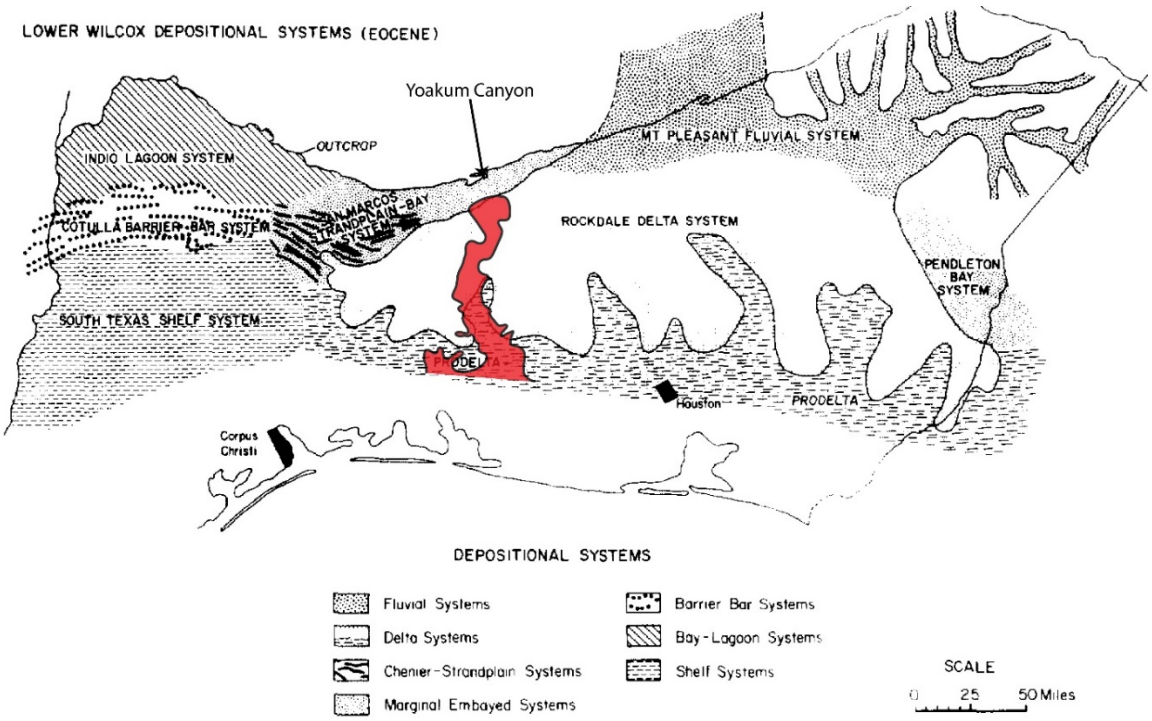

Figure 11: Depositional Environments of the Lower Wilcox in the Houston Embayment and relationship with the Yoakum Canyon (modified from Fisher and McGowen [1967]).

The two deltas in this projects study area, Colorado and Guadalupe (Figure 10) are in the proximity of Yoakum Canyon and consist of delta A, B, and C. Delta A represents the initial progradation (significant sediment input) of the Wilcox Group after the Midway shale. Delta A, between the Big Shale and Dull Shale, is predominantly prodelta mud in the study area. It is conformable with the underlying Midway shale. Delta B, between the Dull Shale and the top of Delta A, is the largest, thickest, and most progradational delta of the system, which comprises the majority of sand deposition (hundreds of meters thick) within the Lower Wilcox. The progradation of the Delta B unit over the unstable underlying muddy substrate lead to an extensive growth fault-system basinward of the Cretaceous

margin (Fisher and McGowen, 1967; Edwards 1981; Winker, 1983; Olariu and Ambrose, 2016). The youngest Delta C, between the Dull shale and Big shale, is muddier than the underlying Delta B and is the final deposit of the Lower Wilcox that represent an overall backstepping of the delta system (transgression). The most recent published work on the Lower Wilcox, west of the current study, focusses on establishing high-frequency stratigraphic sequences created by the repeated regression and transgression of the Deltas A and B, a discussion of the highly progradational character of the Lr Wilcox shelf-edge trajectory and the possible role of hyperthermal climate forcing during shelf building (Zhang et al.,2016). It has also been suggested that the early phase of Lr. Wilcox shelf building was coeval with the bulk of the recently discovered Wilcox turbidite succession in the ultra-deepwater GOM (Zarra, 2007; Carvajal et al., 2009).

The Middle Wilcox is defined by basal Big Shale and at the top by the Yoakum Shale (Xue and Galloway, 1995) and correspond in large part with Delta C of Fisher and McGowen, (1967). The deposition of Middle Wilcox incorporates the Paleocene/Eocene boundary (Crabaugh and Elsik 2000). Overall the Middle Wilcox is assumed to be a more transgressive and/or aggradational unit associated with a reduction in delivery of Laramide sediments and possibly linked with a eustatic rise in sea level (Liangqing Xue and Galloway 1995). The Middle Wilcox is a significantly muddy unit in the study area with only 20 to 40% sandstone..

The Eocene Upper Wilcox deposition shifts southward to form the Rosita Delta system in the Rio Grande Embayment (Fisher and McGowen 1967) to the southwest of the Yoakum Canyon location (Figure 11). This is the second major basinward shift of clastic

deposition within the Wilcox Group and is attributed to a resurgence in the Laramide orogeny (Crabaugh and Elsik 2000; Galloway et al. 2011; Winker and Edwards 1983). The Recklaw shale caps the top of the Upper Wilcox and marks the end of Wilcox Group deposition (Galloway et al. 2000).

Submarine Canyons:

There are multiple large-scale incisions within the Wilcox Group occurring on the Mexico, Texas, and Louisiana paleo-margins (Hutchinson 1984; Figure 12). Some of the incisions that have been described, from south to north, are: Ovejas, Nautla, Chicontepec, Bejuco-La Laja, Meyersville, Anna Barre, Jennie Bell, Hope, Yoakum, Halletsville, Smothers, Lavaca, Hardin, Tyler, St. Landry, Mississippi Embayment Axis, and Desoto (Hutchinson 1984; Devine and Wheeler 1989; Galloway et al. 1991; Dingus and Galloway 1990; Watkins 2014; Cornish 2013). The canyons tend to occur in clusters (closely spaced) and have similar shale dominated sedimentary fills. Overall the lengths are on the scale of 10's to 100 km, widths exceed 10 km, and depths are 100's to 1000 m (Hutchinson 1984; Chuber and Begeman 1982; Dingus and Galloway 1990; Galloway et al. 1991).

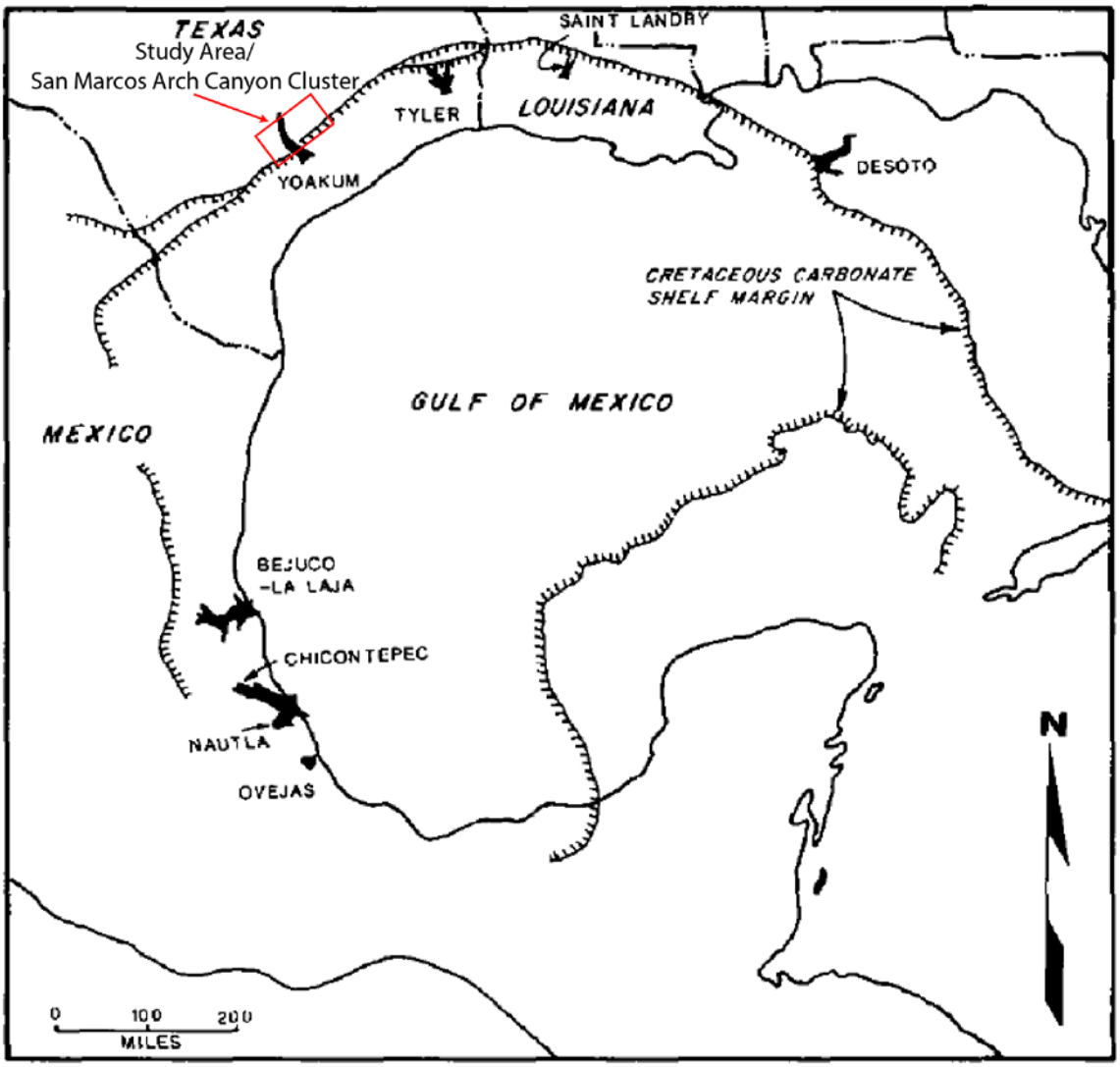

Figure 12: Location of Wilcox Group paleocanyons (Hutchinson, 1984).

In the study area of this project, there is also a cluster of large-scale incisions. From oldest to youngest, the incisions are the Halletsville Complex/Smothers channel, the Lavaca Canyon, the Yoakum Canyon, Jennie Bell, Hope, Meyersville, and Anna Barre

(Devine and Wheeler 1989; Dingus and Galloway 1990; Galloway, Dingus, and Paige 1991; F. G. Cornish 2011; Figure 2).

The two canyons within the Lower Wilcox stratigraphy, the Hallettsville Complex and Lavaca canyon, have similar morphologies and dimensions. The Hallettsville Complex is interpreted to have a strike-width of 142 km and a dip-length upwards of 40 km (Devine and Wheeler 1989). The incision depth is upwards of 120 meters and the feature has a broad, scalloped morphology. This incision cuts through Delta A of the Lower Wilcox into the underlying Midway shale. The incision fill is predominantly marine shales with a higher percentage of sandstone towards the proximal end. Nested above the Halletsville complex, the younger Lavaca Canyon incises through the Lower Wilcox shelf deposits and partially through the Halletsville complex. With a similar broad, scalloped morphology and dimensions (60 km wide and 40 km long) as the Halletsville complex, the Lavaca Canyon is filled with marine shales with a depths greater than 1000 m (Galloway et al. 1991). The Halletsville and Lavaca incisions cuts within the lower part of the Lower Wilcox down to the Midway shale at its greatest depths.

The largest canyon in the San Marcos Arch region, and the focus of this study, is the Yoakum Canyon. The canyon incision dissects for over 100 km across the shelf, has width exceeding 16 km, and depth larger than 1000 m (Dingus and Galloway 1990; Galloway et al. 1991). Due to the canyon incising further back across the shelf than the previous Lower Wilcox canyons, the Yoakum Canyon has an elongate morphology rather than “scalloped”. The canyon fill is also a shale lithology with “erratic” sandstone bodies. Dingus and Galloway (1990) previously interpreted the Yoakum Canyon to be active in

the late Middle Wilcox period, incising through the Middle and Lower Wilcox. The history of this canyon is widely debated and this study proposes a new, more complex evolution of the canyon during multiple high-frequency stratigraphic sequences than a “simple” cut and fill during one sea-level cycle.

The proposed mechanisms for canyon formation varied through time, with four main proposals: I) canyon excavation during lowstand sea level, where the shoreline is at or below the shelf edge allowing a river to cut a shelf valley (Vail 1987; Cornish 2013; Figure 13A). II) Shelf edge failure and headward erosion initially forming gullies. Canyon head sediment failure is enhanced during transgression when canyon excavation through the shelf and subsequent progradation fills the incision (Dingus and Galloway 1990; Galloway et al. 1991; Pratson and Coakley 1996). III) Isolation of the Gulf of Mexico allowing evaporitic drawdown (Pindell, 2002, 2003 Cornish, 2013) IV) Proposed in Chapter 1 of this study, tectonic uplifting enhances mechanisms (could include previously proposed mechanisms) and leads to shelf margin failure. Thus, a tectonic variable controls the location of canyon clusters within the Wilcox Group.

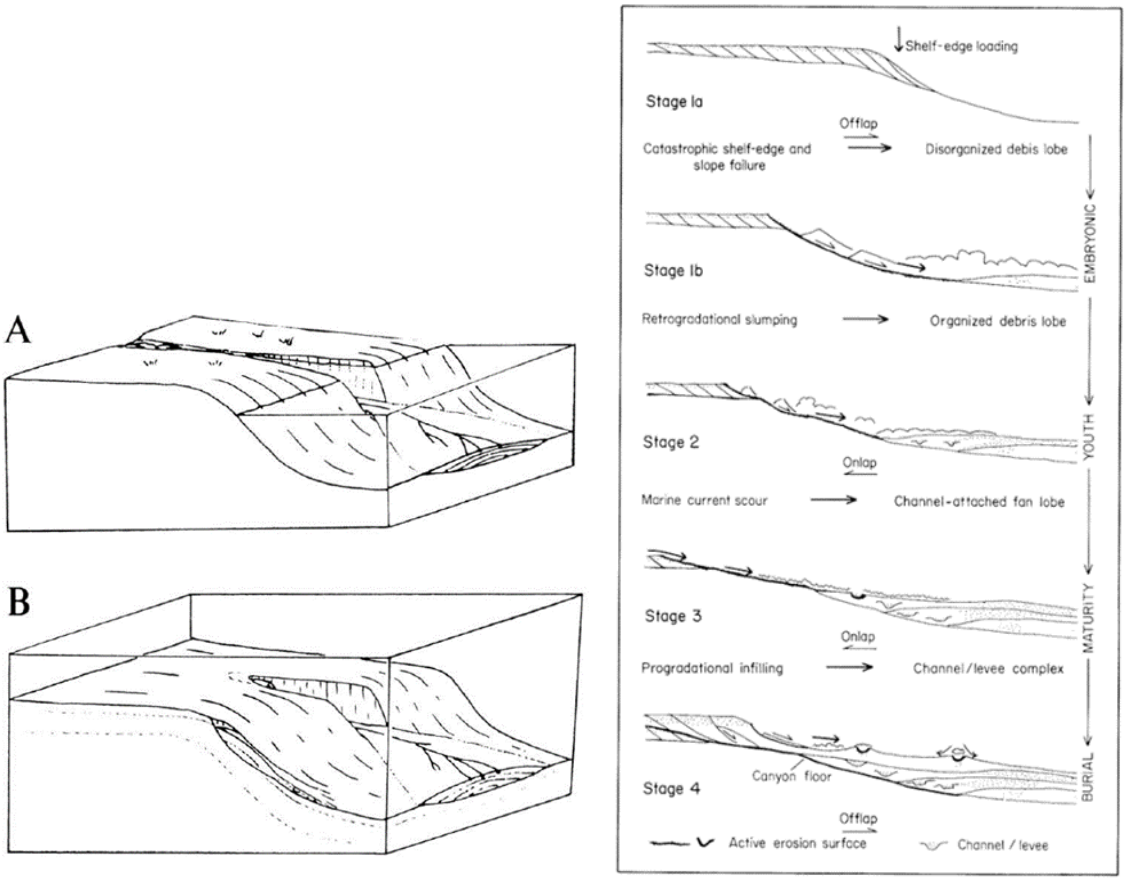

Figure 13: Schematic figures showing mechanisms for canyon cutting. A) Sea level lowing and fluvial incision during lowstand (Vail, 1987; Cornish, 2013). B and Stage 1 through 4) overloading of shelf edge initiating failure and transgressive headward erosion of the canyon within the shelf (Dingus and Galloway, 1990; Galloway et al., 1991).

A study by Harris and Whiteway (2011) identified 5,849 modern submarine canyons and divided them into three categories: Type 1 – shelf incising, river-associated, Type 2 – shelf incising, and Type 3 – blind, confined to the slope. The majority of shelf incising canyons are not river associated, Type2 (1671 canyons or 91.16%), whereas a significantly less percentage (153 canyons, or 8.84%) are associated with rivers (Harris

and Whiteway 2011). The large percentage of non-river associated shelf incising canyons suggests that submarine canyons do not necessarily need a direct river association for growth. Other processes can lead to the excavation of such large submarine features.

METHODS AND DATASET

Dataset

The dataset is entirely subsurface, with the emphasis of the project focusing on well log correlations. A number of 765 well logs were selected for correlations, primarily in the form of raster (TIFF format) image files. In order to create more detailed maps, such as net sandstone thickness, certain raster image files were selected to be digitized and converted to ”LAS” format files. For the maps, a number of 222 LAS files are selected in areas of interest and dispersed throughout the study region. The study area encompassed approximately 8,400 km² over a depositional strike length of 160 km (Figure 14). The average well spacing between .las files is 2 km with a maximum distance between wells of 12 km and a minimum of 700 m.

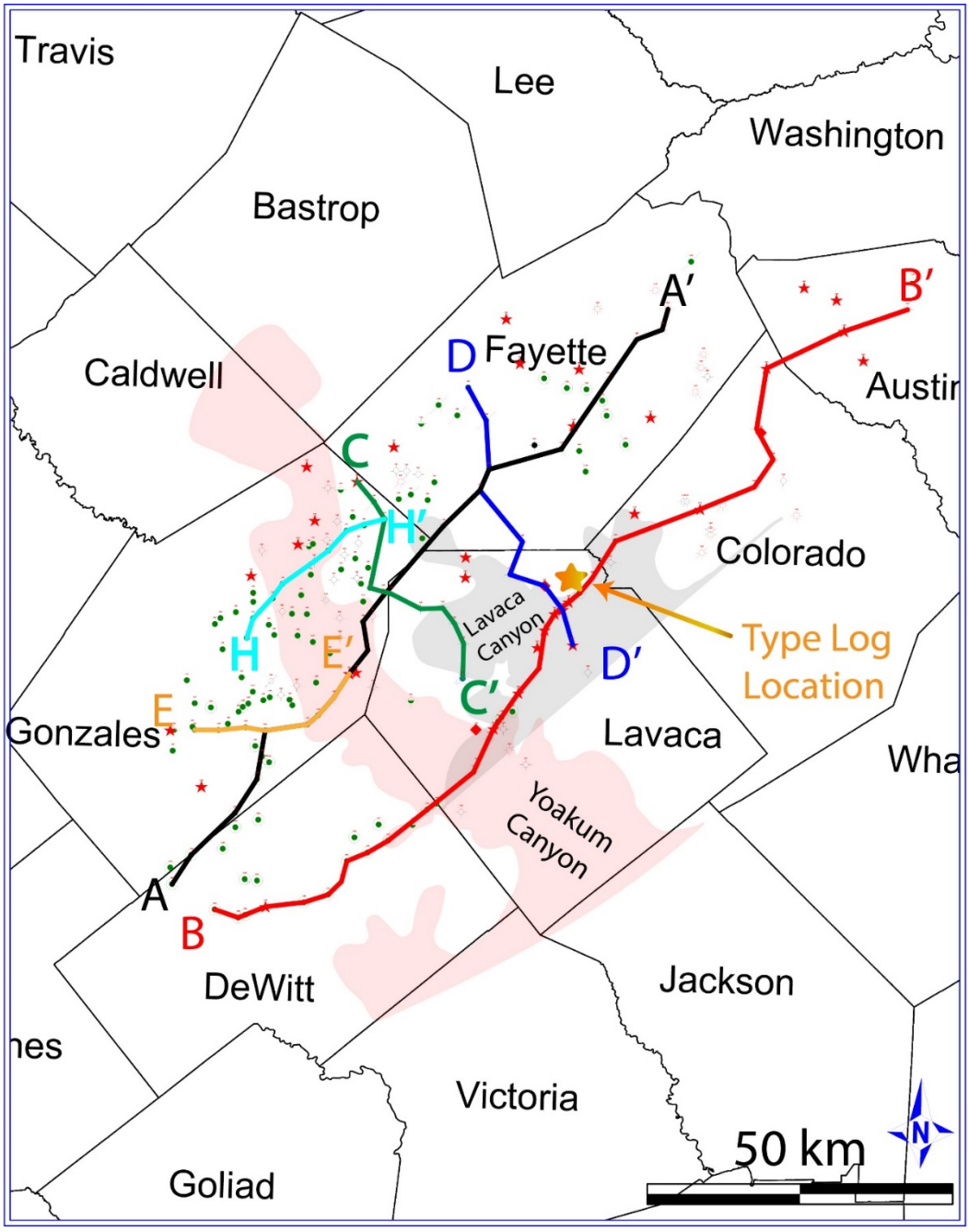

Figure 14: Study Region and location of cross sections and type log.

A previous study by Bebout (1982) provided a general framework for the Wilcox Group stratigraphy. Regional cross-sections that depicted the base of the Wilcox Group,

the top of the Lower Wilcox, the top of the Middle Wilcox, and the top of the Wilcox Group in 42 wells from dip-oriented and strike-oriented cross-sections (Bebout, 1982) that cover this study were used to guide the initial stratigraphy picks. The top of the Wilcox Group is the best surface over the study region to flatten the underlying stratigraphy on, as it is the only surface that is not affected by large deformations and shelf and shelf-edge incisions in the region.

The incisions within the Lower and Middle Wilcox were defined by previous studies (Chuber and Begeman 1982; Dingus and Galloway 1990; Devine and Wheeler 1989). Chuber and Begeman (1982) defined the Lavaca Canyon and Halletsville Complex in cross sections through the study area. Dingus and Galloway (1990) defined the Yoakum Canyon through strike-oriented cross sections. The location of the Yoakum Canyon by this study provided a guideline, but this study will suggest a more complex evolution of the system and thus a more dynamic location of the margin for the Yoakum Canyon system.

This study mapped high-frequency sequences within the Lower Wilcox (primarily Delta B and C from Fisher and McGowen [1967]). Each sequence is a regressive-transgressive cycle bounded by flooding surfaces. The thickness of each of these sequences should be a few 10s of meters, representing a reasonable height of regressive shelf deltas plus the thickness of subsequent retrogressive estuaries or barrier/lagoon systems. Landward transgressions >50km in extent were documented as common by Zhang et al. (2016). Sequence 1, being the oldest, through Sequence 12, the youngest, defines the 12 sequences in the region (Figure 15). Flooding surfaces are regionally correlative high Gamma Ray log or Spontaneous Potential values. The high Gamma Ray value and high

Spontaneous Potential value denotes deposition of finer sediments during a flooding event (delineating the flooding surface) and occurs typically above a fining upwards pattern (Galloway 1989). While there are many high Gamma Ray and Spontaneous Potential value intervals in the Lower Wilcox, the 13 flooding surfaces are the most regionally correlative and mark transitions from fining upwards to coarsening upwards in the majority of wells. In addition to the flooding surfaces, each sequence also has a maximum regressive surface. This surface is the transition from coarsening upwards to fining upwards, and typically has very low (lowest) Gamma Ray and/or Spontaneous Potential value.

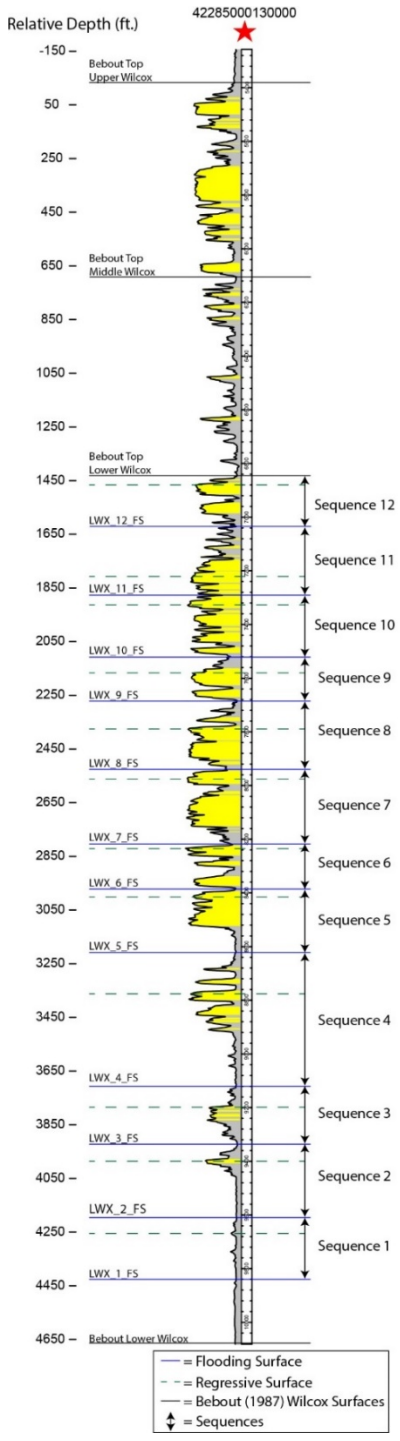

Figure 15: Type log defining sequences, flooding surfaces, regressive surfaces, and Bebout (1987) defined Wilcox surfaces.

Mapping

The different thematic (sequence thickness, sand thickness, net-to-gross) maps are generated from the software Petra. Only digital well logs were used to generate the maps, and the two log curve types are SP (spontaneous potential) and GR (gamma ray). Due to the availability of wells logs, the majority of curves used in the study are SP. Using the Petra software, net sand thickness, gross thickness, and net to gross ratios were computed for each sequence, regressive phase (between underlying flooding surface and maximum regressive surface), and transgressive phase (between maximum regressive surface and overlying flooding surface). Three different sequence properties, gross thickness, net sand thickness, and net to gross ratio, were computed using a cutoff of -40 MV for the SP logs, and 75 GAPI for the GR logs. These cutoffs define the lithology, values less than the cutoff are interpreted to be sandstone, and greater than the cutoff is shale. The gross sequence thickness is the computed thickness between two bounding surfaces. The net sand thickness is the computed thickness of sandstone (values below the cutoff) within two bounding surfaces. The net to gross ratio is the ratio between sandstone thickness and total thickness within two bounding surfaces. Each of these sequence properties were computed for each total sequence, regressive phase, and transgressive phase. In result, 9 maps were generated for each sequence. Using the computed sequence properties, isopach maps were generated by the Petra software. With 9 map types for 12 sequences, there are a total of 108 maps (Figures 18, 19, 20, 22, 24, 26, 27, 29, 30, 32, 33, and 34).

Cross Sections

Cross sections within the study area illustrate main sandstone-mudstone distribution trends seen on the different maps. Some of the cross-section orientations cut across canyon margins to show lithological trends and well log patterns with relation to the canyon margins, regional strike-oriented sections, and regional dip-oriented sections (Figure 16 and 17). For each cross-section, distance between well logs is the true distance between the wells. Sandstone/mudstone cutoffs on each log (to color yellow vs. grey) are the same as previously discussed. Yellow shading denotes a sandier lithology, whereas grey denotes a muddier lithology.

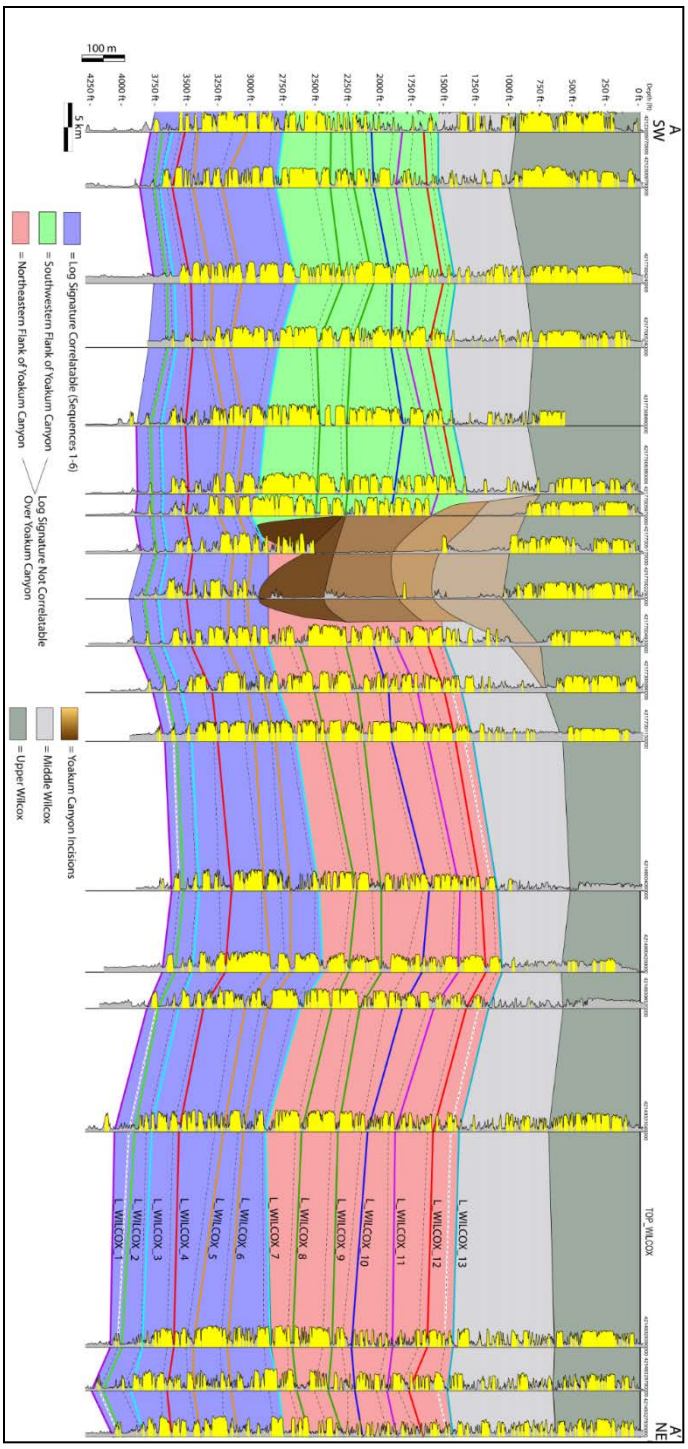

Figure 16: Regional cross section A-A' dissecting the proximal portion of the Yoakum Canyon.

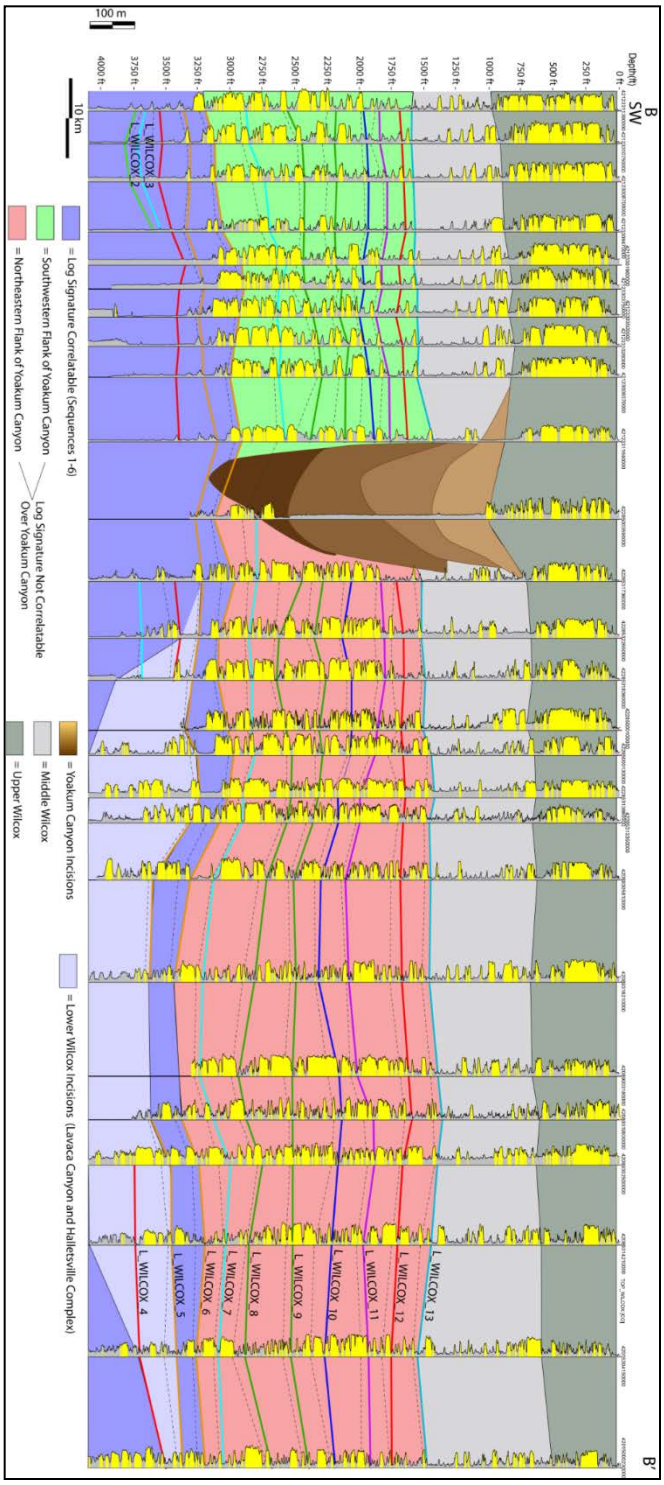

Figure 17: Regional cross section B-B' dissecting the basinward portion of the Yoakum Canyon.

RESULTS

Regional Cross Sections

Two strike-oriented cross-sections, A-A' and B-B', span from southwest to northeast of the Yoakum Canyon (Figure 16 and 17). The cross sections are both approximately 150 km in length, and the well spacing ranges from 3 to 12 km. A-A' cross-section is located in the updip, proximal end and B-B' cross-section is located in the downdip, distal end of the Yoakum canyon. Both of these sections are located updip from the highly growth-faulted region basinward of the Cretaceous margin (Devine and Wheeler 1989; Olariu and Ambrose 2016). Both of the strike-oriented cross sections include wells with the Yoakum Canyon fill.

The proximal A-A' cross-section shows a section that is largely unaffected by the Lower Wilcox canyon systems, Lavaca Canyon and the Halletsville complex. To the southwest of the Yoakum Canyon the overall Lower Wilcox section (Sequences 1 to 12) is approximately 600 meters thick whereas in the northeastern region of the study area this expands to approximately 800 meters thick. Sequence log signatures are similar on both sides of the Yoakum Canyon for sequences 1 through 6 (Blue region on Figure 16), but the log signatures become sandier in the overlying sequences 7 to 12 to the northeast of the canyon (Green and red colors on Figures 16). Note also that the sequences above sequence 6 are much sandier towards the canyon margin than further away from the margin (Figure 16).

The distal B-B' cross section shows a more complex region, with the Halletsville complex and Lavaca canyon incising the oldest Lower Wilcox sequences (Light Blue on Figure 17). Northeast of the Yoakum canyon, these incisions are especially seen in the lowest sequences 1-4, where there are greater gross thicknesses and shaley log signatures. The difference in thickness between the southwest and northeast is more apparent in the distal cross-section where there is a much thicker section but with thinner sandstone units occurring away from the canyon margin to the northeast (colored red on Figure 17). This thickening of the Lower Wilcox section in this region is likely due to the multiple incisions (Halletsville, Lavaca) on the outer shelf to upper slope within the lower sequences. The log signatures throughout all of the Lower Wilcox is largely different within the Yoakum Canyon. While Sequence 5 is somewhat similar, the older sequences 1 to 4 are not relatable due to the Halletsville complex and Lavaca Canyon, and the younger sequences, 6 through 12, are sandier to the northeast with distinct log patterns.

Lower Wilcox Sequence Maps

Sequence thickness, sandstone thickness and net-to-gross maps for the 12 sequences are briefly described below. Emphasize will be given to the depocenter locations relative to the canyons and also as these evolve/ switch from one sequence to next.

Sequence 1

The first interpreted sequence in the study area within the Lower Wilcox, Sequence 1, is dominated by mudstone with largely a prodelta or deepwater slope log facies in the

study area. Sequence 1, between L_WILCOX_1 and L_WILCOX_2 surfaces (Figure 16), has the most constant thickness (about 30 m) over the study region in comparison to the other sequences. The gross thickness and net sandstone thickness maps show a relatively constant thickness (30 m) for the whole sequence and for the regressive phase (Figure 18). The transgressive phase has a slight thickening northeast of the Lavaca Canyon, which is over the eastern portion of the older Halletsville complex.

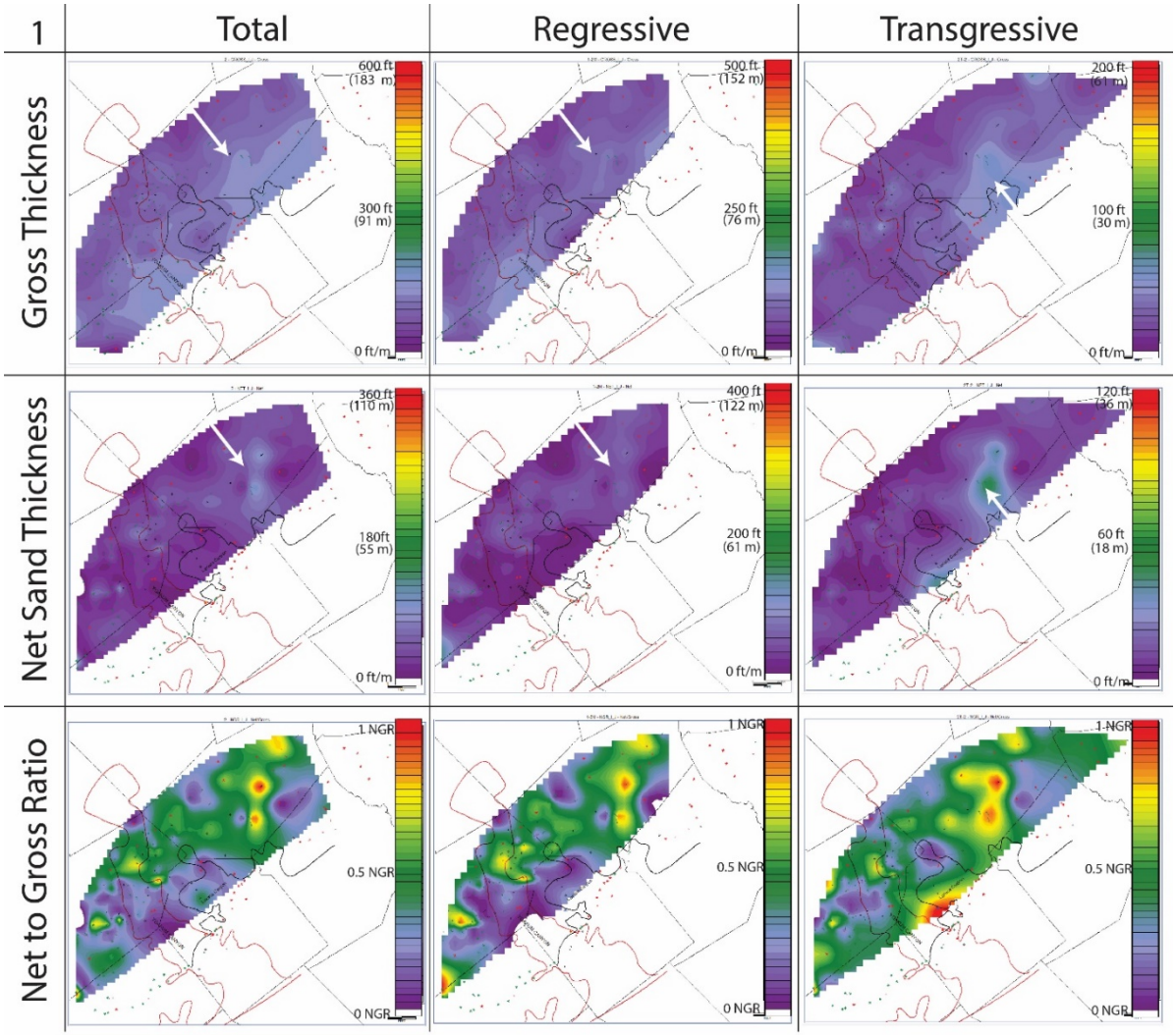

Figure 18: Isopach maps for the total sequence, regressive phase, and transgressive phase for Sequence 1. Isopach maps included are gross thickness, net sand thickness, and net to gross ratio. White arrows indicate location of trends for the sequence.

The net-to-gross ratio maps for the total sequence and the regressive phase illustrates that the proximal portion of the study area has a higher net-to-gross sandstone ratio than the distal portion. This shows that the delta is contributing little sand sediment

to the outer shelf during this early sequence. The transgressive phase of sequence 1 also has a higher net-to-gross ratio in the northeastern portion of the Halletsville complex as seen by the net sand thickness and gross thickness maps.

The regional cross section A-A', illustrates the relative constant thickness of Sequence 1 across the study area (Figure 16). The cross section also illustrates the relative muddy signature of the log facies that dominate Sequence 1 and suggest a prodelta to upper-slope depositional environment. The Sequence 1 is likely the distal end of the deltaic unit that will eventually prograde into the study area and onto the outer shelf/shelf edge to deliver sediment to deeper water.

Sequence 2

Sequence 2, also has a relatively constant thickness (50 m) over the study area. The total and regressive phase gross thickness maps (Figure 19) suggest a slight thickening to the northeastern portion of the study area. Additionally, the net sand thickness map for the total and regressive phase suggests a slight thickening to the northern portion of the study region. The transgressive phase has a thickening to the northern portion of the study region, but slightly south of where the total and regressive phase thicken. The net-to-gross ratio for the total sequence, regressive phase, and transgressive phase all have higher ratio to the northern portion of the study region. This higher net-to-gross ratio suggests a sediment source and a depocenter to the north.

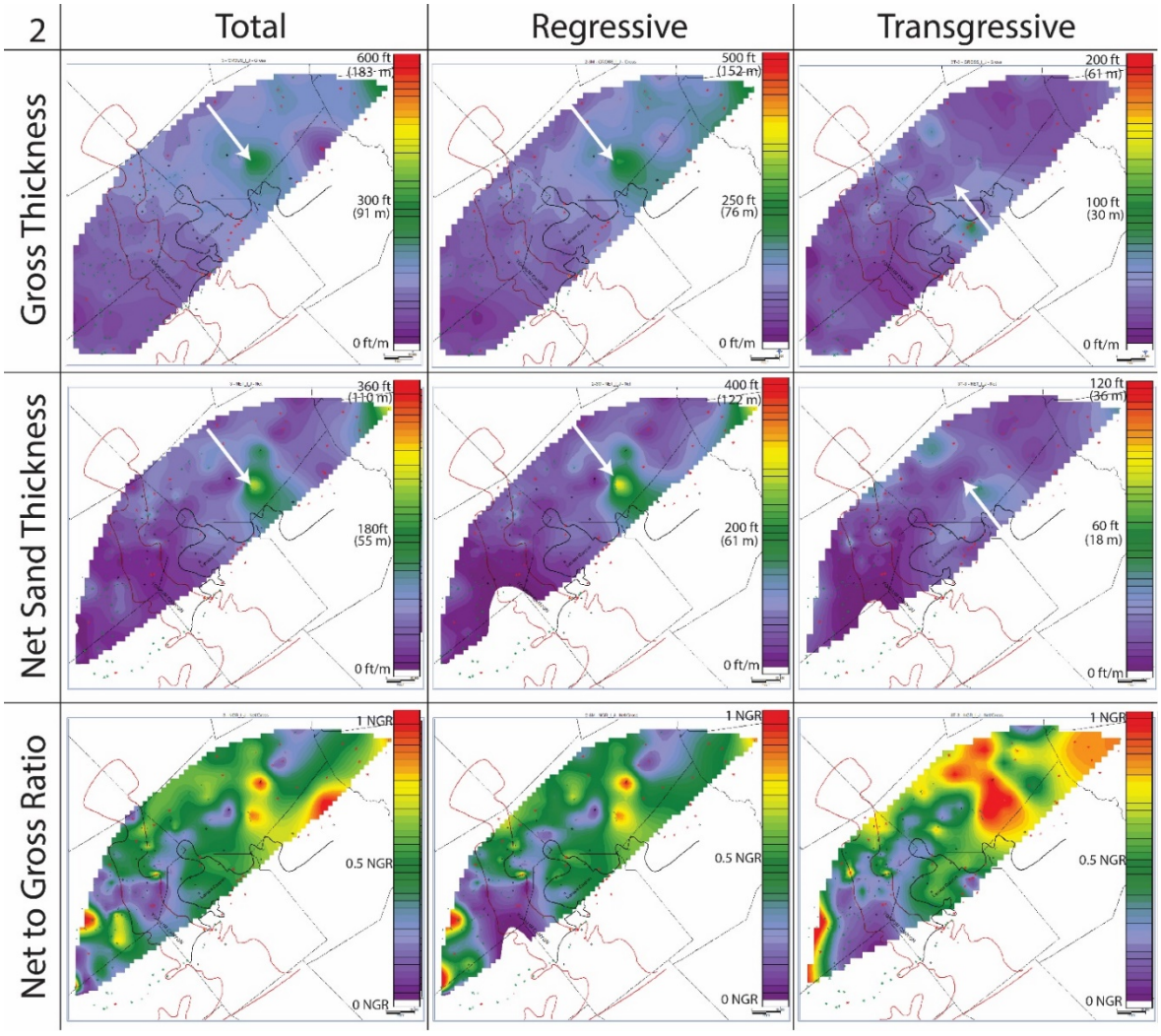

Figure 19: Isopach maps for the total sequence, regressive phase, and transgressive phase for Sequence 2. Isopach maps included are gross thickness, net sand thickness, and net to gross ratio. White arrows indicate location of trends for the sequence.

The cross-section A-A' shows the slight thickening to the north (Figure 16). The log signature to the south is mainly muddy with upward coarsening log facies, suggesting a prodelta to delta front depositional environment. The northern region of the study area is

also composed of primarily muddy deposits but coarsens up into a sandier facies (likely delta front) than the southern portion of the study area.

Sequence 3

Sequence 3, between L_WILCOX_3 and L_WILCOX_4 surfaces (Figure 16), is the first sequence to clearly be affected by incisions. The gross thickness of the whole sequence (~50 m) and the regressive phase deposits thickens over the Lavaca Canyon and Halletsville complex region (Figure 20). In contrast, the net sand thickness thins into the area where the gross thickness expands for both the whole sequence and the regressive phase. In addition to thinning basinward toward the Lavaca Canyon and Halletsville complex region, the net sand for both the total sequence and regressive phase thickens southeastward towards the margin of the incised region. The thickening towards the incision, thinning of sandstone lithology within the incised region, and expansion of gross thickness within the incised region suggests that incision within the shelf was active (canyon was open) during this time period of Sequence 3 (delta) deposition.

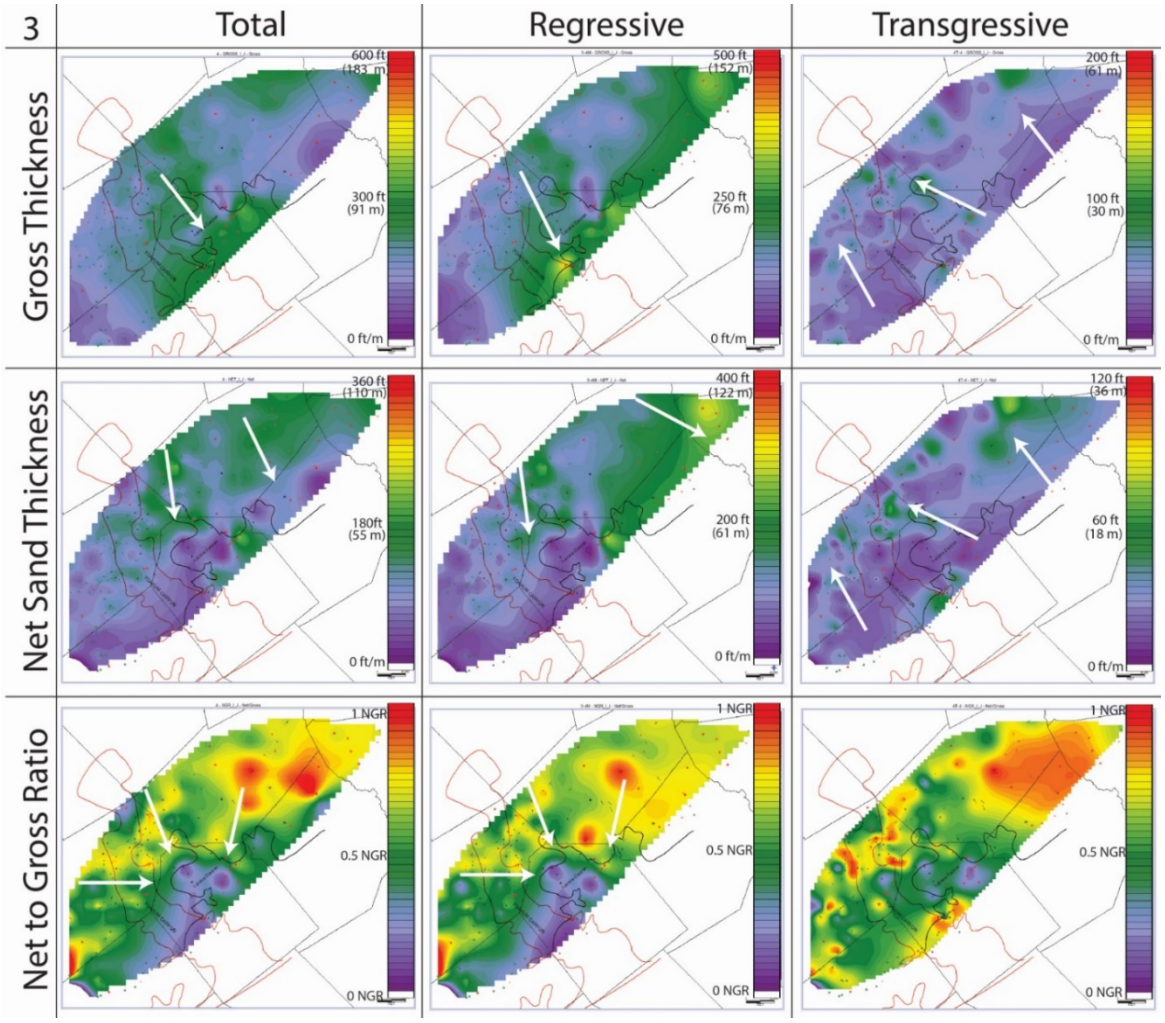

Figure 20: Isopach maps for the total sequence, regressive phase, and transgressive phase for Sequence 3. Isopach maps included are gross thickness, net sand thickness, and net to gross ratio. White arrows indicate location of trends for the sequence.

The transgressive phase also shows that gross thickness is slightly thicker over the incised region (Figure 20). In contrast to the total sequence and regressive phase, the transgressive phase has a thickening of the net sandstone towards the southern basinward

region incision. This thickening of the sandstone could be due to sediment reworking and partial filling of the canyon (incised area) during transgression.

The net-to-gross ratio for the total sequence, regressive phase, and transgressive phase suggests that the main depocenter is concentrated in the northern section of the study area (Figure 20). The sandstone dominates in the northern section to the head (northwest) of the incised Lavaca Canyon and Halletsville complex region. This trend follows the gross thickness and net sand thickness trends.

The cross-section A-A' shows an increase in sandstone thickness along strike to the northern region like the trend seen from the mapping (Figure 16). A dip oriented cross-section dissecting the inner shelf to the incised region, C-C' shows a thickening of the sandstone towards the incised regions margin (Figure 21). The increase in sandstone thickness abruptly thins into the incised region where mud deposition dominates. This abrupt change is over too short of a distance, about 1 km, for the lateral change to be associated with a delta front and prodelta progradation and it is likely that sandstone layers of the Sequence 3 were truncated.

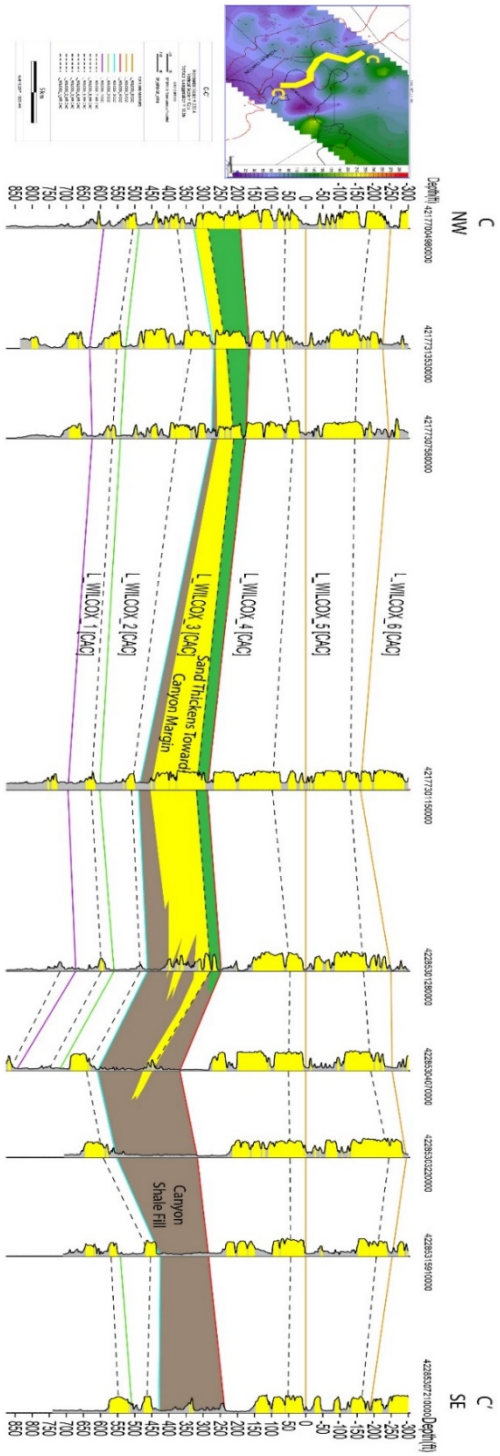

Figure 21: Cross-section C-C’ depicting sand thickening trend towards the Halletsville Complex.

Sequence 4

Sequence 4, between L_WILCOX_4 and L_WILCOX_5 surfaces (Figure 16), is similar to the prior sequence, sequence 3, with incision activity likely affecting the basinward region. The gross thickness for the total sequence and regressive phase shows a shift, about 50 km, southward from the previous sequence (Figure 22). The net sandstone thickness suggests the area of incision has slightly widening and moved northwards from the previous sequence (Figure 22). The net sandstone thickens, similar to sequence 3, towards the incised region margin, and then the area of incision is shale filled with little sand. During the transgressive phase, the gross thickness and net sand thickness denotes the deposition is relatively constant with a slight shift towards the southwest (Figure 22).

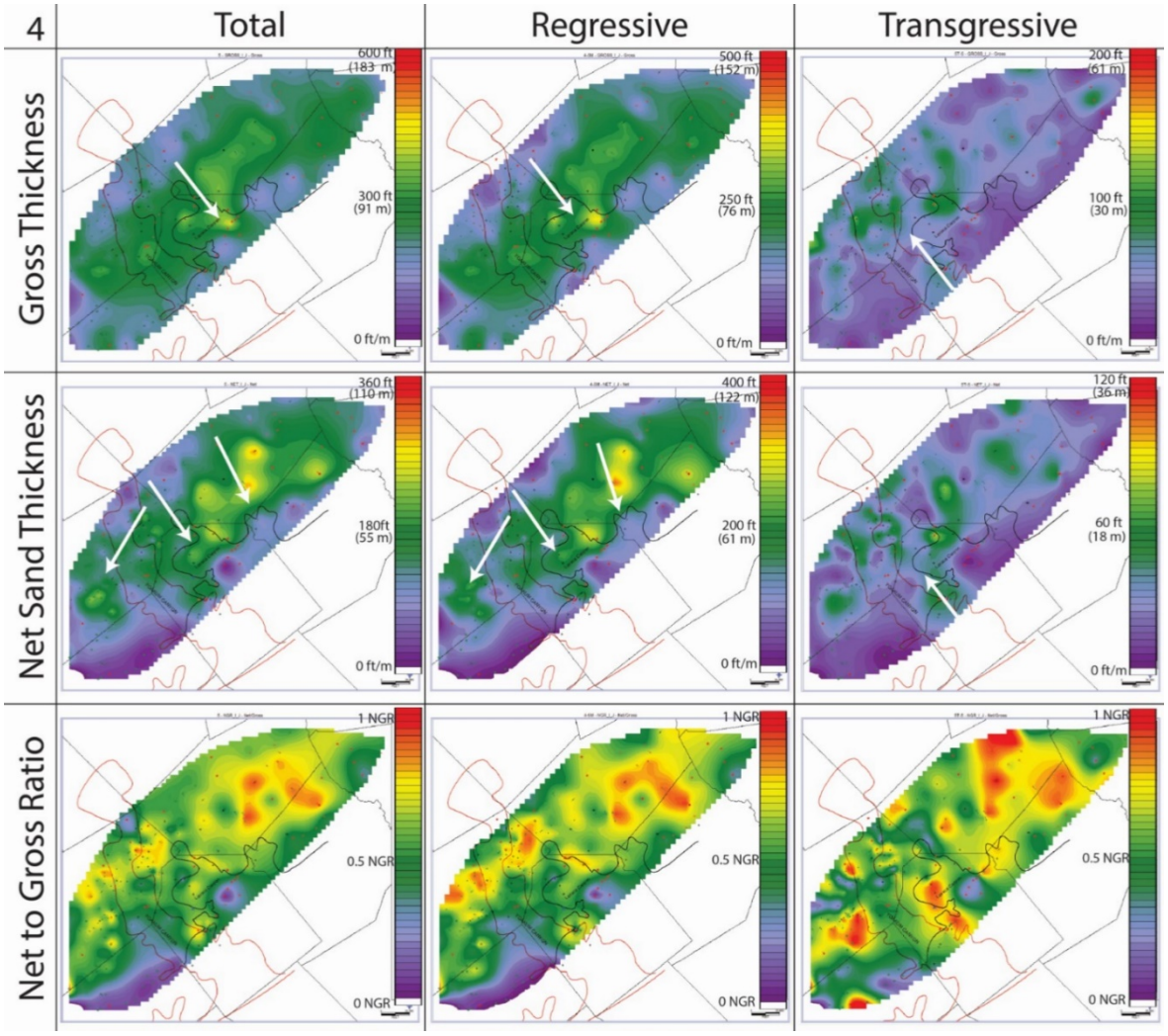

Figure 22: Isopach maps for the total sequence, regressive phase, and transgressive phase for Sequence 4. Isopach maps included are gross thickness, net sand thickness, and net to gross ratio. White arrows indicate location of trends for the sequence.

The net-to-gross ratio confirms the net sandstone thickness trends for the total sequence and regressive phase interaction with the area of incision (Figure 22). Towards the margin of the incised region, the sequence becomes more sand rich and an abrupt shift

to a muddy matrix occurs within the incised region. Additionally, the net-to-gross ratio maps for the whole sequence and the regressive phase suggest a progradation of the system in comparison to the previous Sequence 3.

The cross-section D-D' is a dip-oriented section showing the relation of the sequence with the margin of the incised region (Figure 23). From the distal northeastern portion of the cross section to the basinward southwestern side, the log signature facies change from thin sandstone with fining upward log patterns suggesting non-marine deposition to upward coarsening log pattern indicative of marine deltaic environments, to mud dominated log pattern of distal shelf (or slope) depositional systems. The shift from blocky, thick sandstone to mud dominated deposits is an abrupt change in log facies (Figure 23).

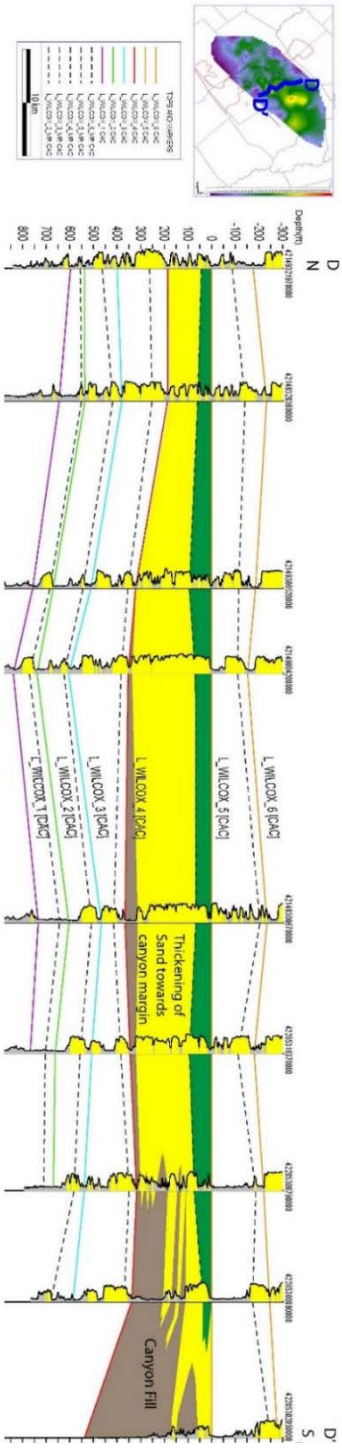

Figure 23: Cross-section D-D’ depicting sand thickening trend towards the Lavaca Canyon.

Sequence 5

Sequence 5, between L_WILCOX_5 and L_WILCOX_6 surfaces (Figure 16), differs from the previous two sequences 3 and 4 by having no clear incision in its deposits. The gross thickness of the total sequence (~ 75m thick) and regressive phase denotes a basinward shift of thickening suggesting an overall progradation of the depocenter (Figure 24). From sequence 4 to sequence 5, the system progrades approximately 20 km (distance between thickest portion of each sequences depocenters). The gross thickness maps also suggest a relatively constant deposition over the study area. There is a slight thickening of both the gross thickness and the net sandstone towards the northern and southern flanks of the study area. The transgressive unit also suggests a relatively constant thickness over the study region through the gross thickness and net sand thickness, but has a slightly thicker region on the northern flank of the Yoakum Canyon.

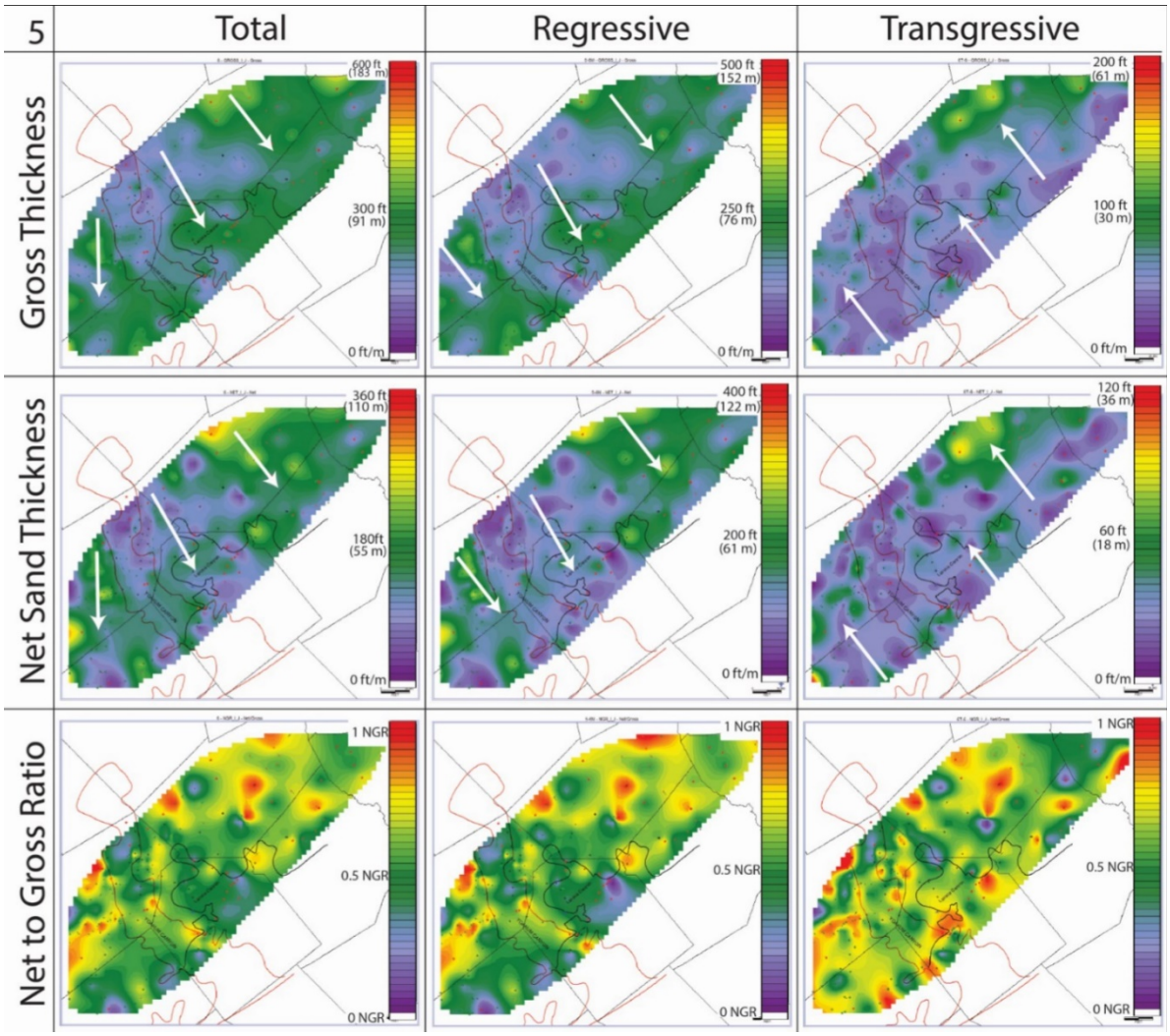

Figure 24: Isopach maps for the total sequence, regressive phase, and transgressive phase for Sequence 5. Isopach maps included are gross thickness, net sand thickness, and net to gross ratio. White arrows indicate location of trends for the sequence.

The net-to-gross ratio maps for the entire sequence 5, regressive phase, and transgressive phase all do not show any significant trends and are relatively constant over the study area. When comparing the net-to-gross ratio maps of sequences 4, 5, and 6 for

the total sequence, an overall progradation of the system is illustrated (Figure 25). By assuming, the shoreline has the highest net-to-gross ratio (cleanest sand unit), the shoreline is interpreted to have moved basinward approximately 25 km beyond the previous sequence, while also switching laterally towards the southern portion of the study region.

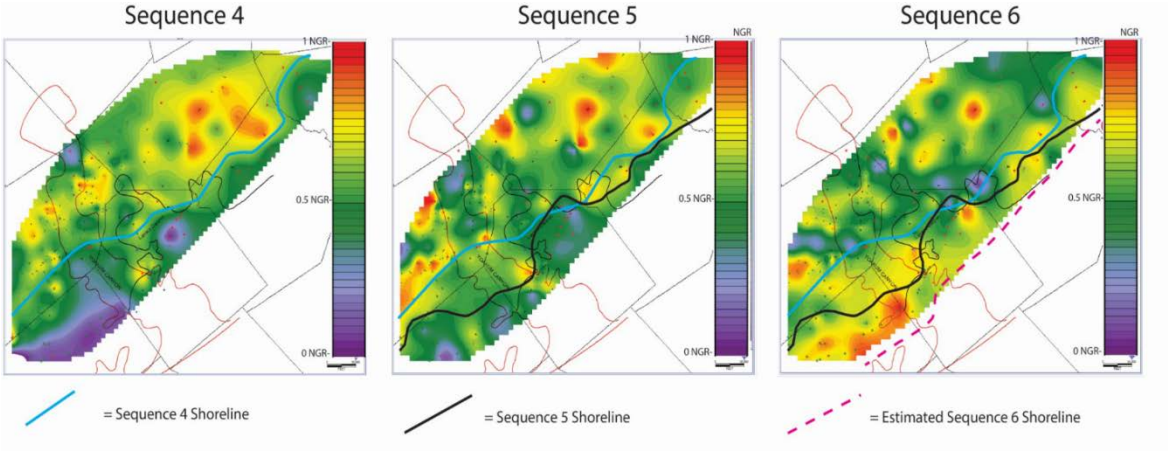

Figure 25: Net sand thickness maps for Sequences 4-6 illustrating the progradation of the system across the shelf. Shorelines (interpreted based on the break between sandy and muddy lithology) represented for Sequences 4 and 5. Sequence 6 shoreline estimated to be basinward of the study area.

Sequence 6

Sequence 6, between L_WILCOX_6 and L_WILCOX_7 surfaces (Figure 16), is distinctly different than the previous 1 to 5 sequences in that the main deposition shifts to the south side of Yoakum Canyon (Figure 26). From the gross thickness (~100 m) and net sandstone thickness maps for the total sequence and the regressive phase, the deposition and concentration of sand is primarily to the southwest of the Yoakum Canyon (Figure 26). There is also a depocenter in the northern section of the study area, but the primary

deposition is in the southern flank. The transgressive phase is relatively constant across the study area as seen by the gross thickness and net sandstone thickness maps (Figure 26).

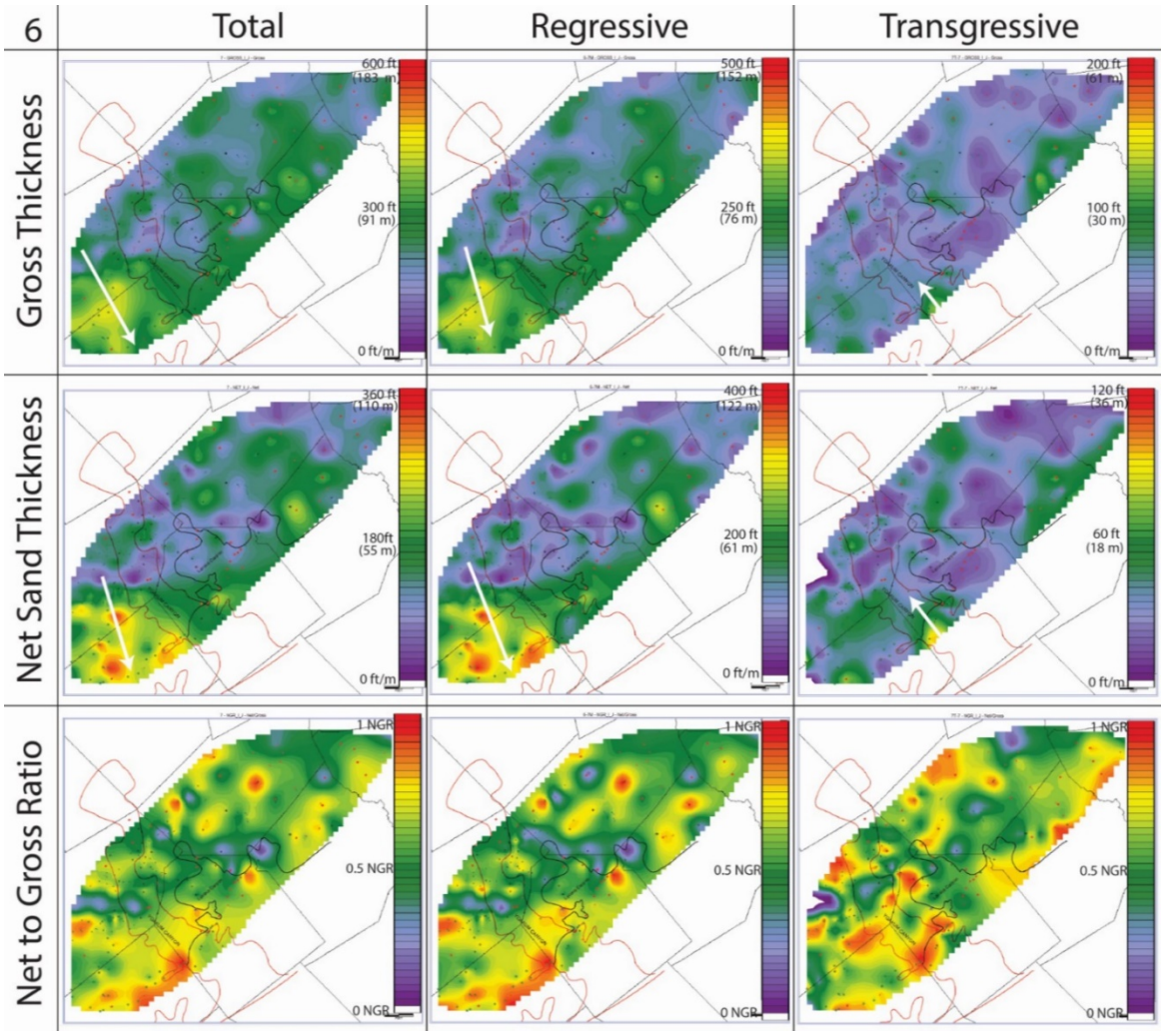

Figure 26: Isopach maps for the total sequence, regressive phase, and transgressive phase for Sequence 6. Isopach maps included are gross thickness, net sand thickness, and net to gross ratio. White arrows indicate location of trends for the sequence.

The net-to-gross ratio for the total sequence and regressive phase emphasizes the main depocenter to the southern flank (Figure 26). The net-to-gross ratio is more evenly distributed for the transgressive phase, but also seems to preserve thicker deposits to the southern flank. In Figure 26 it is apparent that this sequence's shoreline has prograded even further basinwards than sequence 5.

From cross-section A-A' (Figure 16) the log signature of sequence 6 across the Yoakum canyon is easily correlative. The log signature of the sequence 6 is similar across the canyon and only differs when thickening to a blockier sandstone on the southern flank at about 5 km from the canyon due to the concentration of deposition in this area. No clear indication of an incision affecting deposition is present at time of sequence 6, but this is the furthest basinward deposition that occurs in the southern portion of the study area.

Sequence 7

Sequence 7, between L_WILCOX_7 and L_WILCOX_8 surfaces (Figure 16), is the first sequence to show significant relationships with (or affected by) the Yoakum Canyon incisions. While the gross thickness for the total sequence (~90 m) and regressive phase shows relative constant thickness within the depocenters on the southern flank and the north central region of the study area, the net sandstone thickness shows a thickening towards the canyon margin (Figure 27). The net sandstone thickness for both the total sequence and the regressive phase is thickest on the southern side of the study area and remains thick until the area of the Yoakum canyon incision. Another interesting trend is

that the transgressive deposit is far greater, in comparison to the rest of the region, in the Yoakum canyon incision area (Figure 27).

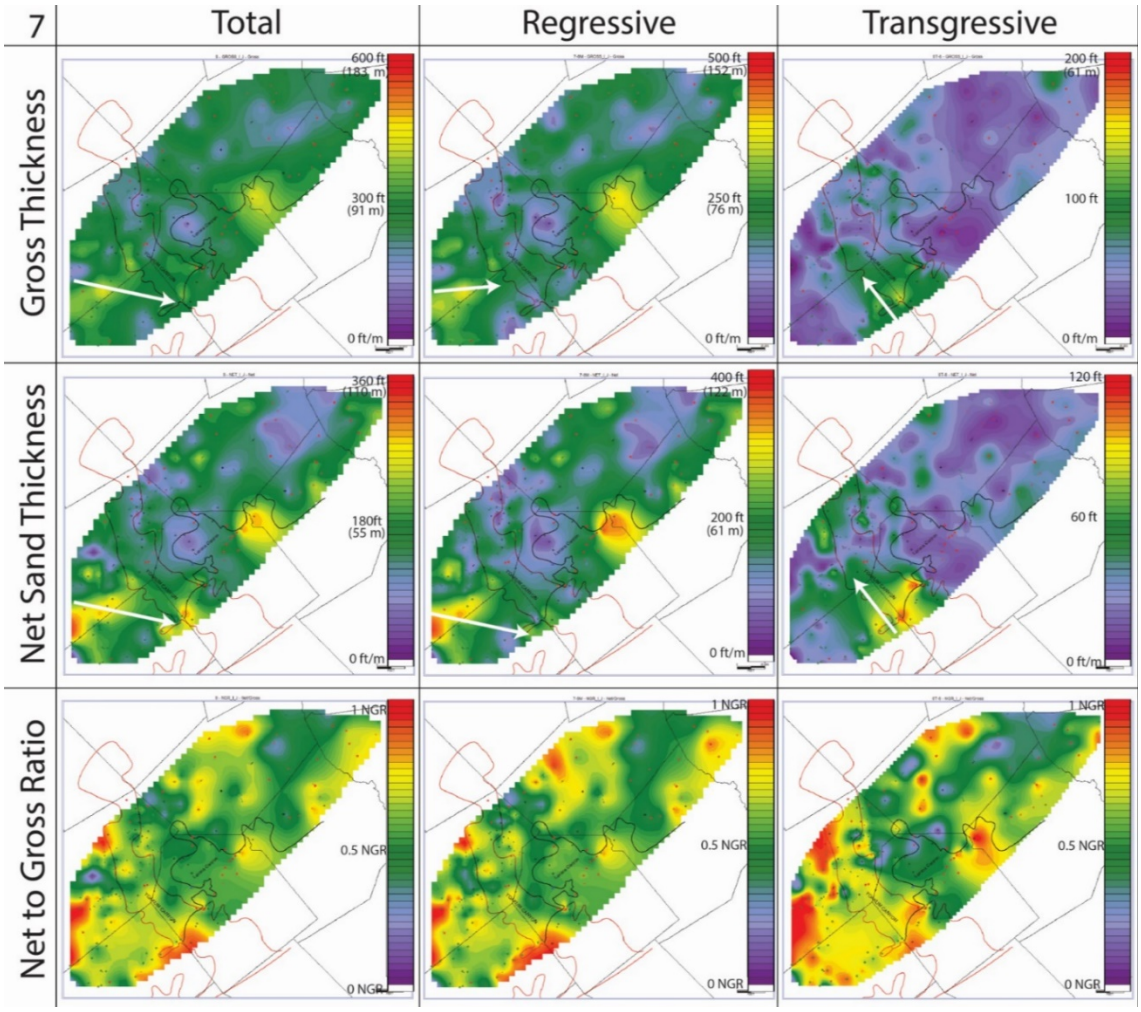

Figure 27: Isopach maps for the total sequence, regressive phase, and transgressive phase for Sequence 7. Isopach maps included are gross thickness, net sand thickness, and net to gross ratio. White arrows indicate location of trends for the sequence.

The net-to-gross ratios for the total sequence, regressive phase, and transgressive phase show a distinct difference in deposition of the southern side to the northern side of

the Yoakum Canyon incision area (Figure 27). The sediment is primarily being deposited in the southern region of the study during the time of sequence 7 when the canyon was actively open in the study area.

Cross-section E-E' illustrates the trend of the southern section in an oblique angle to the strike of deposition where the log signature suggests thicker sandstone toward the Yoakum Canyon then closer to the margin separate into thinner sandstone (Figure 28). Past the Yoakum canyon margin, within the incised area, the log pattern suggests a shale fill with possible thin (10 meters thick) sandstone units within the canyon. The regional cross section A-A' (Figure 16) illustrates a distinctly different log pattern between north and south sides, across the Yoakum Canyon incision. The southwestern side of the canyon is characterized by a thick, blocky sandstone unit, whereas the northeastern side of the canyon is characterized by a thinner and muddier log signature. This log pattern difference is significant over such a small distance between wells, approximately 8 km. The thickening of the sandstone bodies towards the canyon margin (because increased accommodation) and the difference in log patterns across the proposed Yoakum incision area suggests that the canyon was likely active (incision was open) during the deposition of sequence 7.

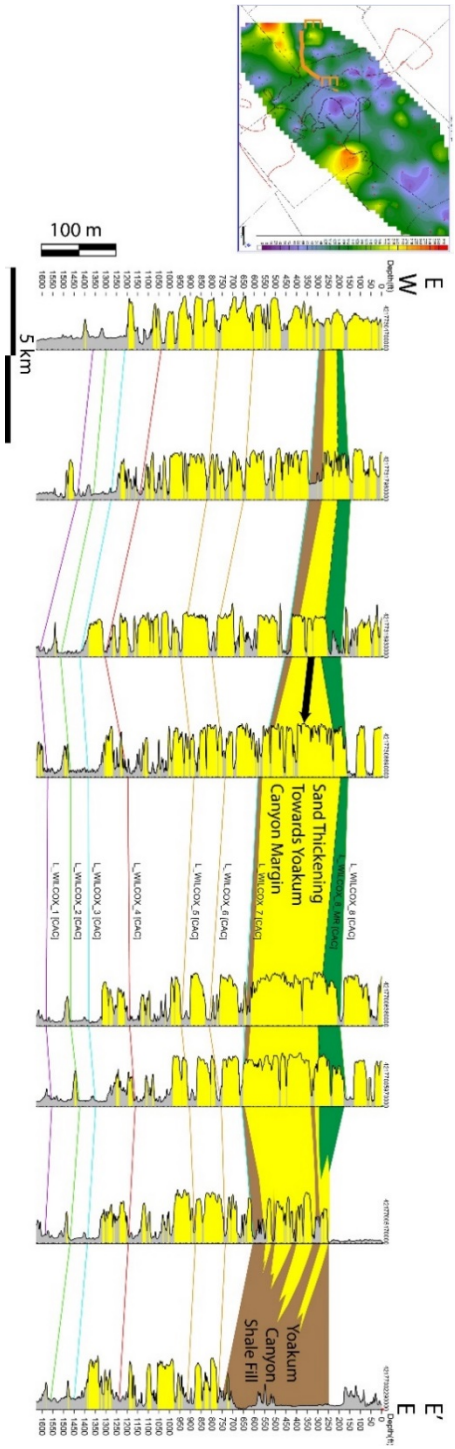

Figure 28: Cross-section E-E' illustrating the sand thickening trend of sequence 7 towards the Yoakum Canyon margin.

Sequence 8

Sequence 8, between L_WILCOX_8 and L_WILCOX_9 surfaces (Figure 16), has a lateral shift in deposition from the previous sequence 7. The gross thickness for the total sequence (~ 90 m) and regressive phase is somewhat constant with a slight thickening over the center of the study region and the northeastern portion of the study region (Figure 29). The net sandstone thickness for the total sequence and regressive phase contrasts with the previous sequence because of an increase in sand deposition to the northeast of the Yoakum Canyon and a decrease in sand deposition to the southwest of the Yoakum Canyon. Within the Yoakum Canyon incision area little sand deposition occurred. On both sides of the Yoakum Canyon, the net sand of Sequence 8 thickens towards the canyon margin. The transgressive phase has primary deposition from the southern flank of the study area to the central region of the study area. There is not significant difference over the Yoakum Canyon for the transgressive phase of Sequence 8.

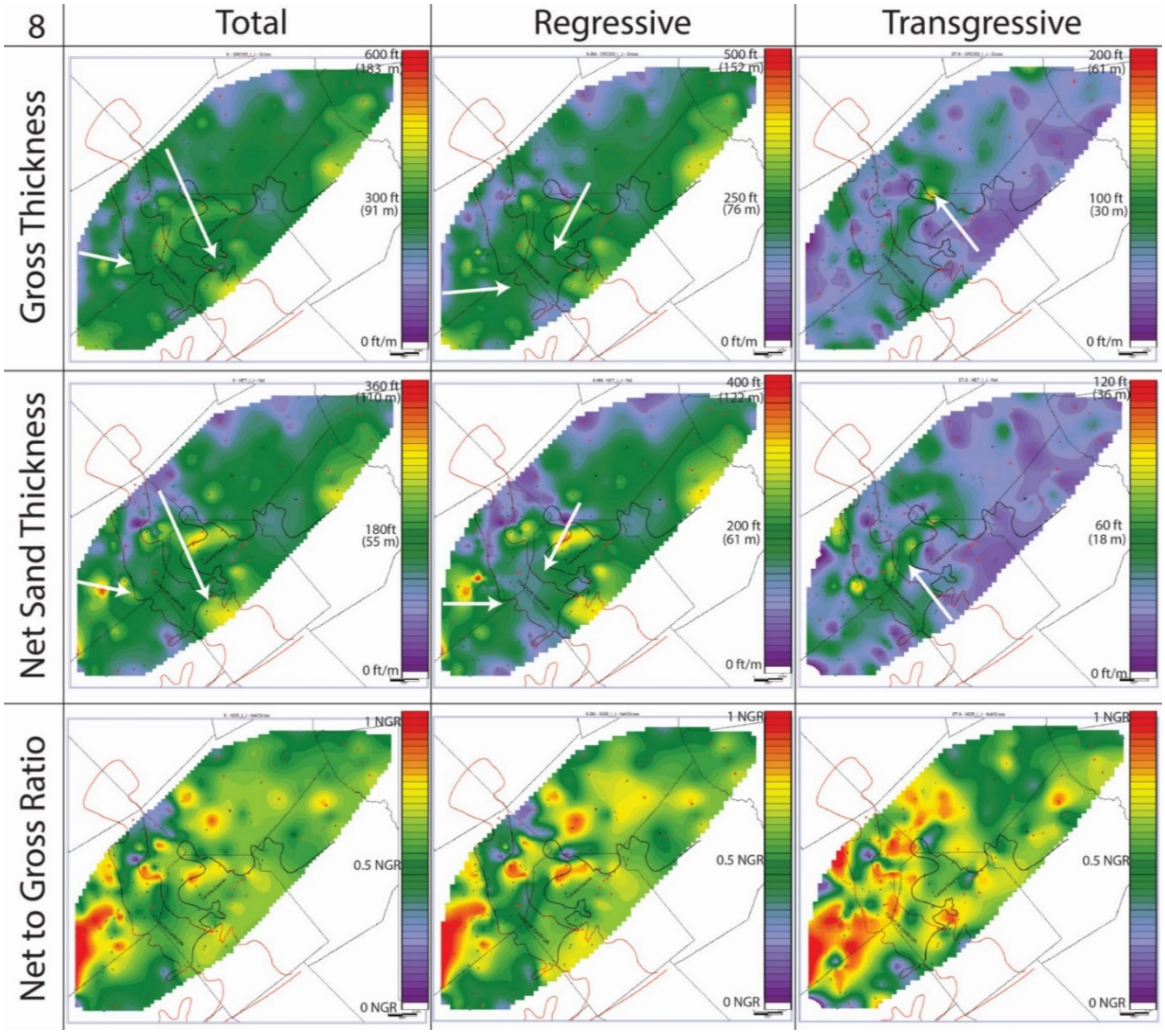

Figure 29: Isopach maps for the total sequence, regressive phase, and transgressive phase for Sequence 8. Isopach maps included are gross thickness, net sand thickness, and net to gross ratio. White arrows indicate location of trends for the sequence.

The net-to-gross ratio maps for the total sequence and the regressive phase again illustrates the concentration of sand deposition on both sides of the canyon margin (Figure 29). Within the Yoakum Canyon incision area there is a lower net-to-gross ratio than the

region outside of the canyon. The transgressive phase does not have any significant net-to-gross relationship with the Yoakum Canyon incision area.

Cross-section H-H' illustrates the thickening of sandstone units of Sequence 8 towards the canyon margin (Figure 30). This strike oriented, landward located cross-section shows a similar log pattern across the canyon, but the further downdip cross section, A-A', has distinctly different log patterns across the canyon (Figure 16). This difference in cross sections can be explained by the location of the incision head within the shelf.

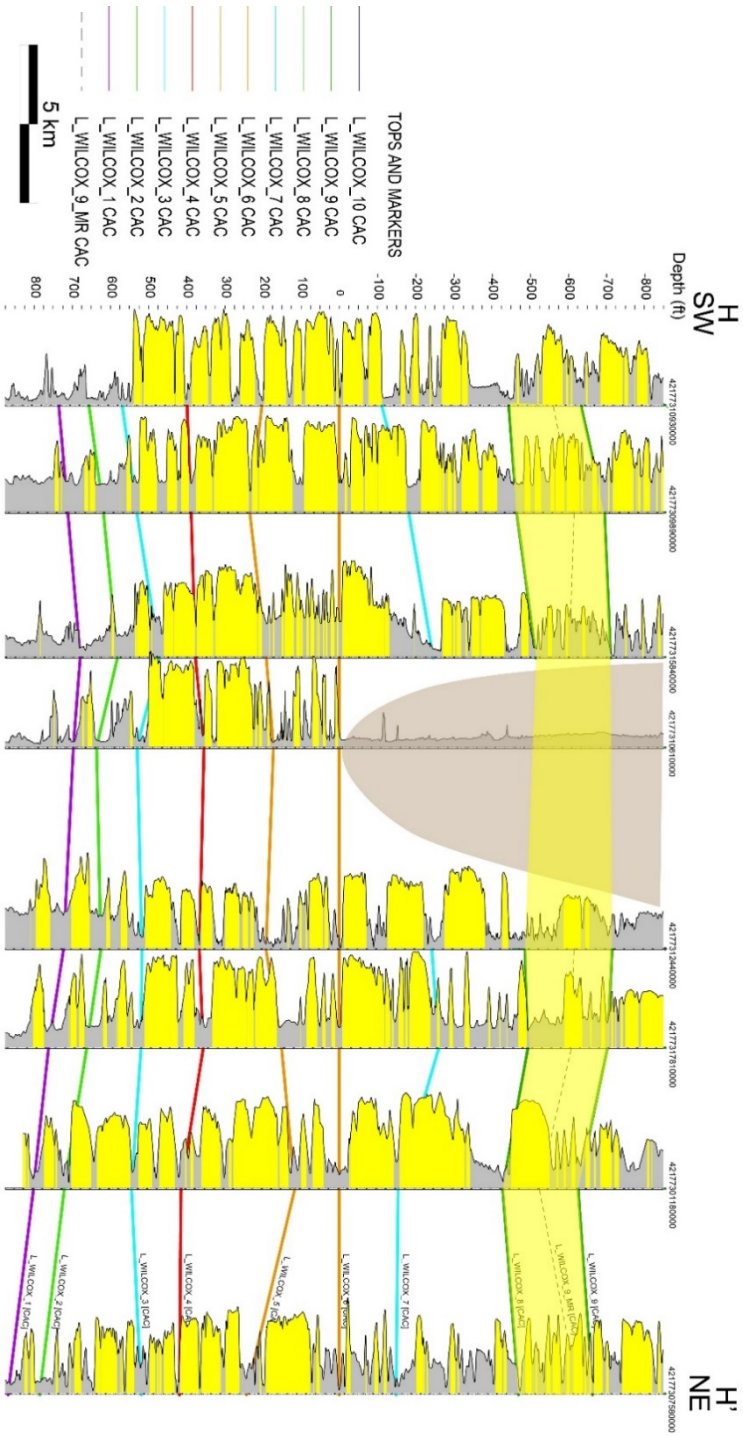

Figure 30: Cross-section H-H’ illustrating matching log patterns across the Yoakum Canyon.

Sequence 9

Sequence 9, between L_WILCOX_9 and L_WILCOX_10 surfaces (Figure 16), is similar to the previous two sequences 7 and 8 with the differences in log pattern of the deposits across the Yoakum Canyon. The gross thickness for the total sequence (~80 m) and regressive phase suggests the overall deposition moving away from the southern portion of the study region and starting to concentrate in the central and northern region of the study area (Figure 31). This trend is also confirmed by the distribution of net sandstone thickness for the total sequence and the regressive phase. Similar to the previous sequences 7 and 8, the net sandstone thickness and gross thickness is significantly thinner within the Yoakum incised area in comparison to the surrounding margins. The transgressive phase is concentrated in the central region of the study area as seen by both the gross thickness and net sand thickness maps.

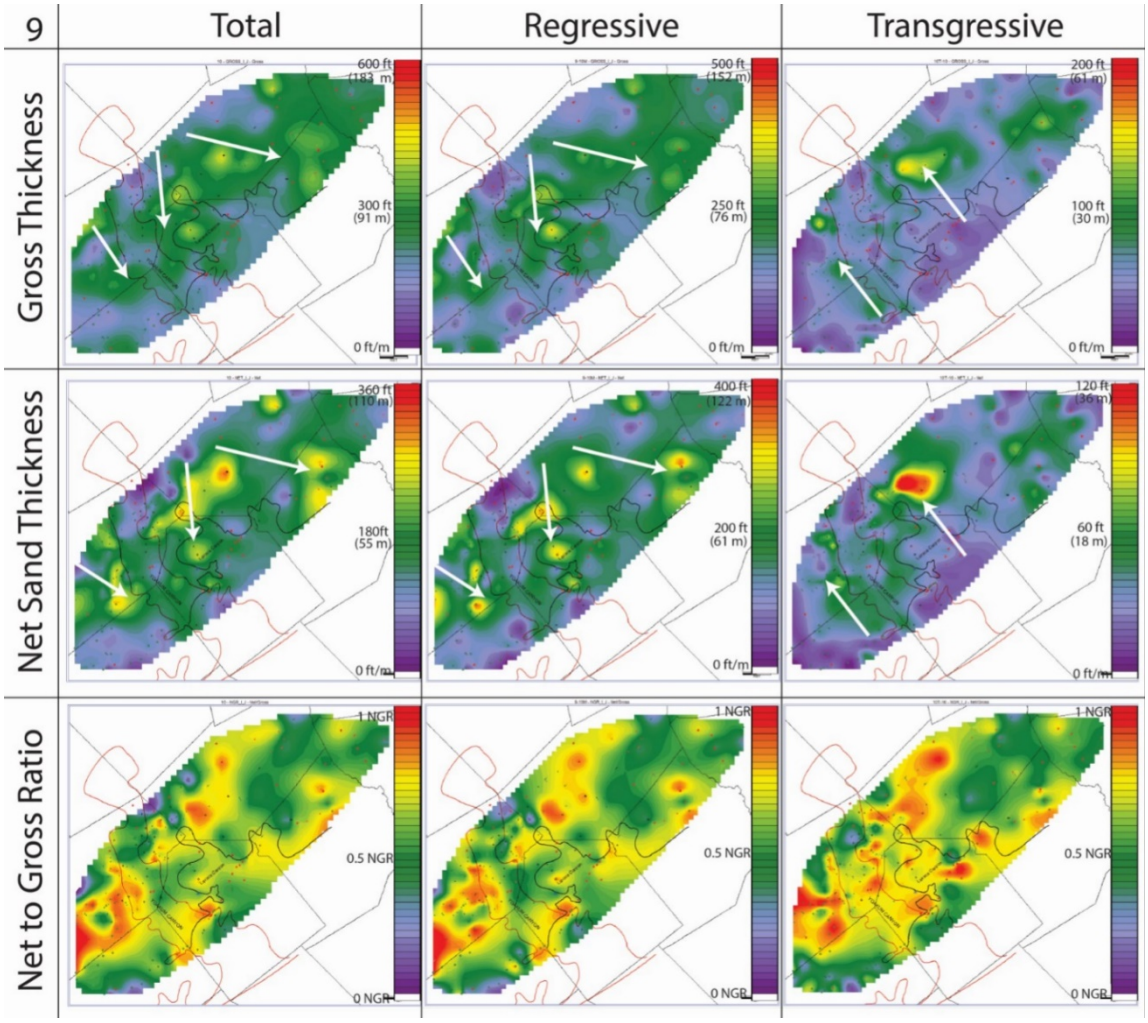

Figure 31: Isopach maps for the total sequence, regressive phase, and transgressive phase for Sequence 9. Isopach maps included are gross thickness, net sand thickness, and net to gross ratio. White arrows indicate location of trends for the sequence.

The net-to-gross ratio for the total sequence and the regressive phase is similar to the previous sequences 7 and 8 with greater sand deposition occurring around the margin of the incised region, and muddier lithology within the incised region. The transgressive phase has a more constant distribution of sandstone thickness throughout the study region.

The cross-section B-B' illustrates that Sequence 9 is much sandier northward of the Yoakum Canyon margin than on the southern side (Figure 17). The log signature of the sequence 9 is significantly different across the canyon area from south to north side over a span of about 10 km. The difference in log signature is also significantly different updip (landward) of cross-section B-B', as seen by cross section A-A' (Figure 16). The sequence 9 is thicker in the updip portion and thickens towards the canyon margin, but with a different log pattern across the canyon that suggests the Yoakum Canyon was active during Sequence 9.

Sequence 10

Sequence 10, between L_WILCOX_10 and L_WILCOX_11 surfaces (Figure 16), further separates the deposition of the south to that of the north of the Yoakum Canyon. Deposition is strongly preferential to the northern region as seen by the gross thickness and net sandstone thickness maps for the total sequence and the regressive phase (Figure 32). The gross thickness and thinning of the net sandstone thickness maps suggest that deposition to the south of the Yoakum area is minor in comparison to the previous sequence and the deposition to the north is becoming more prevalent. The net sandstone thickness maps suggest a thickening towards the canyon margin for the basinward northern portion of the study area. The transgressive phase is also thicker to the northern portion of the study area. The net-to-gross ratio for the total sequence, regressive phase, and transgressive phase emphasizes the further basinward deposition of the northern study area in comparison to the more transgressed southern portion of the study area.

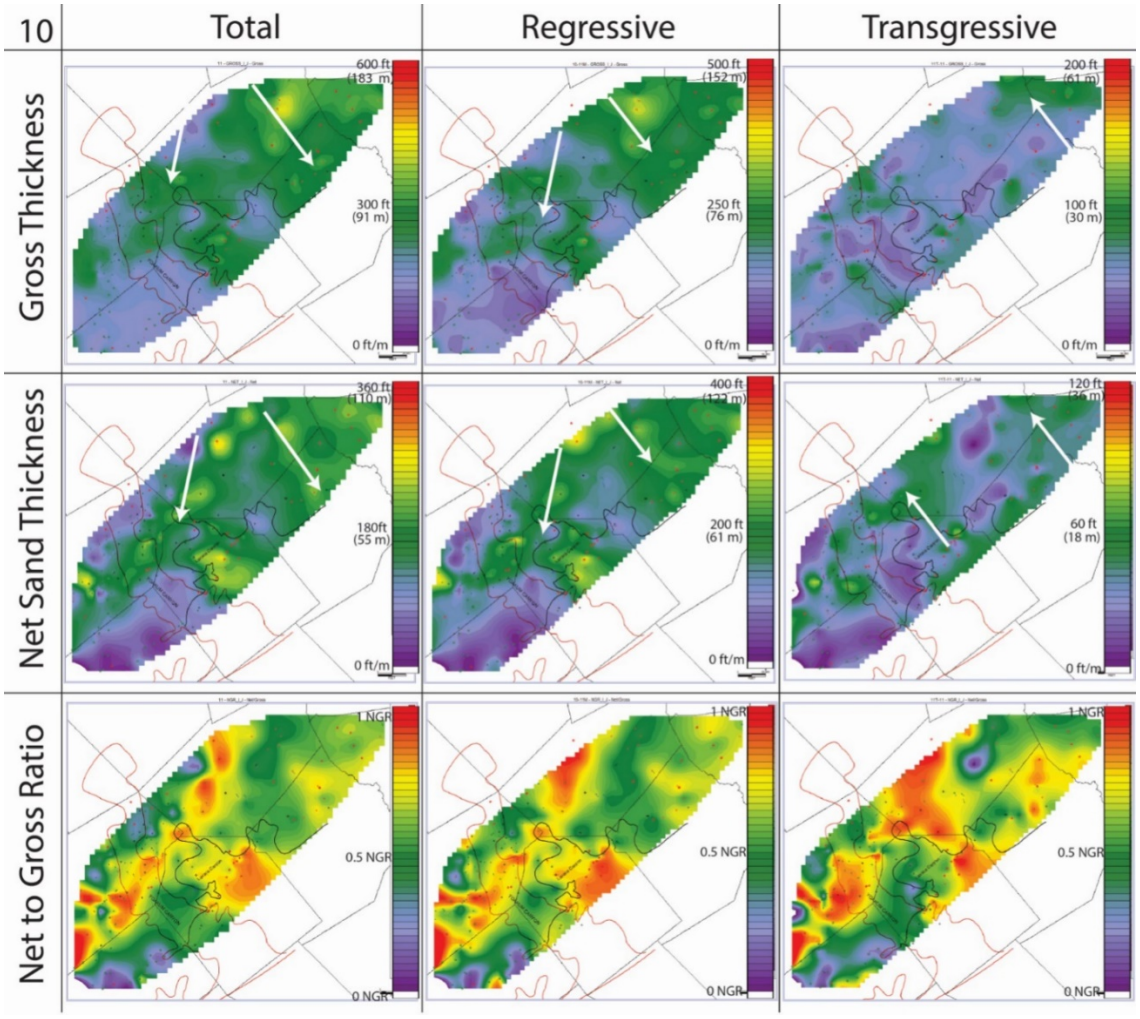

Figure 32: Isopach maps for the total sequence, regressive phase, and transgressive phase for Sequence 10. Isopach maps included are gross thickness, net sand thickness, and net to gross ratio. White arrows indicate location of trends for the sequence.

The regional cross section A-A' shows a distinctly different log signature on either side of the Yoakum Canyon incision area during the Sequence 10 (Figure 16). To the south of the Yoakum Canyon the sequence is much thinner with a slight thickening towards the

canyon margin. North of the Yoakum Canyon the sequence thins into the canyon and thickens away from the canyon with a blocky log pattern.

Sequence 11

Sequence 11, between L_WILCOX_11 and L_WILCOX_12 surfaces (Figure 16), further shifts deposition to the northern portion of the study area. The gross thickness (~90 m) and net sandstone thickness maps for the total sequence and regressive phase illustrates the continuous dominance of northward deposition of the Sequence 11 in comparison to Sequence 10 (Figure 33). There is still some thickening on the southern side, but is thinner overall compared with depocenter on the north side of the canyon. There is no apparent thickening or thinning relationship associated with the Yoakum Canyon area. The transgressive phase also suggests greater deposition to the northern side of the study area but is more continuous over the whole region than the total sequence and regressive phase.

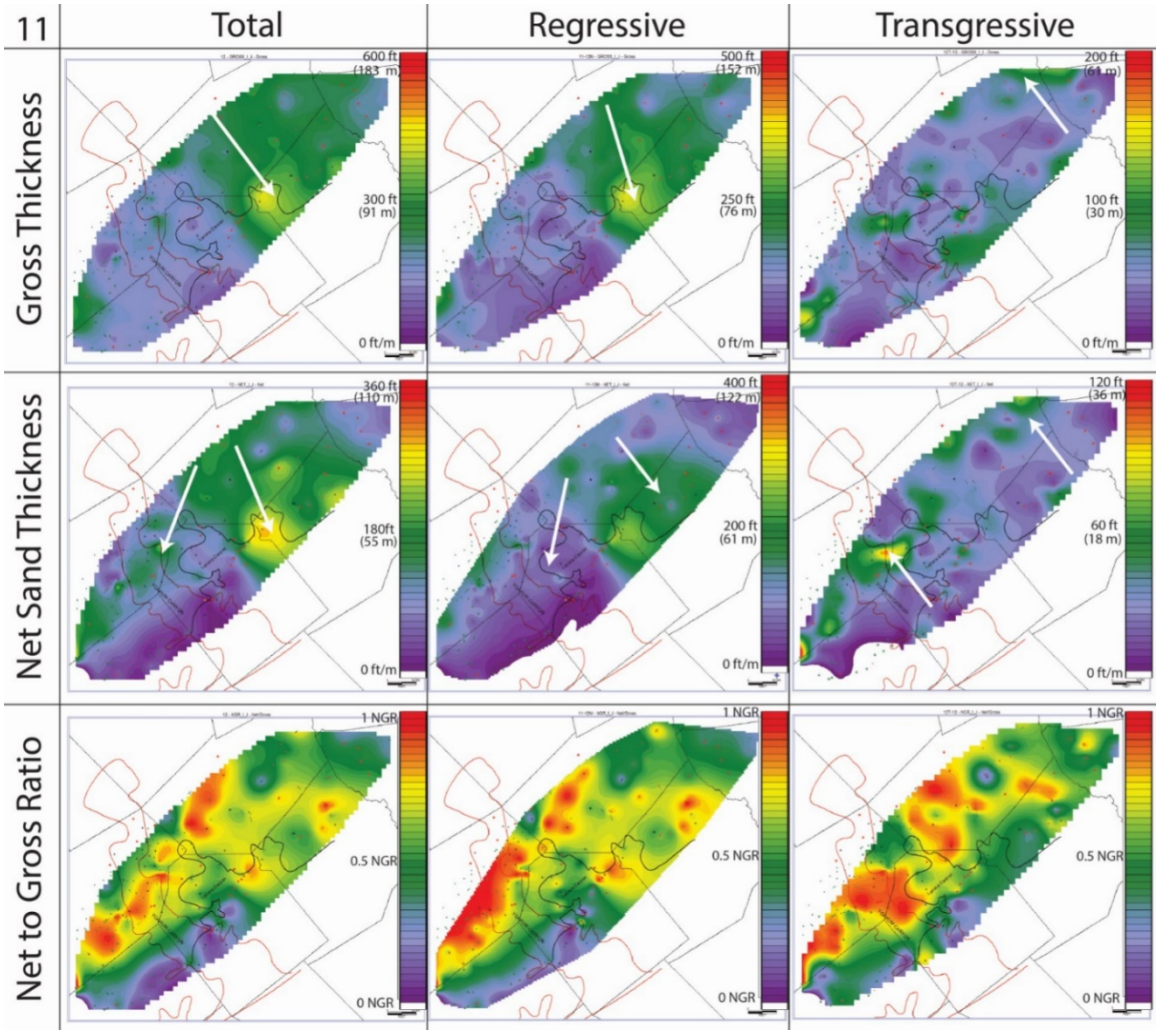

Figure 33: Isopach maps for the total sequence, regressive phase, and transgressive phase for Sequence 11. Isopach maps included are gross thickness, net sand thickness, and net to gross ratio. White arrows indicate location of trends for the sequence.

The net-to-gross ratio for the total sequence, regressive phase, and transgressive phase also suggest more sand deposition to the northern portion of the study region (Figure 33). With comparison to the previous sequence, Sequence 10, the sand deposition shifts

landward on both the southern and northern regions suggesting a retrogradation of the system.

The regional cross section B-B' in the basinward portion of the study area illustrates the difference of Sequence 11 across the study region (Figure 17). The thickest portion of the sequence 11 is in the northern part of the study area. The sequence thins toward the Yoakum Canyon margin. South of the Yoakum Canyon, the sequence is very thin with little sandstone deposition.

Sequence 12

Sequence 12, between L_WILCOX_12 and L_WILCOX_13 surfaces (Figure 16), is the youngest interpreted sequence within the Lower Wilcox of this area. This sequence follows a similar trend to the previous sequence 11 with deposition strongly preferential to the northern portion of the study area (Figure 34). The gross thickness (~60 m) and net sandstone maps for the total sequence and regressive phase denotes the primary deposition to occur in the northern portion of the study area. The net sandstone thickness and gross thickness of the transgressive phase show that deposition stays in the northern section primarily during transgression and moves landward. The net-to-gross ratio for the total sequence, regressive phase, and transgressive phase suggests that sand deposition occurs primarily in the northern section with a muddier lithology in the southern and basinward portion of the study region.

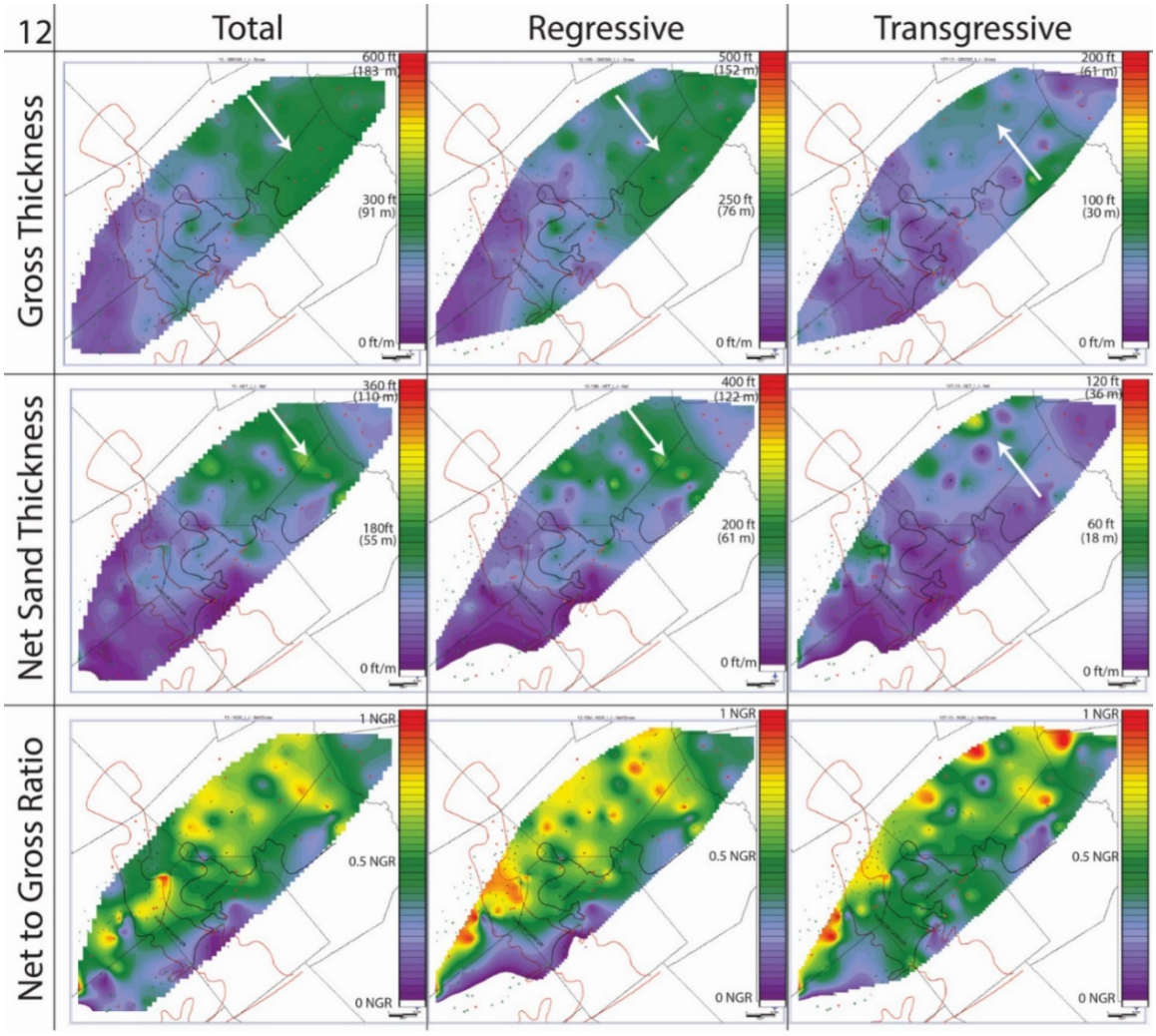

Figure 34: Isopach maps for the total sequence, regressive phase, and transgressive phase for Sequence 12. Isopach maps included are gross thickness, net sand thickness, and net to gross ratio. White arrows indicate location of trends for the sequence.

Both regional cross sections A-A' and B-B' illustrate the thickening to the northern portion of the study area (Figure 16 and Figure 17). The log signature greatly varies from the southern to the northern portion of the study area. No clear trend is associated with the

direct canyon margin, but this is likely due to the depocenters being further landward as the system retrogrades. Also of significance, above this sequence, the Middle Wilcox is much sandier in the northern portion of the study area than the southern region. Additionally, the units of the Middle Wilcox are not correlative across the Yoakum Canyon that suggest at the time of the Middle Wilcox the Yoakum canyon was still separating two distinct depocenters.

DISCUSSION

This study subdivided the Lower Wilcox into 12 regressive-transgressive sequences based on flooding surfaces (Figure 15). The number of sequences is 4 or 5 less than recorded by Zhang et al (2016) in a neighboring easterly area, but the latter authors included several muddy, basal slope sequences that are not included herein. Through mapping the gross thickness, net sand thickness, and net-to-gross ratios for each total sequence, the regressive phase, and the transgressive phase, an overall history of the system has become apparent (Figure 35). Initially, the system's depocenter was located landward of the study area and shelf deposits were overall fine grained (Figure 16 and Figure 17) and probably draped somewhat onto the deepwater slope. The depocenter prograded during the initial sequences with Sequence 1 being the first sand input of the Lower Wilcox within the study area. As the system prograded toward the south-west over the study area, Lower Wilcox incisions became apparent in younger sequences. Sequences 3 and 4 have large scale incisions associated with them which correlate to the previously described Hallettsville Complex and Lavaca Canyon (Devine and Wheeler 1989; Chuber and

Begeman 1982). The geometries of the sandstone bodies around the shale-filled incisions is significant with both 3 and 4 sequences showing thickening near the canyon margin. The thickening of sandstone bodies toward the incision margin abruptly shifts to shale fill within the incision. This trend could be associated to the greater accommodation space available near the canyon margin, thus suggesting that the canyon was active at this time.

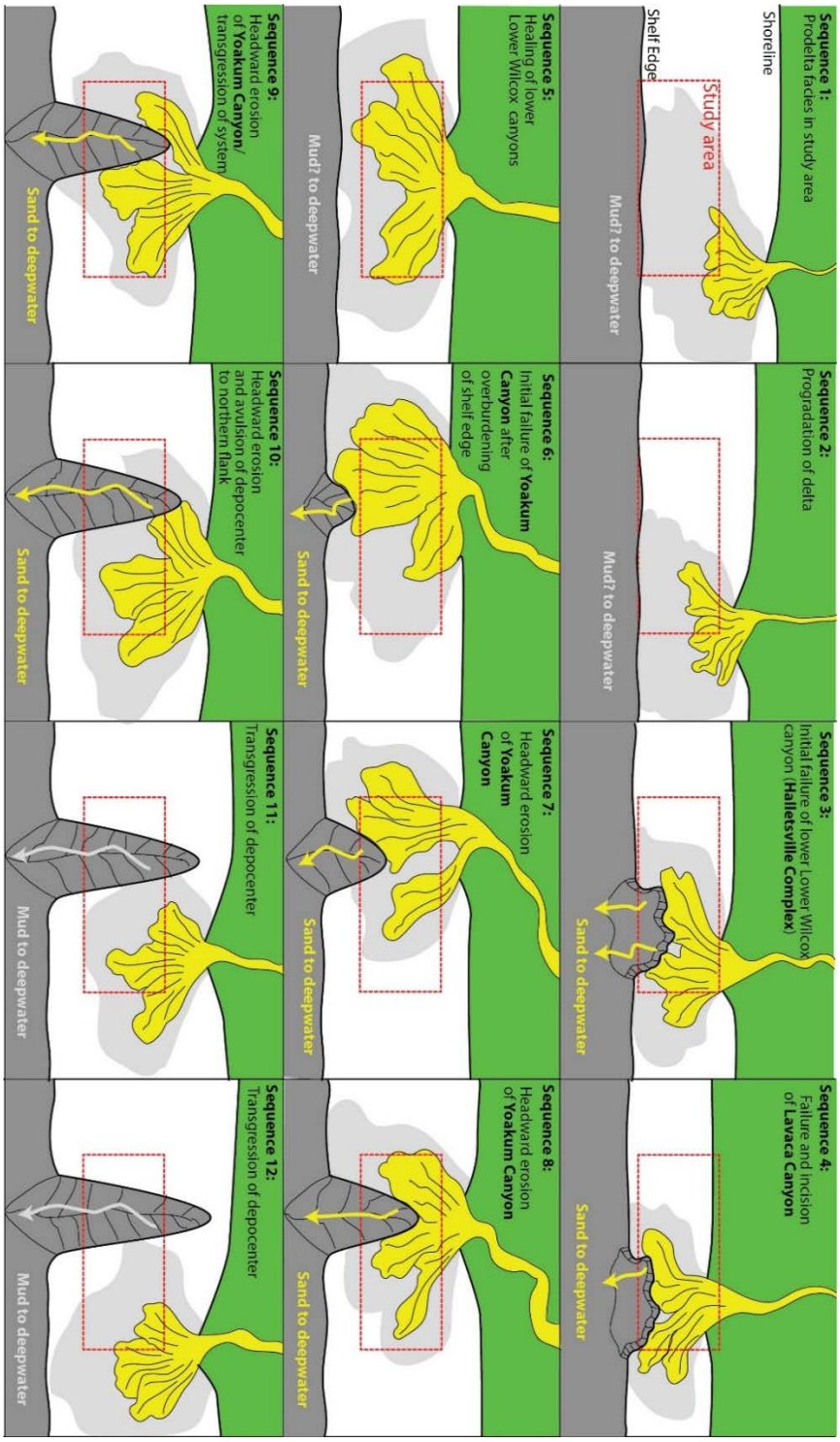

Figure 35: Evolution of the Lower Wilcox sequence depocenters based on trends depicted in isopach maps of each sequence and log patterns. Morphology and

location of depocenters interpreted from isopach maps for the regressive phase of each sequence.

After Sequence 4, there is no longer evidence for incision activity associated with the Hallettsville Complex and Lavaca Canyon. The sequences continue to prograde over the study region and shift from mainly concentrated in the northeastern portion of the study region to spanning over the central and southwestern region. Well log signatures from Sequence 1 to 6 are easily correlatable with no significant changes in log pattern over short distances of a few kilometers (Figures 16).

Sequence 6 marks the maximum basinward progradation of the delta system and there is a thick depocenter at the southeastern portion of the study area. Above sequence 6, log signatures become 'broken' and show a miss-match across the Yoakum Canyon incision region (from north to south). Sequence 7 does not have a correlative log signature across the Yoakum Canyon on the basinward section of the study area. Sandstone thickness trends thicken approaching the margin of the Yoakum Canyon (Figure 16). As a result, Sequence 7 is likely to be the first sequence where the Yoakum Canyon was actively incising the shelf within our study area.

Similar trends have been observed for the next sequences with thickening of sandstone bodies near the canyon margin and log signatures not being similar across the canyon margin (Figure 16). The depocenter transgresses on the southern side of the Yoakum canyon from Sequence 7 through Sequence 9 and eventually shifts to primarily depositing on the northern portion of the study area. The final sequences of the Lower Wilcox, 10 through 12, essentially only contribute sand deposition to the northern portion

of the study region and each sequence moves further northward, away from the canyon. These three sequences also are characteristically distinct across the Yoakum Canyon suggesting that the sediments on either side of the canyon were not interacting. The canyon acted as a "sedimentation barrier" for shelf sediments during this time.

In result, the overall interpretation for the progression of the system is as follows: I) Sequences 1 and 2 prograde over the Midway Shale. II) Cut and infilling of the Halletsville Complex and Lavaca Canyon during Sequences 3 and 4. III) Healing of the Lower Wilcox incisions while the deltaic systems prograded and continued to extend the shelf during Sequences 5 and 6. IV) Initiation of shelf incision by the appearance of the Yoakum Canyon due to overloading of the shelf margin during Sequence 6 (due to the constraint of the study region there is a possibility that the canyon incision could have occurred further basinward during an earlier sequence). V) Headward erosion of the Yoakum Canyon resulted in further shelf dissection during initiation of transgression for Sequences 7, 8 and 9 splitting the deposition in northern and southern depocenters. VI) The depocenter shifted away from the southern portion of the study area and concentrated deposition to the north for sequences 10 through 12 (Figure 35).

Implications for the Evolution of the Yoakum Canyon

This study, by systematic mapping of high frequency regressive-transgressive cycles within the Lower Wilcox, corroborates that large-scale incisions within the Wilcox Group were localized along the San Marcos Arch region. The incisions within the lower portion of the Lower Wilcox, the Halletsville Complex and Lavaca Canyon, have broad

morphologies as previously described and are confined to Sequences 3 and 4. The following two sequences, 5 and 6, prograde over the study region and heal the underlying canyons. Sandstone trends, thickening toward the margin of the incision, associated with the Halletsville Complex and Lavaca Canyon, appear again during Sequence 7 along the Yoakum Canyon margin. Sandstone thickening towards the canyon margin, combined with log signature differences across the area of incision, strongly suggests that the Yoakum Canyon is a longer lived system than previously proposed (Dingus and Galloway 1990) and in fact developed during the Lower Wilcox rather than in Middle Wilcox time.

Dingus and Galloway (1990) suggested that the Yoakum Canyon incision began after a brief progradation during the Middle Wilcox lead to slumping of the shelf margin. Subsequent headward erosion allowed for the shelf dissection of the elongate Yoakum Canyon. The present study doesn't refute a headway erosion genesis, possible triggered by tectonics as showed in Chapter 1, as suggested by Dingus and Galloway (1990) but the sequences mapped rather suggest a complex evolution with multiple cut and fill events and multiple canyon "reactivations" during multiple regression-transgression cycles. The results of this study also suggest the progradation of the Rockdale Delta System overburdened the shelf margin creating instability and failure, and that this process began earlier than the Middle Wilcox during Sequence 7 of the Lower Wilcox. As the Lower Wilcox transgressed following this sequence, there was headward erosion of the incision within the shelf. While sediments of Sequence 7 and younger deposits on the shelf (aggrading and prograding the basin margin), some sediments contributed to the incision and bypassed the slope in addition to enlarging the incision. Because of the high frequency

regression-transgression sequences, partial periods of erosion and filling occured during each sequence with the canyon cutting younger and younger sequences back into the inner shelf. However, an overall further development of the incision took place as the 3rd order system transgressed overall, as Dingus and Galloway (1991) suggested.

Comparison to the Mississippi Canyon

One of the main findings of this study is the prominent shifting of the deltaic depocenter on the shelf from one regressive sequence to the next across the study region (Figures 35). The shifting of the depocenter across the shelf and subsequent failure of the shelf margin provided long term interaction of the depocenter with the shelf incising Yoakum Canyon and the possibility that different sediment caliber fed the basin floor via canyon. Sediment caliber delivered to Yoakum canyon was controlled by the distance to the delta river mouth of each sequence, with sands delivered to the canyon from km distance and muds from tens of km away from river mouth (Sweet and Blum, 2016). The transgression of the deltaic depocenter allowed the Yoakum Canyon to erode headwards across the shelf, but counterintuitively, the depocenter still deposited significant amount of sediments across the shelf while the canyon was active. This trend of shelf sediments switching across the shelf and interacting with a large submarine canyon is seen in the recent Mississippi Delta–Mississippi Canyon system. The Mississippi Delta during the last sea-level lowstand was located west of the head ward Mississippi Canyon. Following transgression, the first highstand delta lobe (Maringouin) of the Mississippi Delta Complex prograded straight toward the canyon head but later avulsed the main depocenter (Balize

Delta) to the east of Mississippi Canyon head (Suter and Beryhill, 1985, Figure 36). The Wilcox deltaic depocenter(s) migration likely contributed sandy sediments to the canyon, as seen by the thickening patterns along the canyon margin, but the canyon did not completely capture the shelfal sediments since some sediments were still deposited on the shelf.

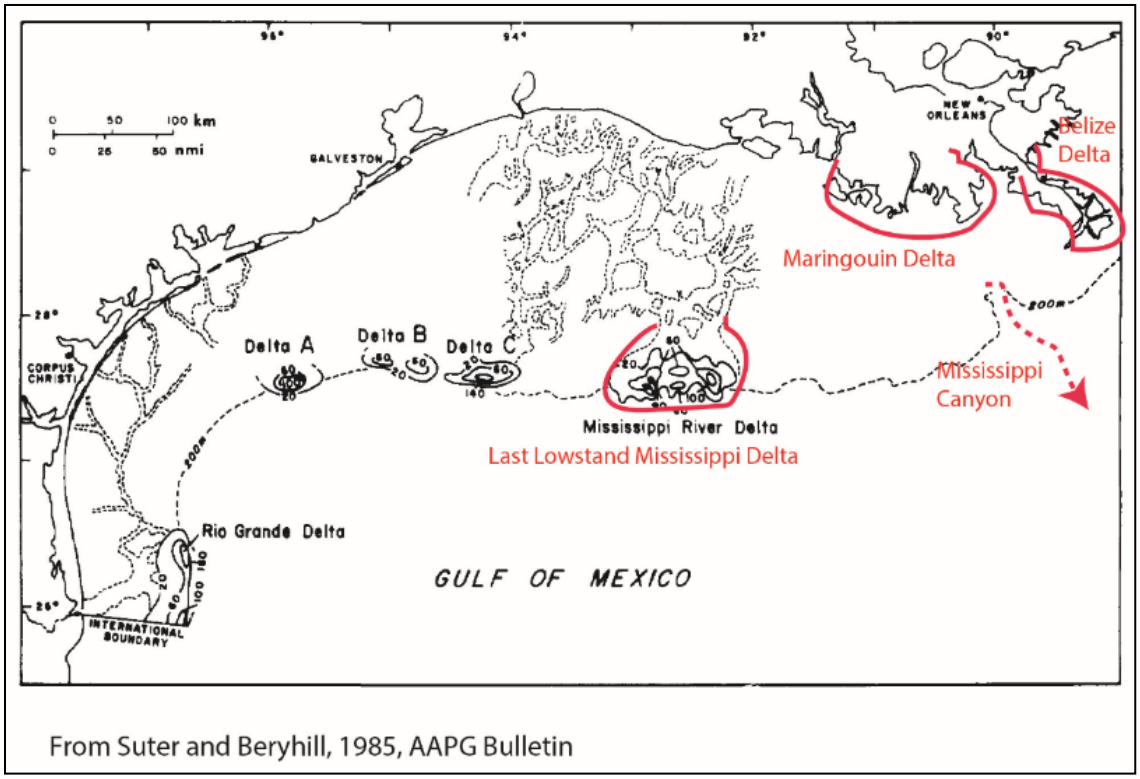

Figure 36: Location of different Delta systems of the Mississippi Delta Complex illustrating that the Mississippi Canyon did not capture shelfal sediments during the last lowstand (Suter and Beryhill, 1985).

Relationship with the Deepwater

The Yoakum Canyon was active for a longer period than previously described (Hoyt, 1959; Dingus and Galloway 1991). Interaction with multiple high frequency (4th order) sequences of the Lower Wilcox shows that the canyon was not confined to just the Middle Wilcox but was likely incised starting half way through Lower Wilcox. This has significant implications for sediments fed to the deepwater basin floor fans. Instead of one single episode of deepwater sediment deposition (single cut and fill), a longer-lived Yoakum Canyon over multiple lowstand-highstand cycles would imply a more continuous feed (in multiple pulses) of sediment to the deepwater.

Zarra (2008) concluded that the Wilcox 2 of the deepwater Wilcox Play (58.5 to 57.2 Ma, possibly correlative to youngest portion of Lower Wilcox [Figure 37]) ranges from 850 to 1,050 feet (over 300 m) in thickness downdip of the Yoakum Canyon. In the other regions of the deep-water Gulf of Mexico, Wilcox 2 is only 600 to 800 feet (200-250 m). This thicker sequence downdip of the Yoakum Canyon formed during Wilcox 2 suggests that the Yoakum Canyon could likely have been feeding the basin floor fan during the Lower Wilcox. The lower 600 feet of the Wilcox 2 downdip of the Yoakum canyon is composed of amalgamated to non-amalgamated turbidite sandstone beds. The overlying remaining portion of the Wilcox 2 is comprised of thicker mudstones and thinner sandstones. The deep-water deposits align with the erosional-depositional trends on the shelf. The initiation of the Yoakum Canyon during Sequence 6 and the following three sequences (Sequence 7-9) where the shelfal depocenter interacted strongest with the

canyon margin and likely fed the deep-water, contributing sand deposition to the turbidite sandstones of the lower portion of Wilcox 2. During Sequences 10-12 the depocenter (sands) shifted away from the canyon margin and did not interact with the canyon as directly as the previous sequences. With the shifting of the depocenter away from the Yoakum Canyon, less sand bypassed the shelf through the canyon and rather more mud was reaching the canyon which, as a consequence, dominated the canyon-basin floor system. This correlates with the upper portion of Wilcox 2 primarily consisting of thick mudstones and thin sandstones on the basin floor (Zarra, 2007). Overlying the Wilcox 2, deposits primarily consist of mudstone with some interbedded sandstones that might correspond with the “abandonment” and fill of the canyon. The initiation of the Yoakum Canyon during the Lower Wilcox and the subsequent longevity of the system links the thick sandstone deposits of Wilcox 2 in the deep-water with the shelfal depositional trends downdip of the San Marcos Arch region. The shelf dissecting Yoakum Canyon is a strong candidate as a link between the shelfal deposits and the deep-water providing a sediment fairway for shelfal bypass during multiple 4th order sea level cycles.

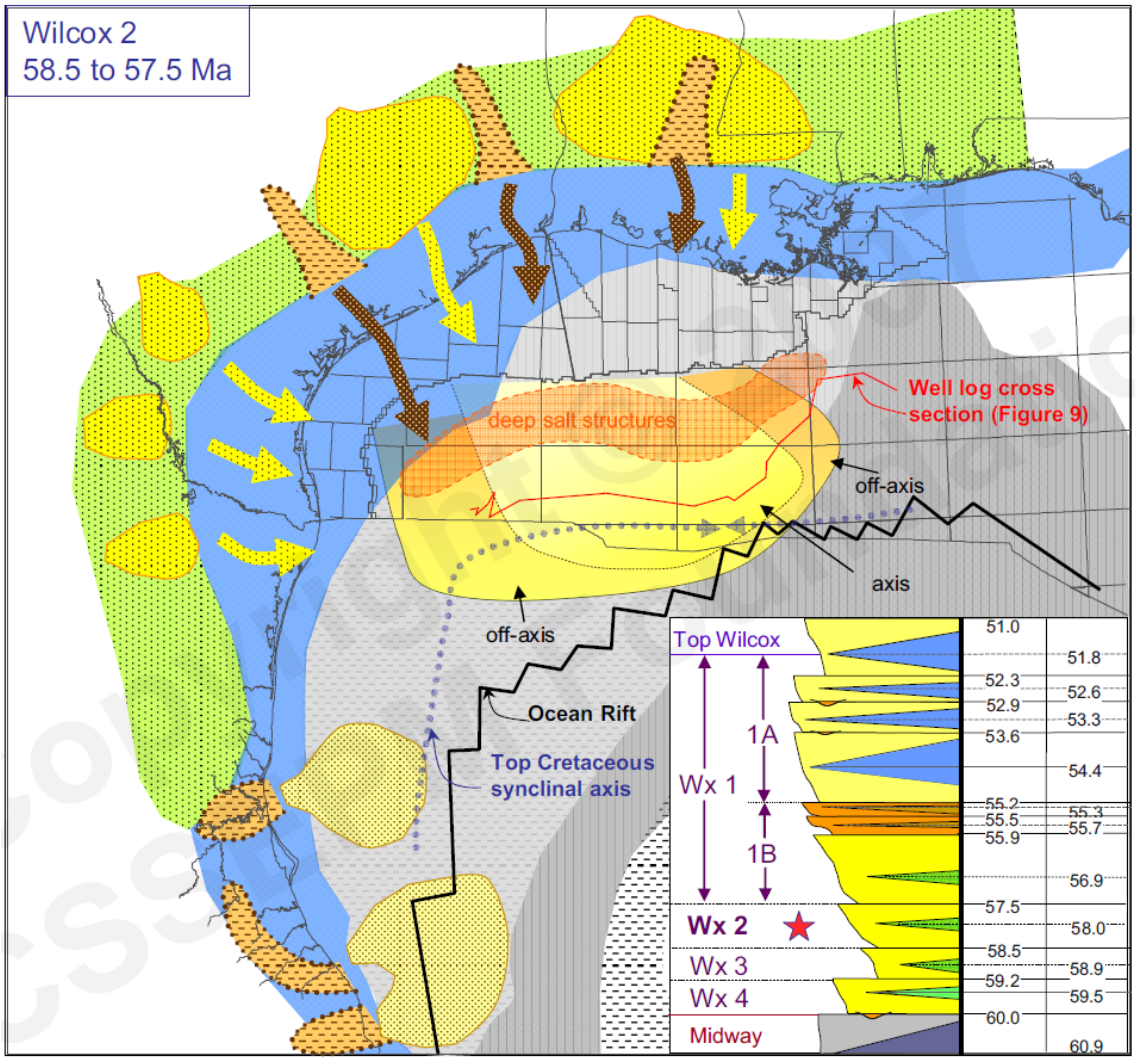

Figure 37: Paleogeographic map of Wilcox 2 showing the basin floor fan downdip of the Yoakum Canyon (Zarra, 2007).

CONCLUSIONS

1. This study divides the Lower Wilcox south east of the Houston Embayment, in the Yoakum Canyon area, into 12 regressive-transgressive high frequency sequences. The high frequency (4th order) sequences define the regressive deltas and associated transgressive estuaries building the margin of the Lower Wilcox. Sequences 1 through 7 mark an overall progradation of the shoreline/ delta and the overall basin margin in this region, whereas the sequences 8-12 follow an overall backstepping of the system.
2. Wilcox Group canyons are confirmed within the San Marcos Arch region. The lower Lower Wilcox Halletsville Complex and Lavaca Canyon incise into Sequences 3 and 4. These incisions healed after Sequence 4.
3. The Yoakum Canyon incision began with an overburdening of the shelf margin during Sequence 7. Backstepping of the system after the initial failure caused headward erosion and shelfal incision of the Yoakum Canyon during sequences 7 to 9. This allowed Lower Wilcox system to contribute significant sediment volumes to the Yoakum Canyon and thus feed the Deepwater Gulf of Mexico. The Yoakum Canyon, as a result, is a longer-lived system (over multiple Lower Wilcox sea level cycles) than previously described.

Chapter 4: Thesis Findings and Future Work

- Tectonic uplift “pulses” causing regional arches of the foreland basin, triggered by Pacific plate subduction under North American, influenced locations of canyons along the Gulf of Mexico Margin.
- Three mechanisms for canyon evolution trigged by tectonic uplift are proposed:
- The low uplift rate (LUR) model proposes fluvial erosion triggered by relative sea-level fall from localized tectonic uplift. The tectonic uplift was slow and a preexisting river would have cut through the uplift to readjust (increase) the stream gradient. Eventually the shelf-edge was incised and the shelf was eroded.
- The shelf edge bulge model proposes that the outer shelf to shelf-edge gradient increased slowly from tectonic uplift creating instability. The instability led to slumping and incision of the shelf-edge. Continuous landward uplift supports subaqueous canyon headward erosion into the shelf edge.
- The high uplift rate (HUR) model bulged the paleo-shoreline creating a headland with a relatively narrow shelf along the uplifted region. This bulging of the shoreline directed longshore currents basinward to the shelf margin triggering dense, with dissolved salts, sediment-laden shelf-water cascading over the shelf-edge.
- The Lower Wilcox in the San Marcos Arch region was sub-divided into 12 regressive-transgressive 4th order sequences. The first seven sequences mark a period of overall progradation and start of shelf incision. This was followed by five

sequences accreting on the shelf while the deltaic system was backstepping landward.

- The Yoakum Canyon initially fails at approximately sequence 6 and incises within the study area during sequences 7 and younger. With the overall transgression of the system, the Yoakum Canyon headwardly erodes within the shelf.
- The proposed evolution of the Yoakum Canyon found by this study possibly correlates with the thick Wilcox 2 (58.5 Ma to 57.2 Ma) unit downdip of the San Marcos Arch region in the deep-water Gulf of Mexico region (Zarra, 2007). This correlation suggests the Yoakum Canyon provided a sediment fairway to the deep-water Gulf of Mexico during the development of the upper part of the deepwater sandy succession.

Future Proposed Research

Recommended studies to build upon this study:

1. A larger study region extending the well log correlations would allow a more complete representation of the trends seen within the shelf deposits. To extend the well log correlations downdip within the shelf, a seismic volume dataset is strongly needed to correlate over the extensive region of growth faulting.
2. A 3-D seismic volume across the San Marcos Arch will increase the confidence of Lower Wilcox sediment interaction with the Yoakum Canyon.
3. Age dating to improve the correlations of the Lower Wilcox 4th order sequences from the shelf with the deep-water Wilcox 2 deposits.

4. Compare rates of uplift for the regional tectonics with Wilcox Group canyon incision depths.

Bibliography

Babonneau, N. et al., 2002. Morphology and architecture of the present canyon and channel system of the Zaire deep-sea fan. *Marine and Petroleum Geology*, 19(4), pp.445–467.

Britt, P., 2006. Texas Grand Canyon of the Eocen. *Houston Geological Society*, 48(8), 1-9.

Boyd, R. et al., 2008. Highstand transport of coastal sand to the deep ocean: A case study from Fraser Island, southeast Australia. *Geology*, 36(1), pp.15–18.

Busch, D.A. & Govela, S.A., 1978. Stratigraphy and structure of Chicontepec turbidites, southeastern Tampico-Misantla Basin, Mexico. *AAPG Bulletin*, 62(2), pp.235–246. Available at: -.

Chuber, S., 1979. Exploration methods of discovery and development of lower Wilcox reservoirs in Valentine and Menking fields, Lavaca county, Texas. *Gulf Coast Association of Geological Societies Transactions*, 32, pp.255–262.

Chuber, S. & Begeman, R.L., 1982. Productive Lower Wilcox Stratigraphic Traps From an Entrenched Valley in Kinkler Field, Lavaca County, Texas.

Cornish, F., 2013. Do Upper Wilcox canyons support Paleogene isolation of the Gulf of Mexico? *Gulf Coast Association of Geological Societies Transactions*, 63(2011), pp.183–204.

Cornish, F.G., 2011. Incised Valleys of the Upper Wilcox, Middle Texas Gulf Coast: Additional Pathways for Wilcox Sand Delivery to the Deep Gulf of Mexico. , pp.1–31.

Cossey, S.P.J. et al., 2016. Compelling evidence from eastern Mexico for a Late Paleocene/Early Eocene isolation, drawdown, and refill of the Gulf of Mexico. *Interpretation*, 4(1), p.SC63-SC80. Available at: http://library.seg.org/doi/10.1190/INT-2015-0107.1.

Covault, J.A. et al., 2007. Highstand fans in the California borderland: The overlooked deep-water depositional systems. *Geology*, 35(9), pp.783–786.

Crabaugh, J.P. & Elsik, W.C., 2000. Calibration of the Texas Wilcox Group to the Revised Cenozoic Time Scale : Recognition of Four , Third-Order Clastic Wedges (2.7-3.3 m.y. in Duration). *STGS Bulletin*, (November 2000), pp.10–17.

Culotta, R. et al., 1992. Deep structure of the Texas Gulf passive margin and its Ouachita- Precambrian basement: results of the COCORP San Marcos Arch Survey. *American Association of Petroleum Geologists Bulletin*, 76(2), pp.270–283.

Devine, P. & Wheeler, D., 1989. Correlation, Interpretation, and Exploration Potential of

Lower Wilcox Valley-Fill Sequences, Colorado and Lavaca Counties, Texas. Available at: http://archives.datapages.com/data/gcags/data/039/039001/0057.htm [Accessed February 1, 2017].

Dingus, W.F. & Galloway, W.E., 1990. Morphology, paleogeographic setting, and origin of the middle Wilcox Yoakum canyon, Texas coastal plain. *American Association of Petroleum Geologists Bulletin*, 74(7), pp.1055–1076.

Fisher, W. & McGowen, J., 1967. Depositional systems in Wilcox Group (Eocene) of Texas and their relation to occurrence of oil and gas. *AAPG Bulletin*. Available at: http://archives.datapages.com/data/doi/10.1306/5D25C591-16C1-11D7-8645000102C1865D.

Galloway, W., Dingus, W. & Paige, R.E., 1991. Seismic and depositional facies of Paleocene-Eocene Wilcox Group submarine canyon fills, northwest Gulf Coast, USA. *New York, Springer-Verlag*, (P., Link, M.H. (Eds.), Seismic Facies and Sedimentary Processes of Submarine Fans and Turbidite Systems), pp.247–271.

Galloway, W.E., 1989. Genetic Stratigraphic Sequences in Basin Analysis II: Application to Northwest Gulf of Mexico Cenozoic Basin. *AAPG Bulletin*, 73(2). Available at: http://search.datapages.com/data/doi/10.1306/703C9AFA-1707-11D7-8645000102C1865D.

Galloway, W.E. & McGilvery, T.A., 1995. Facies of a submarine canyon fill reservoir, Lower Wilcox Group (Paleocene), central Texas coastal plain . *Turbidites and Associated Deep-water Facies*, 20, pp.1–24. Available at: http://notes.sepmonline.org/content/sepswtad/1/SEC1.abstract.

Galloway, W.E., 2005. Gulf of Mexico Basin Depositional Record of Cenozoic North American Drainage Basin Evolution. *Fluvial Sedimentology VII*, pp.409–423. Available at: http://dx.doi.org/10.1002/9781444304350.ch22.

Galloway, W., 2008. Depositional evolution of the Gulf of Mexico sedimentary basin. *Sedimentary basins of the world*. Available at: http://www.sciencedirect.com/science/article/pii/S1874599708000154 [Accessed April 21, 2017].

Galloway, W.E., Whiteaker, T.L. & Ganey-Curry, P., 2011. History of Cenozoic North American drainage basin evolution, sediment yield, and accumulation in the Gulf of Mexico basin. *Geosphere*, 7(4), pp.938–973. Available at: http://geosphere.gsapubs.org/cgi/doi/10.1130/GES00647.1 [Accessed August 12, 2015].

Harris, P.T. & Whiteway, T., 2011. Global distribution of large submarine canyons: Geomorphic differences between active and passive continental margins. *Marine Geology*, 285(1–4), pp.69–86. Available at: http://dx.doi.org/10.1016/j.margeo.2011.05.008.

Hentz, T.F. & Ruppel, S.C., 2010. Regional Lithostratigraphy of the Eagle Ford Shale : Maverick Basin to East Texas Basin. *GCAGS Transactions*, pp.325–337.

Hoyt, W. V, 1959. Erosional Channel in the Middle Wilcox near Yoakum, Lavaca County, Texas. *GCAGS Transactions*, IX, pp.41–50.

Hutchinson, P.J., 1984. Morphology and Evolution of a Shale-Filled Paleo-Channel in the Wilcox Group (Paleocene-Eocene), Southeast Texas. , pp.347–356.

Laubach, S.E. & Jackson, M.L.W., 1990. Geology Origin of arches in the northwestern Gulf of Mexico basin Origin of arches in the northwestern Gulf of Mexico basin. *Geology*, 18, pp.595–589.

Lawless, P. & Hart, G., 1990. The LaSalle Arch and its Effects on Lower Paleogene Genetic Sequence Stratigraphy, Nebo-Hemphill Field, LaSalle Parish, Louisiana. Available at: http://archives.datapages.com/data/gcags/data/040/040001/0459.htm [Accessed February 1, 2017].

Liangqing Xue & Galloway, W.E., 1995. High-resolution depositional framework of the Paleocene middle Wilcox strata, Texas coastal plain. *American Association of Petroleum Geologists Bulletin*, 79(2), pp.205–230.

Mitchum, R.M.J., 1985. Seismic stratigraphic expression of submarine fans. *Seismic stratigraphy II; an integrated approach to hydrocarbon exploration/AAPG Memoir*, 39, pp.117–136. Available at: -.

Olariu, M.I. & Ambrose, W.A., 2016. Process regime variability across growth faults in the Paleogene Lower Wilcox Guadalupe Delta, South Texas Gulf Coast. *Sedimentary Geology*, 341, pp.27–49.

Palanques, A. et al., 2006. Suspended sediment fluxes and transport processes in the Gulf of Lions submarine canyons. The role of storms and dense water cascading. *Marine Geology*, 234(1–4), pp.43–61.

Pindell, J. et al., 2006. Foundations of Gulf of Mexico and Caribbean evolution: Eight controversies resolved. *Geologica Acta*, 4(1–2), pp.303–341.

Posamentier, H. W., Erskine, R.D., and Mitchum Jr., R.M., 1991. Models for submarine-fan deposition within a seqeunce-stratigraphic framework. *Seismic facies and sedimentary proceses of submarine fans and turbidite systems* (pp. 127-136). Springer New York.

Pratson, L.F. & Coakley, B.J., 1996. A model for the headward erosion of submarine canyons induced by downslope-eroding sediment flows. *Bulletin of the Geological Society of America*, 108(2), pp.225–234.

Puig, P., Palanques, A. & Martín, J., 2014. Contemporary sediment-transport processes in submarine canyons. *Annual review of marine science*, 6(July 2013), pp.53–77.

Available at: http://www.ncbi.nlm.nih.gov/pubmed/23937169.

Richard P. McCulloh, L.G.E., 1986. Shale-Filled Channel System in the Wilcox Group (Paleocene-Eocene), North-Central South Louisiana. , 36, pp.213–218.

Riding, R. et al., 1998. Mediterranean Messinian salinity crisis: Constraints from a coeval marginal basin, Sorbas, southeastern Spain. *Marine Geology*, 146(1–4), pp.1–20.

Rosenfeld, J. & Pindell, J., 2003. Early Paleogene Isolation of the Gulf of Mexico from the World's Oceans? Implications for Hydrocarbon Exploration and Eustasy. *Aapg Memoir*, pp.89–103.

Ryan, W.B.F. & Cita, M.B., 1978. The nature and distribution of Messinian erosional surfaces - Indicators of a several-kilometer-deep Mediterranean in the Miocene. *Marine Geology*, 27(3–4), pp.193–230.

Salvador, A., 1991. Origin and development of the Gulf of Mexico basin. *The gulf of Mexico basin*.

Suter, J.R. and Berryhill Jr, H.L., 1985. Late Quaternary shelf-margin deltas, northwest Gulf of Mexico. *AAPG Bulletin*, *69*(1), pp.77-91.

Vail, P.R., 1987. Seismic Stratigraphy Interpretation Using Sequence Stratigraphy Part I : Seismic Stratigraphy Interpretation Procedure. *AAPG Studies in Geology #27, volume 1: Atlas of Seismic Stratigraphy*, 1(1), pp.1–10.

Watkins, J., 2014. The Morphology of an Erosional Paleo-Canyon in the Wilcox Group , Southern Louisiana A Thesis Presented to the Graduate Faculty of the University of Louisiana at Lafayette In Partial Fulfillment of the Requirements for the Degree Master of Science Jin Wat.

Winker, C. & Edwards, M., 1983. Unstable progradational clastic shelf margins. Available at: http://archives.datapages.com/data/sepm_sp/SP33/Unstable_Progradational_Clastic_Shelf_Margins.pdf [Accessed February 1, 2017].

Zaitlin, B.A., Dalrymple, R.W. & Boyd, R., 1994. The Stratigraphic Organization of Incised-Valley Systems Associated with Relative Sea-Level Change. *SEPM Special Publication*, 51(51), pp.45–60.

Zarra, L., Meyer, D. & Neal, S., 2005. Wilcox Depositional Systems : Shelf to Deep Basin Gulf of Mexico. , (May), pp.37–38.

Zhang, J., Steel, R. and Ambrose, W., 2016. Greenhouse shoreline migration: Wilcox deltas. *AAPG Bulletin*, *100*(12), pp.1803-1831.

Vita

C. Austin Clayton was born in San Antonio, Texas. He received his B.S. in Geological Sciences in 2015 from The University of Texas at Austin. He continued his education with the Jackson School of Geosciences at The University of Texas at Austin in 2015. After graduating with a Master of Science in Geology in 2017, Austin will go on to work for Luxe Energy in Austin, Texas.

Permanent email: caclayton@mac.com

This thesis was typed by Clarke Austin Clayton.